THE UNIVERSITY
of EDINBURGH

Phosphorous Three Ways:
Polymers, Monomers, and Catalysts

Emily Kate Macdonald

Doctor of Philosophy

University of Edinburgh

2016

Declaration

The author graduated from The University of Manchester in 2013 with a Masters of Chemistry degree and has since been in full time postgraduate study under the supervision of Dr Michael P. Shaver.

The work described in this thesis is entirely my own, except where I have either acknowledged help from a named person or given reference to a published source. This thesis has not been submitted, in whole or in part, for any other degree.

Emily K. Macdonald

October 2016

Abstract

The existence of numerous phosphorus containing functional groups gives phosphorus chemistry its enormous breadth. The range of functional groups stems from phosphorus' ability to vary its coordination and valance. Phosphorus containing compounds have shown applications in agriculture, biological systems and chemical warfare.

High refractive index polymers are used in lenses, fingerprint recognition and optical coatings. However, often these devices rely on to the materials available. Phosphorus rich polymers have shown promise due to the high level of polarisability. A range of poly(phosphate ester)s and polyphosphonates have been synthesised and their thermal and optical properties tested. Some of the samples prepared boast the highest refractive indices for these types of compounds.

Polymers synthesised via a polycondensation mechanism usually possess a high dispersity, one way to introduce control is via a ring opening polymerisation (ROP). Novel aromatic phosphonate monomers have been prepared and attempted to polymerise. Monomer, catalyst and copolymerisation scope for aliphatic phosphonate ROP has also been explored.

Organocatalysts are becoming increasingly popular in ring opening polymerisation literature, one of the most popular organocatalysts is triazabicyclodecene (TBD). TBD is a dual activating catalyst as it activates both the initiator and monomer via a basic and acidic moiety respectively. Phosphates also have dual activating substituents. A range of aromatic phosphates have been successfully synthesised with varying electron withdrawing/ donating groups. These catalysts were then screened against the polymerisation of β-butyrolactone and their catalytic activity investigated.

Acknowledgements

There are many people who have helped me in a variety of ways over the past 3 years. Firstly, my supervisor Dr Michael Shaver for giving me the opportunity to undertake a PhD. I also want to thank you for all the support, backing and patience you have given me, whilst also keeping me amused with your bad jokes and general manner.

I would like to thank all the members of the Shaver group past and present. Fern for being my partner in crime for the first couple of years and much needed support in the early days. TS5 for constantly making me smile and making Edinburgh life so enjoyable. Thanks to Ben for making sure the lab never became too serious, Jaclyn and Dan for reminding me that lab life is not everything, Gerry, Meng, Mo, Vishal, Vincent, Graham, James, Lorna, Derek, Paniz, David, Yaz, Genny, Kevin, Chris, Arthur and Jannik you have all made being part of the group fun and friendly. Thanks to Dr Laura Allan and Dr Jarret MacDonald for making me the practical chemist that I am. A huge thanks to Dr Ben Lake and Dan Coward for significant help with completing this thesis, and other publications.

I am grateful to the NMR spectroscopy staff Dr Lorna Murray and Juraj Bella for all the help they have given me. The NMR service is brilliant and you have done so much from dealing with low level problems to creating bespoke experiments for me. For help with thermal data analysis I would like to thank Stefan Cairns. This work would have not been possible without all of your help.

Thanks to all my friends, of whom the stresses of PhD life will be all too familiar, for still keeping it fun along the way. Mary for always keeping me cheery and your in depth thoughts and analysis, Lewis for continuously giving me lots to think about, Graham, Priyanka, James and Amy. I would also like to thank my family for all the support they have given during the course of my studies, it is greatly appreciated and I am extremely lucky to not just call you family but friends too.

Lastly, I would like to thank you Ross. You have shown me a different side to life in Edinburgh and never let it become dull. You have given me unshakable support and strength when I thought I had none. For this and so much more I thank you.

Table of Contents

List of Abbreviations

°C	degrees Celsuis
β-BL	beta-butyrolactone
µL	microliter
ATP	adenosine triphosphate
Bn	benzyl
Bu	butyl
^{n}Bu	normal butyl
^{t}Bu	tertiary butyl
Đ	dispersity
d	doublet resonance
Da	daltons
DBN	1,5-Diazabicyclo[4.3.0]non-5-ene
DBU	diazabicyclo[5.4.0]undec-7-ene
DCM	dichloromethane
DFT	density functional theory
DMAP	4-diaminopyridine
DMSO	dimethyl sulfoxide
BOE	2-(benzyloxy)ethanol
DSC	differential scanning calorimetry
Et	ethyl
ESI	electrospray ionisation mass spectrometry
FTIR	fourier transform infrared spectroscopy
g	gram
GPC	gel permeation chromatography
HMBC	heteronuclear multiple-bond correlation spectroscopy
hr	hour
HRIP	high refractive index polymer

HSQC	heteronuclear single-quantum correlation spectroscopy
Hz	hertz
IPA	isopropyl alcohol
IR	infrared
^{i}Pr	iso-propyl
J	NMR coupling constant
k	rate constant
K_a	acid dissociation constant
NMR	nuclear magnetic resonance
M	molar
m	multiplet resonance
MALDI-TOF-MS	matrix assisted laser desorption/ionisation time of flight mass spectrometry
mL	millilitre
M_n	number average molecular weight
$M_{n,th}$	theoretical molecular weight
M_w	weight average molecular weight
Me	methyl
mg	milligrams
MHz	megahertz
min	minute
mmol	millimole
MO	molecular orbital
mol	mole
ms	mass spectrometry
m/z	mass to charge ratio
NAD	nicotinamide adenine dicucleotide
nm	nanometer
Ph	phenyl

PHB	poly(hydroxyl butyrate)
PLA	poly(lactic acid)
PPA	3-phenyl-1-propanol
ppm	parts per million
Pr	propyl
q	quartet resonance
R_m	molar refraction
rac	racemic
rt	room temperature
sec	second
t	triplet resonance
T_g	glass transition temperature
T_m	melting temperature
TEA	triethyl amine
TMG	1,1,3,-tetramethylguanidine
TMP	2,2,6,6-tetramethylpiperidine
TBD	1,3,5-triazabicyclo[4.4.0]dec-5-ene
TGA	thermograimetric analysis
THF	tetrahydrofuran
TU	thiourea
UV	ultraviolet
UV-vis	ultraviolet - visible
V_m	molar volume

List of Figures

Chapter One

Chapter Two

Chapter Three

Chapter Four

Chapter Five

List of Schemes

Chapter One

Chapter Two

Chapter Three

Chapter Four

Chapter Five

List of Tables

Chapter One

Chapter Two

Chapter Three

Chapter Four

‘Life can multiply until all the phosphorus has gone and then there is an inexorable halt which nothing can prevent’

Isaac Asimov, 1974.

Chapter One

Organophosphorus Chemistry

1.1 Nature of Organophosphorus Chemistry

"The Devil's element" was first isolated in 1669 by Hennig Brand, a German physician and alchemist. He boiled, filtered and processed nearly 60 buckets of urine in the hope of finding the Philosopher's Stone.[1,2] The process instead isolated white phosphorus, which, when exposed to oxygen, ignites spontaneously to burn with a brilliant white light. Thus the name "phosphorus" is derived from the Greek word for "light-bearer".[3] There are now more than 10^6 known phosphorus compounds, many of which are utilised in organophosphorus chemistry.

Elemental phosphorous is usually dangerous and flammable so therefore it is found in minerals primarily as a phosphate.[4] A staggering 153 million tonnes of phosphorous is produced on average every year.[4] Minerals containing phosphorus are processed by either dissolution in sulfuric acid, which converts the phosphate to phosphoric acid, or by heating with coke in a furnace. There are reports that with the current demand for phosphorus to increase we will reach 'peak phosphorus' where supply will no longer

cover demand. This leads to the possibility of phosphorus shortages in decades to come.[5,6]

The study of organophosphorus, alongside a great deal of synthetic chemistry, began in the nineteenth century. August Michaelis, pioneering this work at the University of Rostock, discovered and characterised some of the major phosphorus containing functional groups. Aleksander Arbusov was also of great importance in the development of organophosphorus chemistry and was awarded the Stalin award in 1943. These two prominent scientists will always be associated with organophosphorus chemistry through the Michaelis-Arbusov reaction, seen in Scheme 1.1.

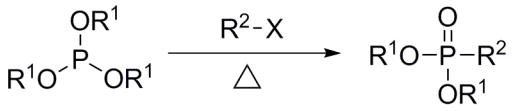

Scheme 1.1: Michaelis-Arbusov reaction

Discovered in 1898 by Michaelis and then further investigated by Arbusov shortly after,[7,8] the commonly used Michaelis-Arbusov reaction is used to synthesise phosphonates,[9-11] phosphinates[12,13] and phosphine oxides.[14,15] This occurs in two steps, as seen in Scheme 1.2. The first step is an S_N2 reaction of the nucleophilic phosphorus centre with an alkyl halide. The phosphonium intermediate then undergoes a second S_N2 reaction with the displaced halide,[16] with inversion of configuration.[17]

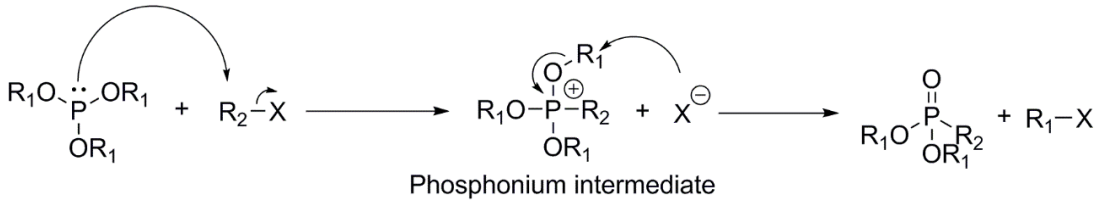

Scheme 1.2: Michaelis-Arbuzov reaction mechanism.

Normally the Michaelis-Arbuzov reaction does not need a catalyst to proceed, but in some situations a catalyst is needed. One of the commonly used catalysts is palladium chloride,[18-20] and some photocatalysts have been explored.[21,22]

Most organophosphorus compounds up until late 1950s had either three or four atoms attached to phosphorus, classified as trivalent or tetravalent respectively. In recent decades, however, compounds with one, two, five and six atoms bonded to phosphorus have been discovered. The first examples of phosphorus breaking the octet rule emerged in the 1960s where stable structures were reported with five and six bonds,[23] two of which are shown in Figure 1.1.

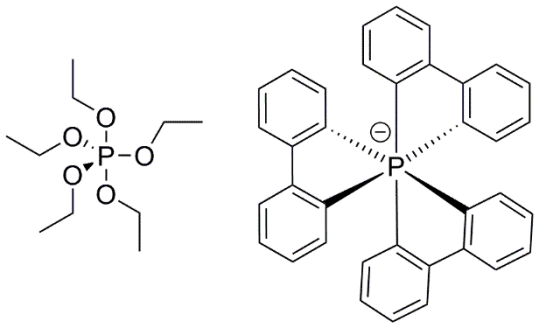

Figure 1.1: Phosphorus in 5 and 6 coordination environments.

The discovery of low and hyper coordinate species demanded a new classification scheme. First, phosphorus is assigned a *coordination number*: the number of atoms directly bonded to the phosphorus atoms and is described using the notation σ^X. The second number is called the *valence number* and is equal to the number of bonds

phosphorus has made, labelled by λ^Y. Table 1.1 shows some common organophosphorus compounds with their classification.

Table 1.1: Classification of some common organophosphorus compounds

Classification	Structure	Name
$\sigma^1\lambda^1$		Phosphinidenes
$\sigma^1\lambda^3$	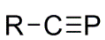	Phosphaalkynes
$\sigma^2\lambda^3$	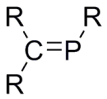	Phosphaalkene
$\sigma^2\lambda^3$	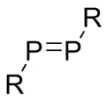	Diphosphenes
$\sigma^2\lambda^2$		Phosphenium cations
$\sigma^3\lambda^3$		Phosphines
$\sigma^3\lambda^3$		Dialkylphosphine halides
$\sigma^3\lambda^5$		Dioxophosphoranes
$\sigma^4\lambda^4$		Phosphonium cations
$\sigma^4\lambda^5$	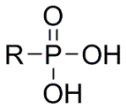	Phosphonic acids
$\sigma^4\lambda^5$	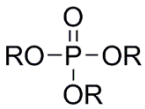	Phosphates

$\sigma^4\lambda^5$	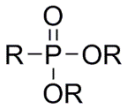	Phosphonates
$\sigma^4\lambda^5$	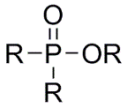	Phosphinates
$\sigma^4\lambda^5$	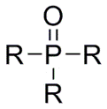	Phosphine oxides
$\sigma^5\lambda^5$		Phosphoranes
$\sigma^6\lambda^6$		No common name

1.2 Heterocyclic Chemistry

Nearly half of all known organic compounds contain at least one heterocycle. They have a wide range of applications, for example in antioxidants and additives. Heterocyclic compounds are also commonly found in nature from nucleic acid bases to many vital vitamins. As a result of this a large amount of current research concerns heterocyclic chemistry, in particular ring synthesis and cleavage.

Whilst advances were being made in heterocyclic nitrogen, oxygen and sulfur chemistry, heterocyclic phosphorus chemistry discoveries came much later. This is evident in the fact that no discussion of phosphorus heterocyclic chemistry can be found in any textbooks until 1996; where the second edition of Comprehensive Heterocyclic Chemistry[24] included chapters on this important topic. However, recent

research effort has made phosphorus heterocyclic chemistry an essential section of heterocyclic chemistry. For example, the structures in Figure 1.2 are now well recognised and used.

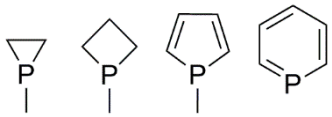

Figure 1.2: Fundamental monocyclic phosphorus systems, from left phosphirane, phosphetane, 1-methylphosphole and phosphinine.

The main difference between cyclic and acyclic compounds is the constraints present in the cyclic species. Acyclic flexible molecules adopt confirmations with 'natural' bond angles and lengths. In cyclic systems the presence of the ring can force the molecule to adopt a strained structure. This strain is made up of bond angle strain, bond stretching or compression and bond torsion, however all the components of strain are interdependent.[25]

Most heterocyclic phosphorus compounds are synthesised by either a reaction of bifunctional carbon compounds with a phosphorus species, or an intramolecular cyclization reaction. One of the most well-known phosphorus heterocycles is 1,3,2-dioxaphospholane, known in a range of functionalities, some of which are shown in Figure 1.3.

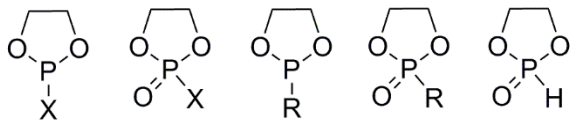

Figure 1.3: Different functionalities of 1,3,2-dioxaphospholane.

1.3 The Phosphoryl Group

The phosphoryl (P=O) group is present in many of the important organophosphorus compounds and is widely abundant in nature. The bond is easily formed and resistant to many chemical reactions: it has a bond dissociation of 536-582 $KJmol^{-1}$.[26] Phosphines can be readily oxidised to incorporate a phosphoryl bond by a huge range of oxidising agents including atmospheric oxygen. Phosphine oxides, however, require very strong reducing agents to return to phosphines. The great stability of this bond comes from the multiple bonding present. The strength of the bonding is determined by the substituents connected to phosphorus. Electron withdrawing substituents increases the strength of the phosphoryl bond. This can be seen using infrared spectroscopy, in $F_3P=O$ the P=O stretching frequency is $1418cm^{-1}$ compared to $1170cm^{-1}$ in $Me_3P=O$. There are many theories that explain the type of bonding present. In early literature, the theory is that there is donation from the phosphorus to the oxygen and then back bonding of a pair of electrons from oxygen into one of the vacant 3d-orbitals of phosphorus, and this has led to a simple resonance structure, demonstrated in Figure 1.4a.[27] Figure 1.4b shows the orbital overlap involved.

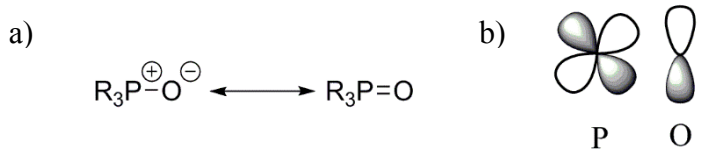

Figure 1.4: a) Resonance expression b) of orbital overlap

Common phases such as “there is expansion of the octet on phosphorus to allow back-bonding from oxygen lone pairs into low-lying empty d-orbitals” are widely accepted.[28,29] Using modern computational calculations, it has been shown that no vacant d-orbitals are used in phosphoryl bonding. Now the generally accepted view is interaction of a 2p orbital on oxygen with an antibonding orbital on the R_3P moiety,[30,31] giving the bond some triple bond character which could explain its strength. This is seen as a form of negative conjugation.[32,33] There have been reports of calculations showing a usual σ bond and an ionic charge on both phosphorus and oxygen,[34] this ionic interaction then shortens and strengthens that σ bond. This model does account for the experimental electron paramagnetic resonance reported for phosphine oxides and phosphates in the early 90s.[35] It is clear, however, that there is no definitive answer to the exact nature of the multiple bonding in the phosphoryl bond, which for the purpose of this thesis will be represented as P=O.

1.4 Analogies between Phosphorus and Nitrogen

The similarities and differences between phosphorus and nitrogen have been a core part of undergraduate inorganic and organic lectures for some time. Elemental nitrogen occurs as gaseous N_2, whereas elemental phosphorus occurs in many allotropes including white, red and black,[36] seen in Figure 1.5.

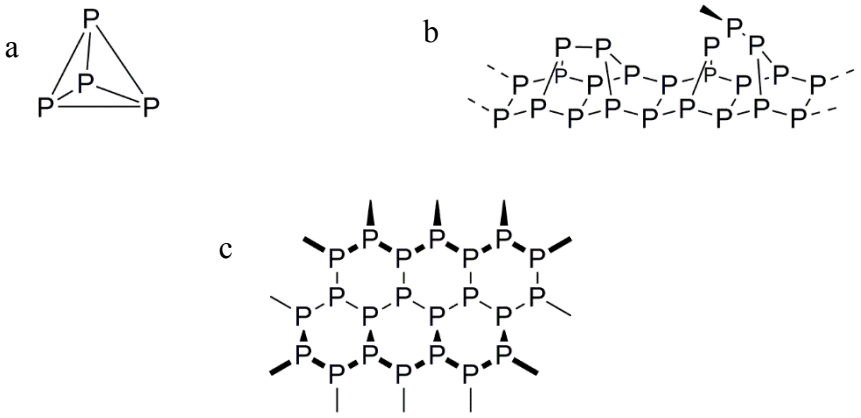

Figure 1.5: Allotropes of phosphorus a) white, b) red and c) black.

White phosphorus is a discrete P_4 unit, and this arrangement results in ring strain and resulting instability. Red phosphorus is an amorphous network formed by exposing white phosphorus to sunlight in anaerobic conditions. Black phosphorus is the most thermodynamically stable allotrope of phosphorus. It is likened to graphite, in terms of appearance and the sheets of linked atoms that make up its structure.[37]

One of the basic differences is in electronegativity, with nitrogen at 3.0 and phosphorus at a lower 2.2 on the Pauling scale. A second basic difference is in their comparable sizes, nitrogen has a Van der Waals radius of 155 pm and phosphorus 195 pm. One of the most commonly noticed differences is the ability of phosphorus to partake in higher coordination environments and multiple bonding to elements such as oxygen. This is due, in part, to phosphorus being more stable in higher coordination environments. This is evident by the ease in which phosphines are oxidised to phosphine oxides compared to amines. Nitrogen is more stable in low coordinate environments than phosphorus. Structures with unsaturation are common with both nitrogen and phosphorus. The Schiff base imine is very well known and a wide range

are accessible by a condensation reaction. However, their phosphorus counterparts, phosphaalkenes, are less well known.

Phosphines resemble amines in a variety of ways such as nucleophility. With phosphines, the barrier to pyramidal inversion is much higher. This means**,** with chiral phosphines**,** optically active enantiomers can be isolated. With amines**,** the pyramidal inversion is rapid, so they are constantly flipping between enantiomers, seen in Figure 1.6.[38]

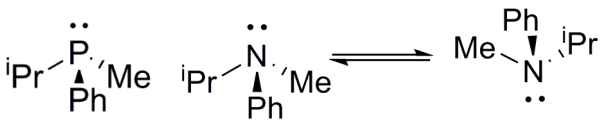

Figure 1.6: Isolable phosphine and rapid inversion of amines.

1.5 General Considerations of ^{31}P NMR Spectroscopy

Working with phosphorus has the major benefit that its nuclei is active for NMR spectroscopy. Phosphorus NMR spectra are easy to prepare and highly informative about the environment. Phosphorus has one naturally occurring isotope that is 100% abundant, with mass 31, so there are no satellites or problems with concentrations of samples. ^{31}P also has a spin quantum number of ½, the same as for ^{1}H NMR spectroscopy, making coupling patterns simple. One disadvantage is the lower

sensitivity of ^{31}P nucleus compared to ^{1}H, but this can be solved by increasing the number of scans run.[39] The range for ^{31}P extents roughly 2000 ppm, but most common shifts fall between -200 and +300 ppm. Functional groups tend to have their own range of shifts within a region, which can be seen in Figure 1.7.

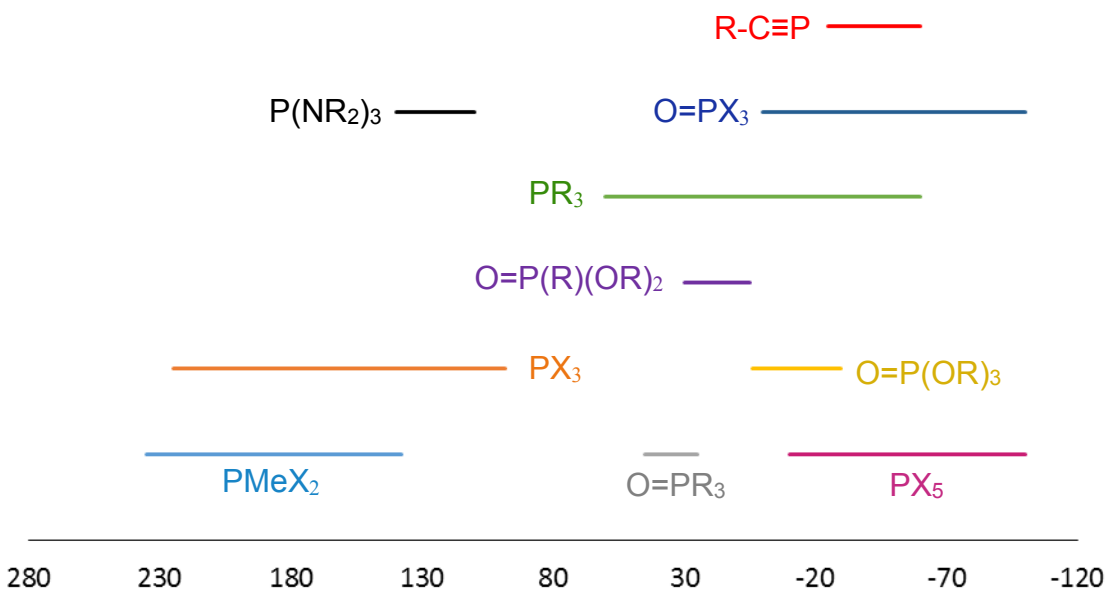

Figure 1.7: ^{31}P NMR shifts of common functional groups.

There are many reasons as to why a shift is at a specific ppm. Electronegative groups are believed to contract the p-orbitals on phosphorus, causing a deshielding effect.[40] Where phosphorus is involved with conjugation, electron density can change either way. An increase in bond angle at phosphorus can have a deshielding effect with three coordinate phosphorus, but a shielding effect with five coordinate.[41]

1.6 Common Uses of Organophosphorus Chemistry

Organophosphorus compounds are widely used around the globe. Not just in active academic research, but also in industry: from chemical warfare to therapeutic agents. Organophosphoruses are also rife in nature, in the human body it is the 6th most abundant element after oxygen, carbon, hydrogen, nitrogen and calcium. In teeth and bones some of the calcium is present as calcium phosphate. Surprisingly the richest phosphorus organ is brain tissue.[4] DNA is a polymer that carries a genetic code that is key for living organisms, made up of nucleotide monomers. It contains a sugar phosphate backbone. The phosphate substituent is highlighted in Figure 1.8 of the nucleotide adenine.

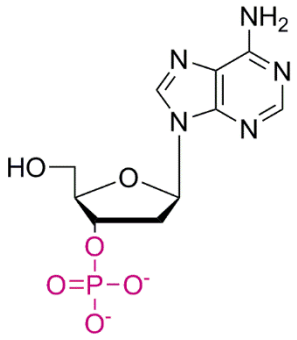

Figure 1.8: Structure of nucleotide

Nucleotides are also the currency of energy used in the body, by the species adenosine triphosphate (ATP). ATP transfers energy by cleavage of a phosphate group and the release of energy. This energy can then facilitate such processes as muscle contraction,

active transport and nerve excitation.[42] The human body produces, uses and recycles over 1 kilogram of ATP every hour.[4]

Phosphorus has been used in warfare in recent centuries, it was used in tracer bullets that would inflict burning phosphorus wounds. White phosphorus is also used in bombs where it burns fiercely and can burn other combustibles in close proximity. The bombs also create a blanket of smoke once dropped. During World War II phosphorus fire bombs were dropped over several cities, as many as 25,000 were dropped on Hamburg during July 1943 alone. Since then white phosphorus bombs have been used in Iraq, Vietnam, Lebanon and Afghanistan.

Organophosphorus compounds have been used in chemical warfare since World War II. There are two main classes of nerve gases, the first is the G-series discovered by German chemist Gerhard Schrader, the second type is the V-series discovered by Ranajit Ghosh working at ICI. Both classes were originally being investigated as pesticides. Blocking acetylcholinesterase causes major body organs to malfunction resulting in death. Three examples of nerve gas are shown in Figure 1.9.

Tabun was the first nerve agent to be discovered. Tabun and Sarin were found to be incorporated into artillery shells produced by Nazi Germany, which were not used. Sarin and Tabun were employed by Iraqi forces in the Iran-Iraq War. During the 2013 Syrian Civil War Sarin was used to kill several hundred people. It is suspected that the Syrian government were responsible for the attacks however this has never been

confirmed. Tetram was one of the first compounds to be discovered in the V-Series of nerve gases. It's thought that North Korea have stockpiles of this compound.

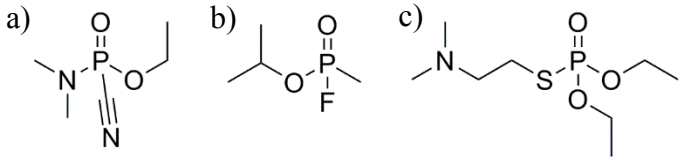

Figure 1.9: Chemical structures of 3 nerve gas agents, a) Tabun, b) Sarin and c) Tetram

The use of polymers as flame retardants has been of great interest since DuPont's discovery of Nomex® and Kevlar® in the 1960s. Phosphorus containing polymers are becoming increasingly successful as halogen free flame retardants.[43,44] One commonly used flame retardant phosphorus containing polymers is melamine polyphosphate, seen in Figure 1.10a. It decomposes endothermically making it a heat sink and also releases nitrogen gases that dilute oxygen. It also favours insulating char formation on the polymer.[45,46]

Red phosphorus, itself a polymer, has been used as a flame retardant. It has been added to materials like polyamides, polycarbonates and polyesters.[47] Phosphorus based products are forecasted to have the largest growing share of the flame retardant market. Some of the commercially available compounds are shown in Figure 1.10b. As a general rule the higher the phosphorus content the better the flame retardant.[48]

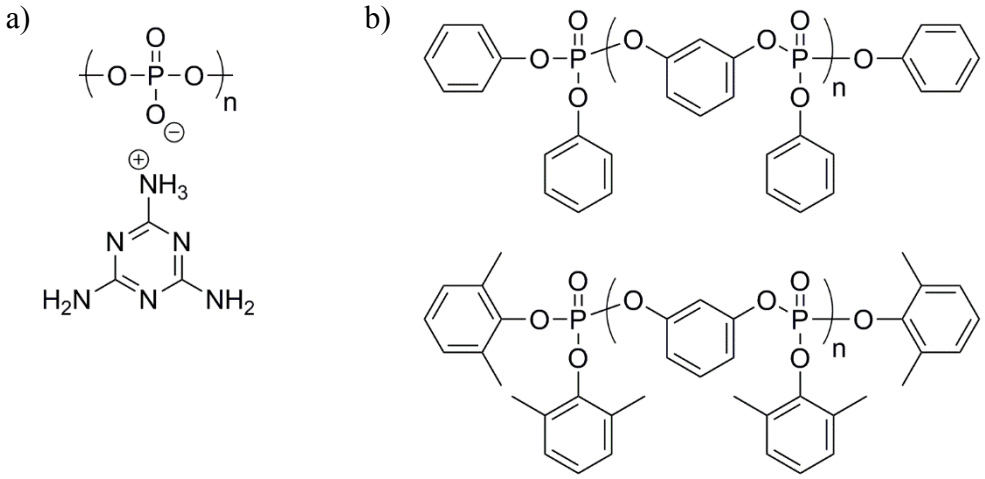

Figure 1.10: a) Structure of melamine polyphosphate b) commercially available flame retardants.

Organophosphorus compounds have also found use in medicine. One early compound is called *Fosfomycin* (Figure 1.11), a phosphonic acid and broad-spectrum antibiotic. It is produced by the bacterium *Stereptomyces fradiae.* It primarily works by inhibiting bacteria cell wall synthesis.[49]

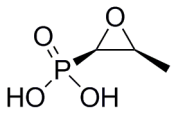

Figure 1.11: Fosfomycin, a broad-spectrum antibiotic.

After the discovery of *Fosfomycin* several phosphonic and phosphinic acids were found in the formation of other bacteria that showed antibiotic activity. The majority of these naturally occurring antibiotics contain amino groups, *Bialophos*,[50] *Plumbemycin A*[51,52] and *Fosmidomycin*[53] are shown in Figure 1.12.

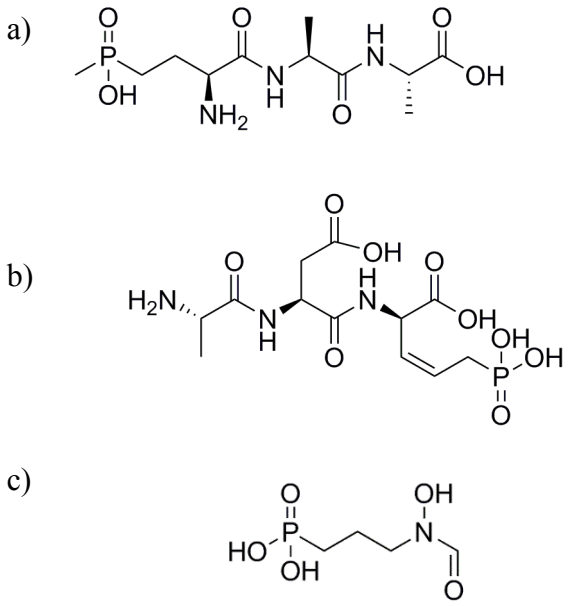

Figure 1.12: Structures of naturally occuring antibiotics with amino groups a) *Bialophos* b) *Plumbemycin A* and c) *Fosidomycin.*

The first organophosphorus compound that showed anticancer activity is shown in Figure 1.13a, a cyclophosphamide. Discovered in 1958,[54] it is still used today. Some phosphonate analogous of biologically active phosphates have been explored. The theory is that the high stability of P-C bonds would prevent any processes involving cleavage of the P-O bond in the phosphate. Phosphonic acids are also thought to inhibit the work of the counter carboxylic acid. The potent anticancer drug in Figure 1.13b is expected to work by this mechanism.[55]

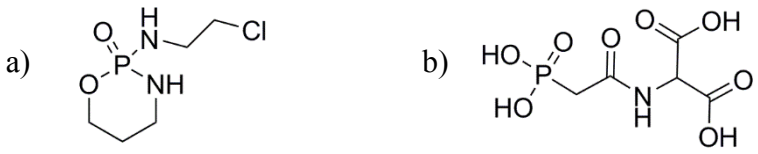

Figure 1.13: Organophosphorus anticancer drugs

Many reactions involving phosphorous compounds produce phosphorus free compounds that are useful in synthetic chemistry. The most well-known is the Wittig reaction, the discovery of which won Georg Wittig the Nobel Prize in 1979.[56,57] The Wittig reaction is one of the most important synthetic routes to produce alkenes.[58] An aldehyde or ketone is reacted with a nucleophilic ylide to produce a four membered ring oxaphosphetane species, this is unstable and undergoes elimination to give the alkene and phosphine oxide. Formation of the strong phosphoryl bond is the driving force for the Wittig reaction. An ylide is formed by deprotonation of a phosphonium salt by a strong base, and phosphonium salts are readily synthesised by reacting a phosphine with an alkyl halide. Ylides can also be represented as phosphoranes. Scheme 1.3. shows ylide formation and the Wittig reaction.[59]

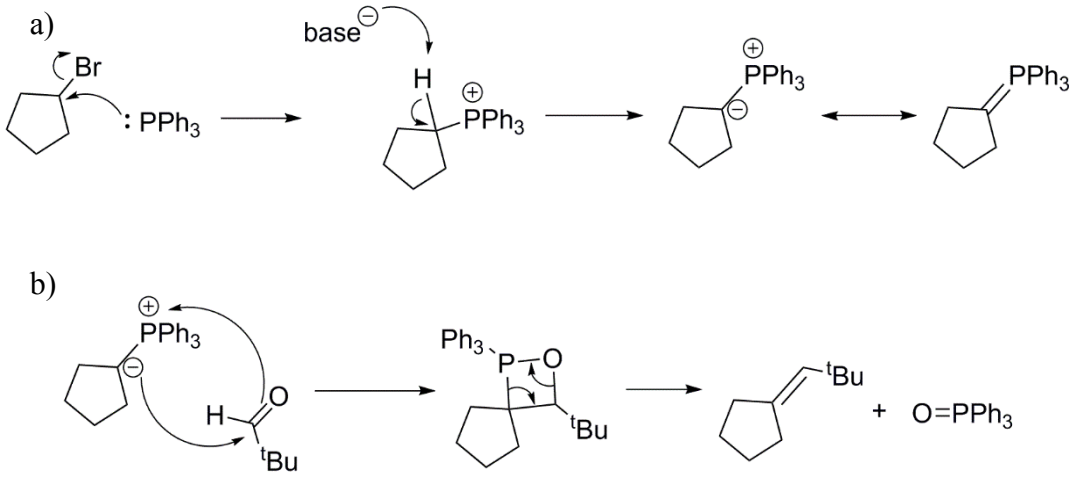

Scheme 1.3: Reaction schemes of a) Ylide formation b) Wittig reaction.

Another way in which organophosphorus compounds are useful as reagents in the synthesis of organic compounds is in the Appel reaction. This reaction converts an alcohol into an alkyl halide and is named after Rolf Appel.[60] In Scheme 1.4, we can

see the Appel reaction using bromine, however carbon tetrachloride, methyl iodide and other halogen sources can also be used.

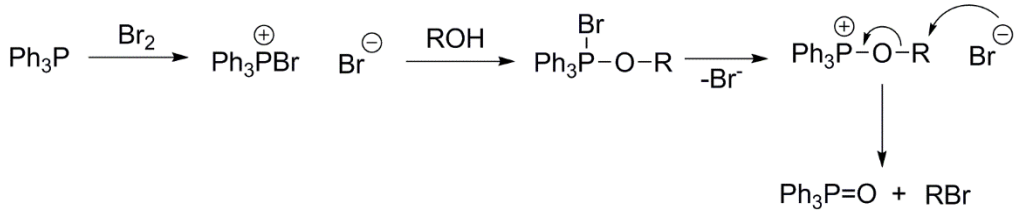

Scheme 1.4: Appel reaction.

With primary and secondary alcohols, the last step happens in a S_N2 process and a S_N1 manner with tertiary alcohols. The driving force for this reaction is the formation of the strong phosphoryl bond.

1.7 Project Aims

This project began as a Samsung funded project exploring phosphorus containing intrinsic high refractive index materials. After meeting Samsung's target refractive indices in Year 1, the company patented the intellectual property and stopped funding. We thus decided to explore the broader roles of organophosphorus compounds in polymer chemistry. There are three principal applications targeted in this thesis. Chapter Two investigates synthesising polymers containing phosphorous *via* polycondensation reactions and their uses as high refractive index polymers (HRIPs). The effect of conjugation length and composition of the polymer backbone on the refractive index of the polymer are addressed. The resultant thermal properties and

optical properties of the polymer can be tuned. Chapter Three first explores synthesising phosphorus containing HRIPs though ring opening polymerisation (ROP). To date no aromatic or bicyclic phosphonates have been synthesised and screened for ROP. The second aim of this chapter is to expand the catalyst scope for phosphonate ROP, extending to a range of organocatalysts and the first examples of metal catalysed ROP of polyphosphonates. Lastly, Chapter Four explores phosphoric acid derivatives as catalysts for the ROP of cyclic esters. In particular, mechanistic considerations in the ROP of β-BL compared to ε-caprolactone and *rac*-lactide.

1.8 References

(1) Prinzler, H. W. *Phosphorus, Sulfur Silicon Ret. Elem.* **1993**, *78*, 1-13.

(2) Maier, L. *Phosphorus, Sulfur Silicon Ret. Elem.* **1998**, *143*, 249-251.

(3) Ashley, K.; Cordell, D.; Mavinic, D. *Chemosphere* **2011**, *84*, 737-746.

(4) Emsley, J.: *Nature's Building Blocks: An A-Z Guide to the Elements*; Oxford University Press: New York, 2001.

(5) Cordell, D.; Drangert, J.-O.; White, S. *Glob. Environ. Change* **2009**, *19*, 292-305.

(6) Stephen, R. C.; Elena, M. B. *Environ. Res. Lett.* **2011**, *6*, 014009.

(7) Michaelis, A.; Kaehne, R. *Berichte der Deutschen Chemischen Gesellschaft* **1898**, *31*, 1048-1055.

(8) Arbusov, A. E. *J. Russ. Phys. Chem. Soc.* **1906**, *38*, 687-713.

(9) Kosolapoff, G. M. *Org. React.* **1951**, *6*, 273-338.

(10) Kosolapoff, G. M. *J. Am. Chem. Soc.* **1945**, *67*, 2259-2260.

(11) Kosolapoff, G. M. *J. Am. Chem. Soc.* **1944**, *66*, 1511-1512.

(12) Hennig, H. G. *J. Prakt. Chem.* **1965**, *29*, 93.

(13) Baldwin, R. A.; Wilson, C. O.; Wagner, R. I. *The Journal of Organic Chemistry* **1967**, *32*, 2172-2176.

(14) Sander, M. *Chem. Ber.* **1960**, *93*, 1220-1230.

(15) Michaelis, A.; LaCoste, W. *Chem. Ber.* **1885**, *18*, 2109-2118.

(16) Bhattacharya, A. K.; Thyagarajan, G. *Chem. Rev.* **1981**, *81*, 415-430.

(17) Gerrard, W.; Green, W. J. *J. Chem. Soc. (Resumed)* **1951**, 2550-2553.

(18) Tavs, P. *Chem. Ber.* **1970**, *103*, 2428-2436.

(19) Tavs, P.; Korte, F. *Tetrahedron* **1967**, *23*, 4677-4679.

(20) Tavs, P.; Weitkamp, H. *Tetrahedron* **1970**, *26*, 5529-5534.

(21) Fu, J.-J. L.; Bentrude, W. G. *J. Am. Chem. Soc.* **1972**, *94*, 7710-7717.

(22) Fu, J.-J. L.; Bentrude, W. G.; Griffin, C. E. *J. Am. Chem. Soc.* **1972**, *94*, 7717-7722.

(23) Denney, B. D.; Relles, H. M. *J. Am. Chem. Soc.* **1964**, *38*, 3897-3898.

(24) Katritzhy, A. R.; Rees, C. W.; Scriven, E. F. V.: *Comprehensive Heterocyclic Chemistry II*; Pergamon Press: Oxford, 1996.

(25) Gilchrist, T. L.: *Hetercyclic Chemistry*; Wiley: Essex, 1992.

(26) Hartley, F. R.: *The Chemistry of Organophosphorus Compounds*; John Wiley & Sons: New York, 1990; Vol. 2.

(27) Kwart, H.; King, K.: *D-Orbitals in Chemistry of Silicon, Phosphorus and Sulfur*; Pringer-Verlag: Berlin, 1977.

(28) Mitchell, K. A. *Chem. Rev.* **1969**, *69*, 157-178.

(29) Corbridge, D. E. C.: *The Structural Chemistry of Phosphorus*; Elsevier: Amsterdam, 1974.

(30) Gilheany, D. G. *Chem. Rev.* **1994**, *94*, 1339-1374.

(31) Kutzelnigg, W. *Angew. Chem. Int. Ed.* **1984**, *23*, 272-295.

(32) Reed, A. E.; Schleyer, P. v. R. *J. Am. Chem. Soc.* **1990**, *112*, 1434-1445.

(33) Quin, L. D.: *A guide to organophosphorus chemistry*; New York : Wiley-Interscience, 2000.

(34) Chesnut, D. B. *J. Am. Chem. Soc.* **1998**, *120*, 10504-10510.

(35) Rai, U. S.; Symons, M. C. R. *J. Chem. Soc., Faraday Trans.* **1994**, *90*, 2649-2652.

(36) Housecroft, C. E.: *Inorganic Chemistry*; 3rd ed.; Prentice Hall: Harlow, 2008.

(37) Schlesinger, M. E. *Chem. Rev.* **2002**, *102*, 4267-4302.

(38) Greenwood, N. N.: *Chemistry of the elements*; Repr. with corrections.. ed.; Oxford : Butterworth-Heinemann: Oxford, 1985.

(39) Kuhl, O.: *Phosphorus-31 NMR Spectroscopy*; Springer: Berlin, 2008.

(40) Karplus, M.; Pople, J. A. *J. Chem. Phys.* **1963**, *38*, 2803-2807.

(41) Gorenstein, D. G.; Kar, D. *Biochem. Biophys. Res. Commun.* **1975**, *65*, 1073-1080.

(42) Maruyama, K. *J. Hist. Biol.* **1991**, *24*, 145-154.

(43) Schartel, B. *Materials* **2010**, *3*, 4710-4745.

(44) Rakotomalala, M.; Wagner, S.; Doring, M. *Materials* **2010**, *3*, 4300-4327.

(45) Jahromi, S.; Gabriëlse, W.; Braam, A. *Polymer* **2003**, *44*, 25-37.

(46) Braun, U.; Schartel, B. *J. Fire Sci.* **2005**, *23*, 5-30.

(47) Levchik, S. V.; Levchik, G. F.; Balabanovich, A. I.; Camino, G.; Costa, L. *Polym. Degrad. Stab.* **1996**, *54*, 217-222.

(48) Levchik, S. V.; Weil, E. D. *J. Fire Sci.* **2006**, *24*, 345-364.

(49) Patel, S.; Balfour, J.; Bryson, H. *Drugs* **1997**, *53*, 637-656.

(50) Seto, H.; Imai, S.; Tsuruoka, T.; Satoh, A.; Kojima, M.; Inouye, S.; Susaki, T.; Otake, N. *J. Antibiot.* **1982**, *35*, 1719-1721.

(51) Gahungu, M.; Arguelles-Arias, A.; Fickers, P.; Zervosen, A.; Joris, B.; Damblon, C.; Luxen, A. *Bioorg. Med. Chem.* **2013**, *21*, 4958-4967.

(52) Diddens, H.; Dorgerloh, M.; Zahner, H. *J. Antibiot.* **1979**, *32*, 87-90.

(53) Iguchi, E.; Okuhara, M.; Kohsaka, M.; Aoki, H.; Imanaka, H. *J. Antibiot.* **1980**, *33*, 18-23.

(54) Arnold, H.; Bourseaux, F. *Angew. Chem.* **1958**, *70*, 539-544.

(55) Kafarski, P.; Lejczak, B.; Mastalerz, P.; Dus, D.; Radzikowski, C. *J. Med. Chem.* **1985**, *28*, 1555-1558.

(56) Wittig, G.; Haag, W. *Chem Ber.* **1955**, *88*, 1654-1666.

(57) Wittig, G.; Schöllkopf, U. *Chem. Ber.* **1954**, *87*, 1318-1330.

(58) Hoffman, R. W. *Angew. Chem. Int. Ed.* **2001**, *40*, 1411-1416.

(59) Clayden, J.; Greeves, N.; Warren, S.; Wothers, P.: *Organic Chemistry*: Oxford, 2009; Vol. Oxford University Press.

(60) Appel, R. *Angew. Chem. Int. Ed.* **1975**, *14*, 801-811.

Chapter Two

Phosphorous Containing Polymers as High Refractive Index Polymers

2.1 Introduction to Intrinsic High Refractive Index Polymers

2.1.1 Main Classes of High Refractive Index Polymers

Advances in optical devices are dependent on the materials available at present. Materials with a high refractive index are an active area of research. Recently interest has turned to polymers as light weight and tuneable alternatives to traditional materials such as glass.[1,2] High refractive index polymers (HRIPs) are used in various applications such as lenses,[3] antireflective coatings,[4] ophthalmic devices[5] and image sensors.[6] The refractive index of a material is a measure of how light propagates through the medium compared to that of vacuum. When light hits the interface of two materials possessing different refractive indices it can change speed and direction, as seen in Figure 2.1.

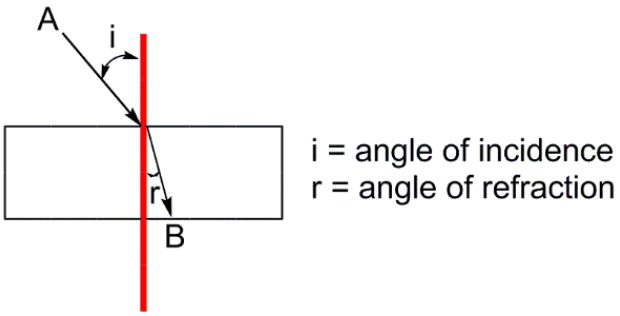

Figure 2.1: Schematic of refraction of light at the interface between two media.

Typically polymers have refractive indices within the range of 1.3-1.7.[7] Refractive index can change with wavelength of light, and the optical dispersity of a material is measured by its Abbé number.[3] The Abbé number is usually calculated using refractive indices at three different wavelengths, the Fraunhofer lines, as in Eqn 2.1[8]

$$\upsilon_d = \frac{\eta_D - 1}{\eta_F + \eta_C} \qquad \text{(Eqn 2.1)}$$

These wavelengths D, F and C are at 589.3, 486.1 and 656.6 nm, respectively. To have applicability in optical applications HRIPs need a low dispersion, shown by a high Abbé number and a high refractive index. There is often a trade-off between refractive index and Abbé number. A material that has a high refractive index and Abbé number removes the need to layer multiple materials to obtain a high refractive index at a wide range of wavelengths of light.

Nanocomposite and intrinsic are the two main classes of HRIPs. Nanocomposites are inorganic/organic hybrid materials where a polymer chain is tethered to a nanoparticle surface, and were first reported in the early 1990s.[9] Titania is a common nanoparticle of choice, itself having a high refractive index, boosting the refractive index of the nanocomposite.[10,11] Zinc sulphide is also a popular choice of nanoparticle.[10] A wide

range of polymer chains have been incorporated into nanocomposites, including polyimides[12] and methacrylates.[13] Unfortunately, nanocomposite materials can aggregate which leads to problems in stability, processability and transport.[14] If a lens or optical device is to be produced by injection moulding nanocomposites are not useful. Intrinsic HRIPs do not reach the same high refractive indices as nanocomposites but can offer advantages in stability and processability.

2.1.2 Principles of Intrinsic High Refractive Index Polymers

An intrinsic HRIP can be prepared by introducing a functionality or element with a high molar refraction into the polymer. The refractive index of a moiety can be predicted using the Lorentz-Lorenz equation:[8]

$$\frac{\eta^2-1}{\eta^2+1} = \frac{R}{M} \times \frac{M}{V} = \frac{R_m}{V_m} \qquad \text{(Eqn 2.2)}$$

where R and V are the molecular refraction and volume respectively and M is the molecular weight of the repeat unit. R/M can be simplified to molar refraction (R_m) and M/V as the inverse of molar volume (V_m). Therefore, a substituent with high molar refraction and low molar volume will increase the refractive index of a polymer including halogens, aromatics, sulfur and heavier main group elements. The more polarisable the material the higher the molar refraction. As light enters a medium the electron density is disrupted, slowing the beam of light down. The more polarisable

the material the more the electron density is disrupted, the slower the wave travels and hence the higher the refractive index.

2.1.3 Halogen Containing Polymers

As mentioned previously halogens are substituents that can increase the refractive index of a polymer, with the exception of fluorine as it is not polarisable. Gaudiana *et al.* reported one of the first intrinsic HRIPs containing halogens. [15 17] It was found that the refractive index is dependent on the halogen incorporated (I> Br> Cl), parallel to their polarisability, all within the range of 1.67-1.77.

2.1.4 Sulfur Rich Polymers

One of the most well studied types of intrinsic HRIPs are sulfur rich, and they have incorporated many moieties including thioethers,[16] thianthrenes,[17] sulfones.[18] This work is predominantly driven by Ueda and colleagues, who confirmed that the higher the sulfur content the higher the refractive index. They also focused on effects from molecular packing, which can be controlled by steric bulk in the backbone of the polymer. They investigated the difference between polymers with a *meta* and *para* linkage in the repeat unit; the *meta* polymers gave the highest refractive index, possibly due to better chain flexibility and less chain-chain interactions.[16] The importance of

low molar volume was shown by the exchange of a sulfonyl (O=S=O) with a thioether (-S-), giving an increase of refractive index in 0.015.[18] More recently HRIPs containing thioethers and sulfones have boosted refractive indices up to 1.725, with heterocycles giving better solubility in polar aprotic solvents.[19] One of the highest reported HRIP is a polymer containing thiophene rings in the backbone and pendent fullerenes.

2.1.5 Heavy Main Group Polymers

A newer area of research is HRIPs containing heavier main group compounds,[20,21] including silicon, germanium and tin. The polymers synthesised had high mechanical strength, due to the high level of crosslinking. They gave refractive indices in the range 1.590-1.703.[20] They were synthesised by a thiol-ene coupling reaction, the monomers used are shown in Figure 2.2a. Silicon containing copolymers have also been synthesised *via* a hydrosilylation reaction, giving refractive indices as high as 1.605.[22] In particular silicon based HRIPs offer excellent stability.

2.1.6 Organometallic Polymers

Nanocomposites give such a high refractive index due to the high metal content, so organometallic HRIPs have been a logical research effort as they combine the highly

refractive metal and synthetic nature of intrinsic HRIPs. Manners *et al.*[23] reported a range of polyferrocenes with high refractive indices and low optical dispersion, which were synthesised by ring opening of the cyclic monomer. One of the highest reported intrinsic HRIPs, produced by Tang *et al.*[24] is an organocolbalt that has a high refractive index of 1.813, as shown in Figure 2.2b. Due to its thermal properties it cannot be injection moulded but can be spin-coated.

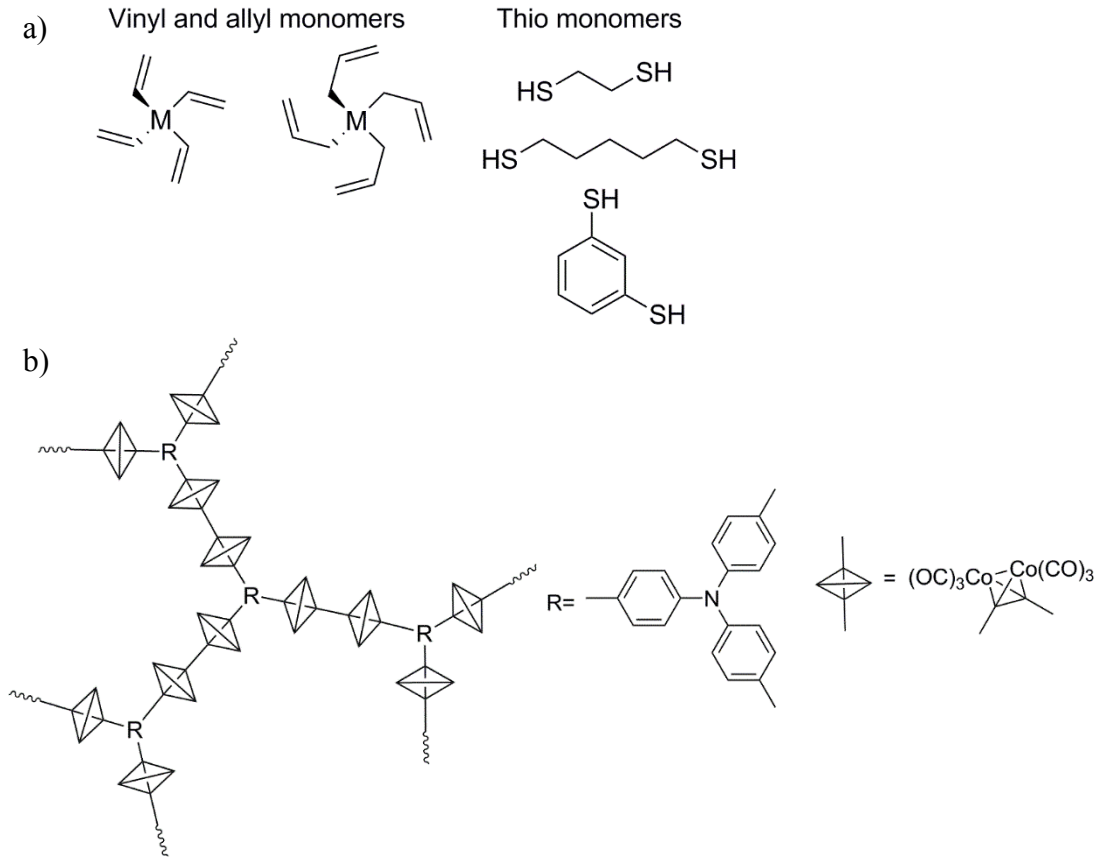

Figure 2.2: a) Vinyl, allyl and dithiol monomers used in thiol-ene coupling reactions b) HRIP of the $Co_2(CO)_6$ dimer with triphenylamine linkers.

2.1.7 Phosphorus Rich Polymers

Phosphorus also been investigated as a candidate componet for HRIPs, as it has a high level of polarisability due to its electron structure, which is shown in Figure 2.3.

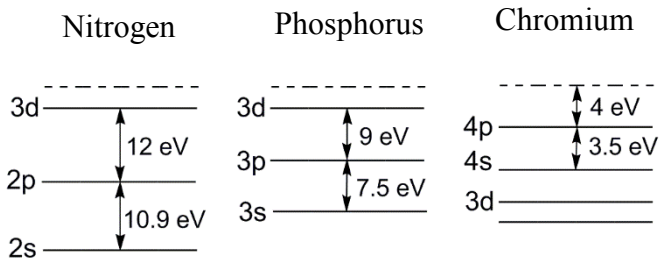

Figure 2.3: Atomic energy levels of nitrogen, phosphorus and chromium.

It was outlined in Section 1.4 that there are many differences between phosphorus and nitrogen. A further difference is the promotional energy for the electron orbitals; 17 eV for phosphorus compared to 23 eV for nitrogen.[25] This energy gap is lower due to a greater contribution from higher energy levels (4s, 4p, 5s) to stabilise electronic distortions. This gives phosphorus a higher degree of polarisability and hence a higher molar refraction. Figure 2.3 shows that this is also lower for metals such as chromium, which is why nanocomposites and organometallic species have a high refractive index. Phosphorus containing HRIPs also give low optical dispersion and good optical clarity,[3] making them excellent choices for incorporation into HRIPs.

One of the first examples of phosphorous containing HRIPs is from McGrath *et al.*[26,27] where they synthesised two polyphosphonates, a biphenol and a bisphenol A system, *via* a polycondensation reaction. The biphenol system is shown in Scheme 2.1.

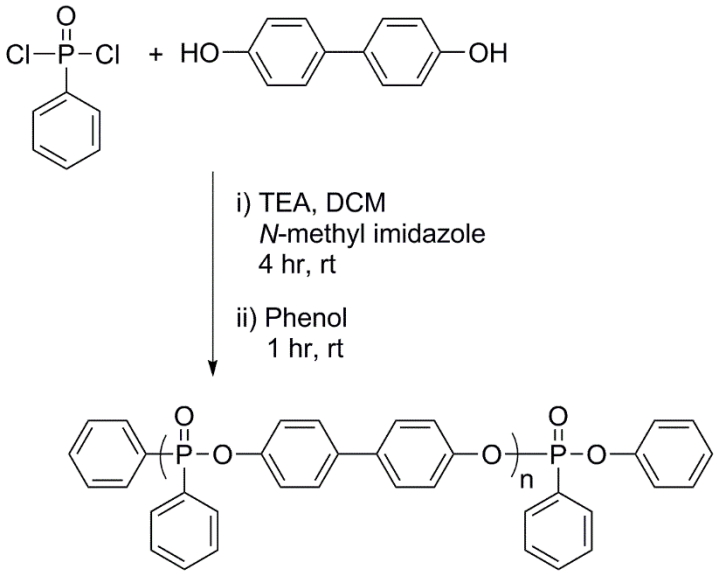

Scheme 2.1: Polycondensation synthesis of McGrath's polyphosphonates.

The reactions were carried out in the presence of base and an organocatalyst, *N*-methyl imidazole. Compared to their carbonate analogues the polyphosphonates had an increase in refractive index of 0.02, and when the backbone was conjugated compared to non-conjugated the refractive index also improved, by 0.04. A series of polyphosphazenes were synthesised by Allcock and colleagues,[28,29] *via* ring opening polymerisation (ROP). Polymers containing pendant naphthyl groups showed short UV-cut off points making their use limited. With biphenyl functionality the systems gave refractive indices as high as 1.755, although gave modest Abbé numbers in the range of 20-25. Compared to sulfur rich HRIPs there has been considerably less research into structure-property relationship of phosphorous containing HRIPs.

In the literature there are many examples of heteroatom containing intrinsic HRIPs. However, there is limited reported research on phosphorus containing HRIPs, even

though studies have demonstrated they are good HRIP candidates. The aim of the research described in this chapter is to expand the scope of phosphorus rich HRIPs, with direction from Samsung for the application of a lens to be used in mobile phones. It first explores poly(phosphate ester)s and then further investigates polyphosphonates to complement the two published systems from McGrath, containing a biphenol and bisphenol A backbone.[26] It will explore the effects of conjugation length, connectivity and composition within the backbone of the polymer, as well as their thermal properties.

2.2 Phosphate Esters as High Refractive Index Polymers

2.2.1 Synthesis and Characterisation of Polyphosphonates

Poly(phosphate ester)s had never been investigated in the literature as HRIPs, and the starting materials gave a greater scope to investigate than the previously reported polyphosphonates, so a range of them were synthesised *via* the polycondensation shown in Scheme 2.2, similar to the conditions McGrath reported.

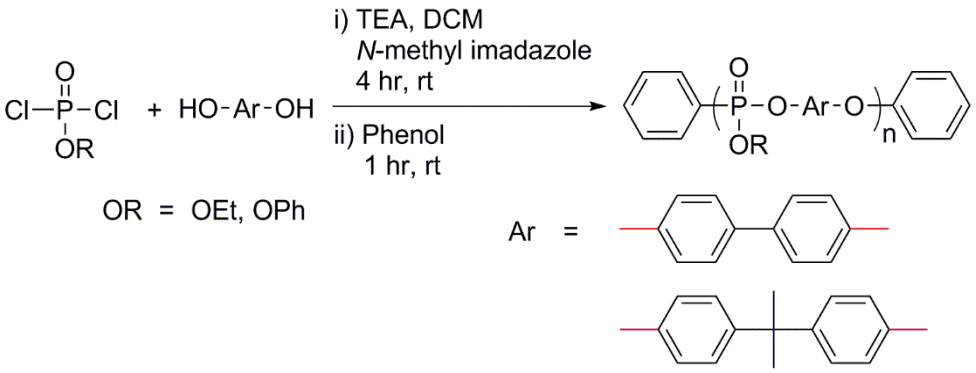

Scheme 2.2: Polycondensation synthesis of poly(phosphate ester)s.

The poly(phosphate ester)s were synthesised by reacting a dichloride phosphate and a biphenol in a 1:1 stoichiometry using triethylamine (TEA) as a base and *N*-methyl imidazole as a catalyst (3% mol loading). Phenol was used as an end capper to prevent the reactive chain ends reacting any further. Table 2.1 shows the polymers synthesised, along with their ^{31}P NMR chemical shift, molecular weight, dispersity (Đ) and melting points.

Table 2.1: ^{31}P NMR, GPC and melting data for poly(phosphate ester)s.

Polymer	Ar	R	^{31}P δ / ppm	M_n / Da[a]	Đ[a]	T_m / °C
P1	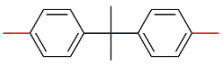	Et	-11.61	46,300	1.31	312
P2	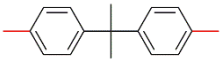	Ph	-17.02	24,800	1.55	362
P2	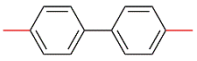	Et	-11.58	22,700	1.60	553

P4	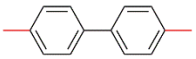	Ph	-17.26	21,200	1.33	332

[a] calculated from GPC data using polystyrene standards

The polymers synthesised were confirmed by ^{1}H and ^{31}P NMR spectroscopy. All the ^{31}P NMR spectra contained one single peak in the expected region for aromatic phosphate esters, and the exact shifts are shown in Table 2.1. The polymers have high molecular weights and reasonable dispersities for condensation polymers, as condensation polymers tend to have broad dispersities. To be useful in an industrial application, the polymers would need to be injection moulded and possibly melted, so their melting points were measured. However, it was noted that high temperatures caused the polymer samples to discolour.

2.2.2 UV-vis Study Before and After Melting Phase

As stated previously the polymers discoloured before melting. Figure 2.4a shows the UV-vis spectrum of the polymers before heating and Figure 2.4b shows the spectrum after the samples experienced a colour change. Before heating, the samples absorb up to 380 nm only absorbing UV light, hence, being colourless. From Figure 2.4 it can be seen that all polymer samples absorb light up to 480 nm, the samples are absorbing blue and violet visible light giving them an orange/red colour. For the application of a lens all samples would need to remain colourless, especially after being injection moulded.

The only sample that did not change colour was a literature polyphosphonate that was made for calibration purposes, attention turned to synthesising polyphosphonates.

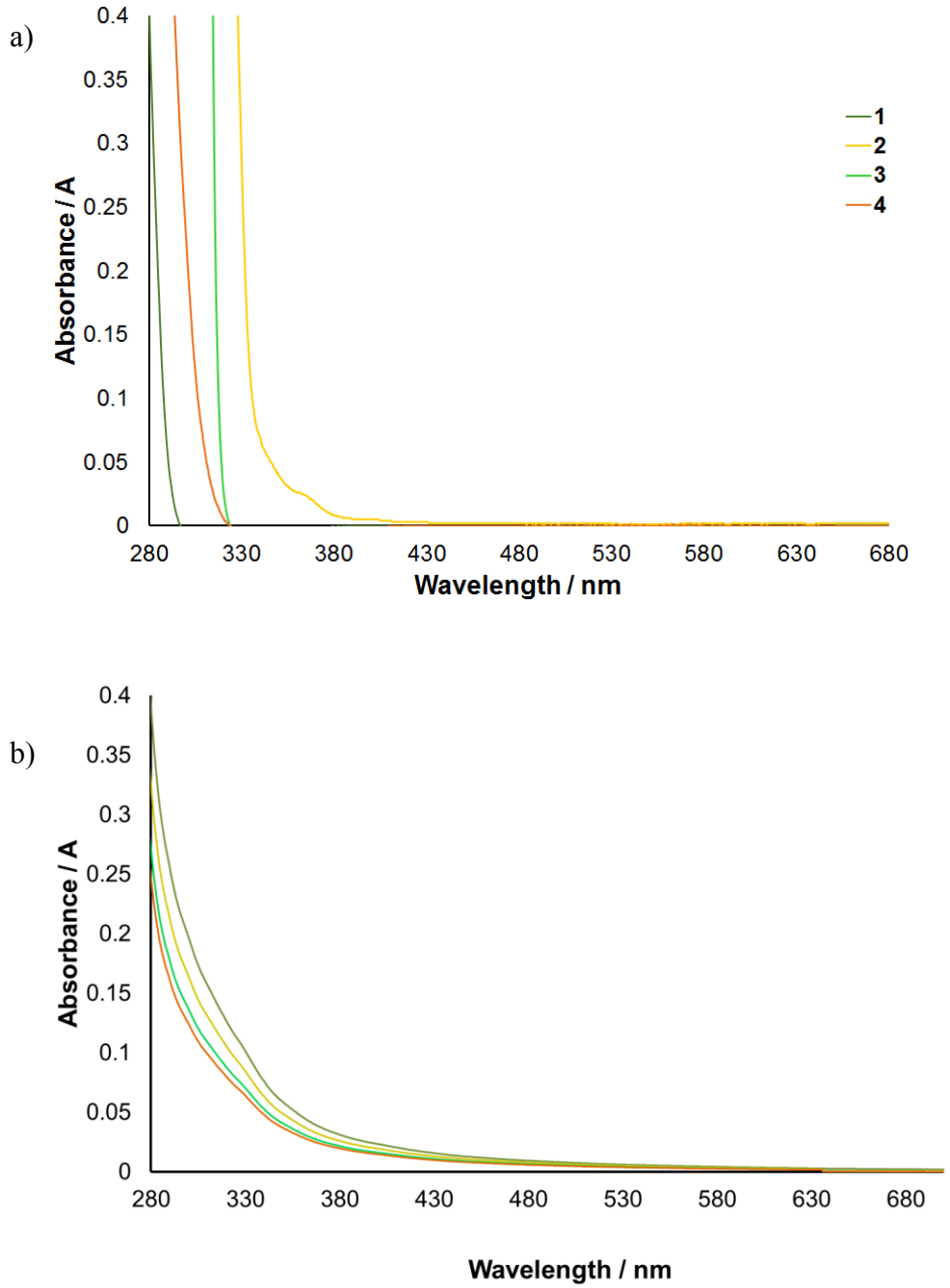

Figure 2.4: UV-vis spectrum a) before and b) after heating.

2.3 Phosphonates as High Refractive Index Polymers

2.3.1 Synthesis and Characterisation of Polyphosphonates

Synthesis of polyphosphonates was carried out under the same conditions as for poly (phosphate ester)s, this work looked at expanding the range of backbones from Mcgrath's work and look at the polymers optical dispersion. This procedure involved stoichiometric amounts of phosphonic dichloride and diols using TEA as a base and *N*-methyl imidazole as an organocatalyst (3% mol loading), again phenol was used to cap the reactive chain ends (Scheme 2.3). For those polymers where the diol was less nucleophilic, such as chlorine containing diols, DMAP was used as a catalyst and reaction times were extended. The range of polyphosphonates synthesised can be seen in Table 2.2, along with their molecular weights and dispersities.

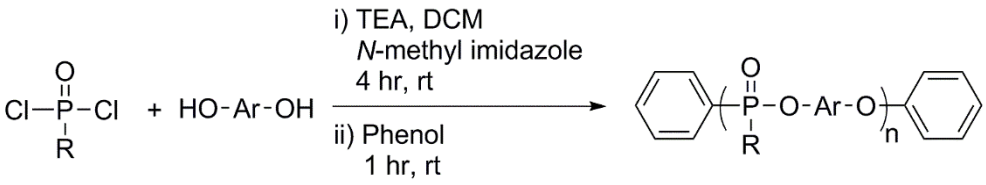

Scheme 2.3: Polycondensation synthesis of polyphosphonates.

Table 2.2: Molecular weight and dispersities of a series of polyphosphonates.

Polymer	Ar	R	M_n / Da[a]	Đ[a]
P5	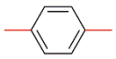	Ph	98,100	1.45
P6	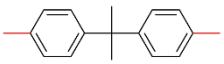	Ph	12,400	1.47
P7	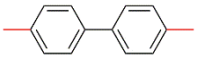	Ph	12,600	1.80
P8	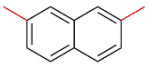	Ph	48,700	1.32
P9	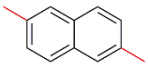	Ph	13,200	1.48
P10	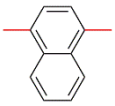	Ph	159,800	1.03
P11	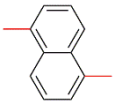	Ph	46,800	1.31
P12	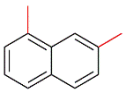	Ph	148,700	1.14
P13	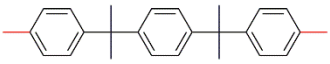	Ph	30,700	1.82
P14	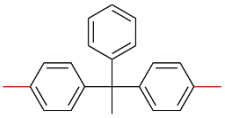	Ph	28,400	1.85
P15	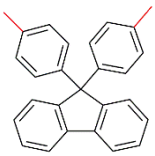	Ph	11,200	1.38
P16	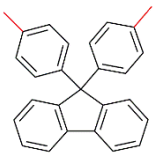	Me	15,100	1.26

17	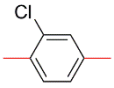	Ph	80,600	1.28
18	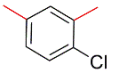	Ph	13,000	1.68
19	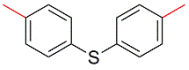	Ph	21,100	1.45

[a] calculated from GPC data using polystyrene standards

The polymers were prepared in good yields and in modest to high molecular weights (11,000 – 160,000) and dispersities as expected for this type of polymerisation. The ^{1}H NMR spectrum for polymer **P19** is shown in Figure 2.5. The assignment of the proton signals were determined by 2D NMR spectroscopy. It is unexpected that H_b is at a higher chemical shift than H_a and H_c. It is possible that the phosphorus atom is electron donating through the π-system so pushes electron density on to the *ortho* and *para* positions. ^{1}H, ^{13}C, ^{31}P NMR and IR spectroscopy confirmed the structure of all polymers.

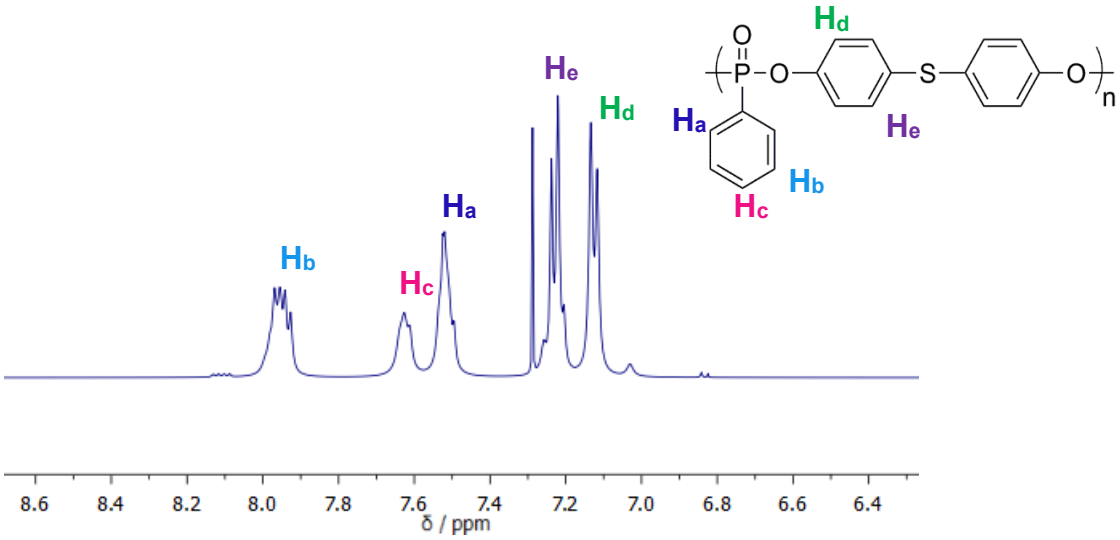

Figure 2.5: ^{1}H NMR spectrum of polymer **P19** (*$CDCl_3$, at 500 MHz).

Figure 2.6 shows the ^{1}H-^{31}P HMBC NMR spectrum of polymer **P19**. The single phosphorus signal at 12.17 ppm strongly couples to protons H_a and H_b and the resonance also couples to the protons in the backbone of the polymer (H_d and H_e), confirming that the synthesis was successful. Figure 2.7 shows two ^{13}C NMR resonances that are part of the polymer backbone, which are split into doublets, due to ^{13}C-^{31}P coupling. The resonances at 149.5 and 121.5 ppm have coupling constants $^{2}J_{CP}$ = 7.4 and $^{3}J_{CP}$ = 4.5 Hz respectively. It is normally expected that $^{3}J_{CP} > {}^{2}J_{CP}$,[30] However, as with ^{1}H-^{1}H coupling ^{13}C-^{31}P coupling is affected by the dihedral angle.[31] It is possible that the three bond fragment P-O-C-C is at an angle resulting in a lower than expected coupling constant. For the phenyl ring directly bonded to the phosphorus centre the magnitude of coupling constants is in agreement with the expected values, where $^{1}J_{CP} > {}^{3}J_{CP} > {}^{2}J_{CP}$.

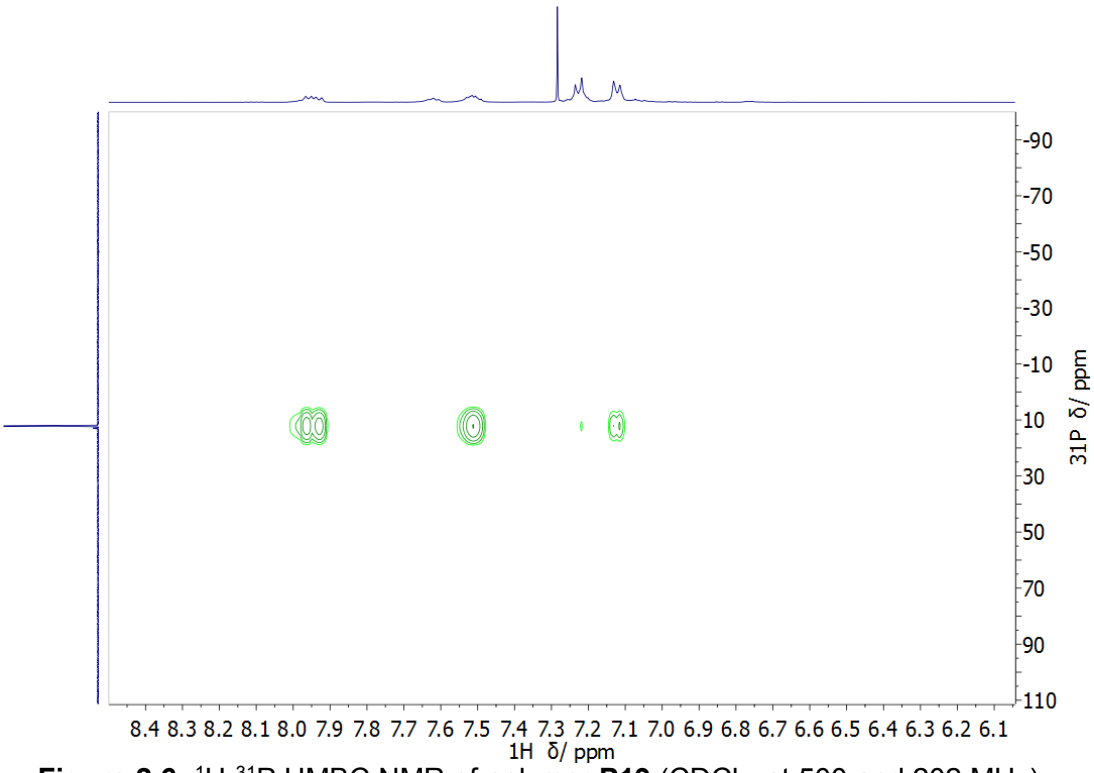

Figure 2.6: ^{1}H-^{31}P HMBC NMR of polymer **P19** ($CDCl_3$, at 500 and 202 MHz).

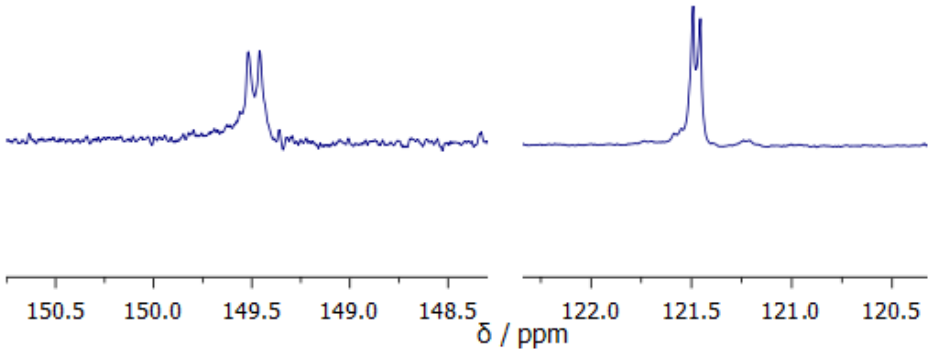

Figure 2.7: ^{13}C NMR resonances at 149.49 and 121.47 ppm, ($CDCl_3$, at 500 MHz).

2.3.2 Thermal Analysis

Thermal stability of these polymers is greatly important for manufacturing and conditions that any resulting device is used under. Investigation into the thermal properties was carried out using thermogravimetric analysis (TGA) and differential scanning calorimetry (DSC), with the results summarised in Table 2.3.

Figure 2.8 shows the TGA traces for the polymers. The polymer samples demonstrated respectable thermal properties, with 5% weight loss being over 350°C for some of the samples. For most of the polyphosphonates 10% weight was above 400°C and residual weight loss at 750°C being above 30%. The polymers showed good to modest glass transition temperatures (T_g). Polymer **P15** showed the highest T_g, probably due to the rigid and sterically encumbered fluorenyl containing backbone. Polymer **P19** has a much lower T_g than polymer **P7**, since thiol linkages are known to increase chain flexibility.

It was then investigated as to how capping agents would affect T_g. A range of polyphosphonates were made using different capping agents, as seen in Table 2.4.

Table 2.3: Thermal properties of polyphosphonates.

Polymer	$T_{5\%}$/°C[a]	$T_{10\%}$/°C[a]	RW_{750}/%[b]	T_g/°C[c]
P5	162	357	41	105
P6	319	412	21	98
P7	363	466	53	140
P8	165	485	51	106
P9	375	483	50	99
P10	328	344	36	124
P11	155	470	29	91
P12	226	401	44	101
P13	119	141	16	112
P14	117	250	22	123
P15	343	403	50	214
P16	461	515	49	208
P17	183	316	36	59
P18	248	316	34	85
P19	426	453	33	81

[a]$T_{5\%}$, $T_{10\%}$: temperatures at 5% and 10% weight loss, respectively; [b]RW_{750}: residual weight ratio at 750°C under nitrogen, [c] DSC data

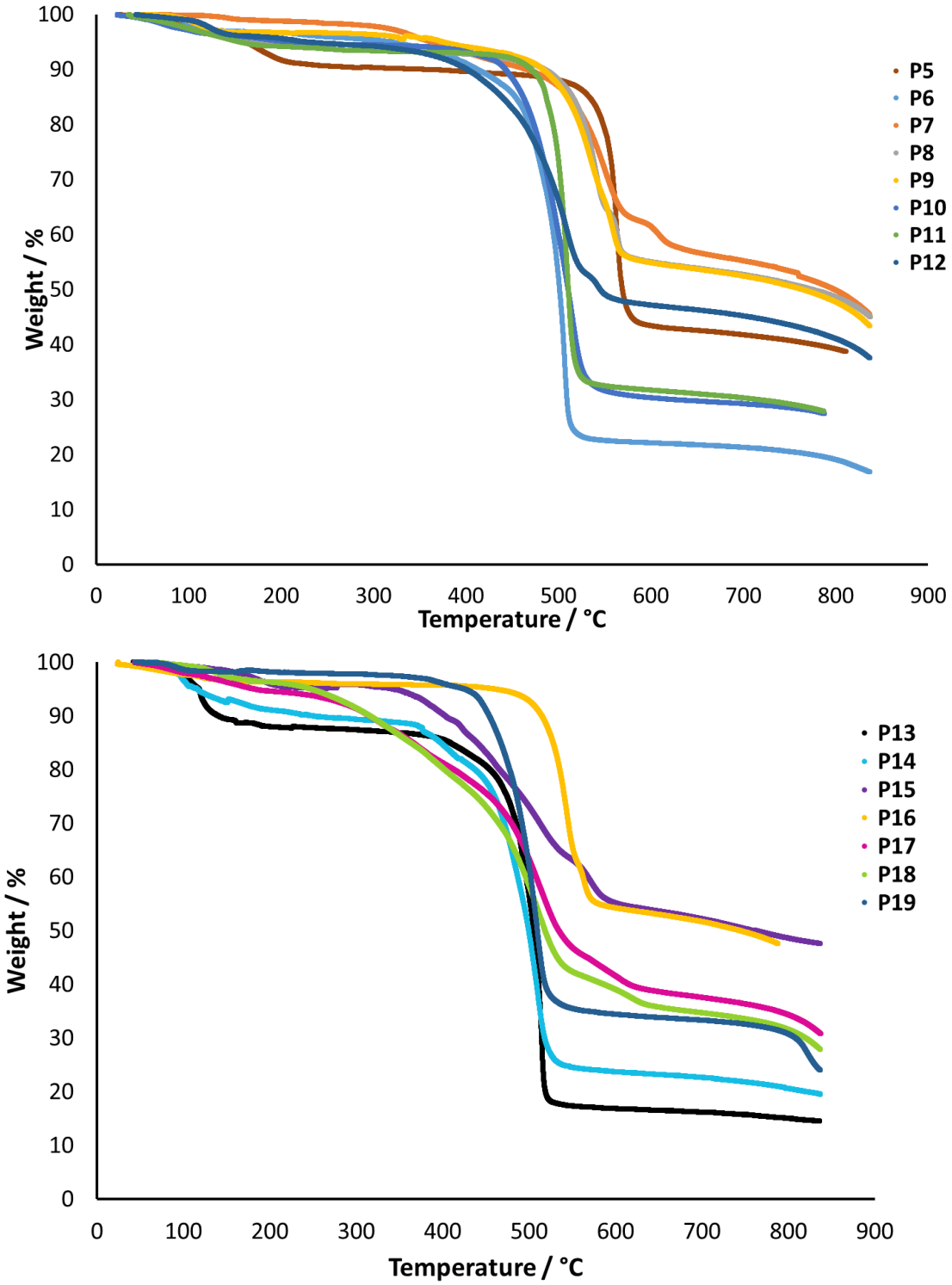

Figure 2.8: TGA curves for polyphosphonates.

Table 2.4: Glass transition temperature using different capping agents.

Polymer	Ar	End capper	Mn / Da[a]	T_g / °C
P7	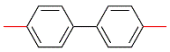		12,600	140
P20	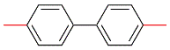	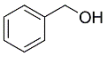	10,400	137
P21	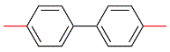	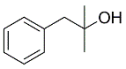	23,400	143
P22	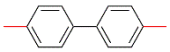	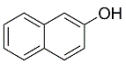	41,400	136
P23	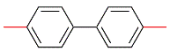	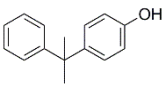	13,800	98
P24	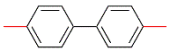	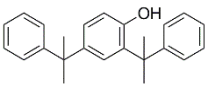	10,700	97
P15	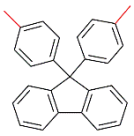		11,200	214
P25	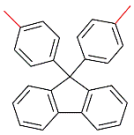	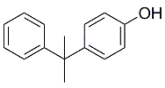	13,300	205

[a] calculated from GPC data using polystyrene standards

T_g did not significantly change between polymers **P7**, **P20**, **P21** and **P22,** although it did drastically reduce in polymer **P23**. This could be due to the added flexibility of the gem dimethyl group. Polymer **P24** shows that adding a second gem dimethyl group did not reduce the T_g any further. The same trend was seen with polymer **P25**, although the T_g was only reduced by 9°C, in this instance.

2.3.3 Optical Data

Optical transparency, high refractive index and low optical dispersion are the three focal optical characteristics needed for HRIPs. The UV-vis spectra of the polyphosphonates is shown in Figure 2.9. UV cut off points, refractive indices and Abbé numbers are shown in Table 2.5.

Table 2.5: Optical data of polyphosphonates.

Polymer	Ar	R	λ_{cutoff}/nm[a]	$\eta_{633\ nm}$[b]	ν_D[c]
P5	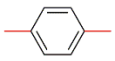	Ph	389	1.60	29.9
P6	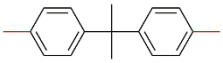	Ph	399	1.60	22.9
P7	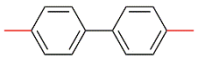	Ph	357	1.64	31.0
P8	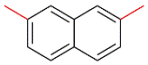	Ph	374	1.61	24.6
P9	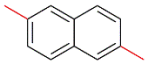	Ph	393	1.64	24.7
P10	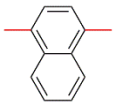	Ph	408	1.64	22.8
P11	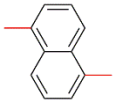	Ph	386	1.64	23.2

P12	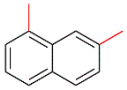	Ph	367	1.63	23.8
P13	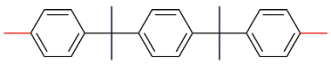	Ph	387	1.60	31.6
P14	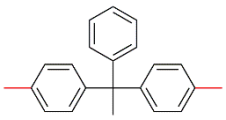	Ph	379	1.61	31.0
P15	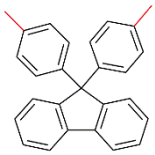	Ph	352	1.66	22.4
P16	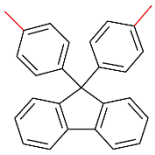	Me	349	1.65	22.8
P17	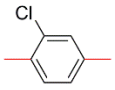	Ph	350	1.61	28.2
P18	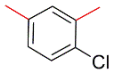	Ph	422	1.62	25.2
P19	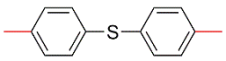	Ph	341	1.65	n/a[d]

[a] λ_{cutoff}: cut off wavelength, [b] measured at 633 nm, [c] calculated using Eq 2.1, [d] could not be calculated due to variation of refractive index at 486.1 nm.

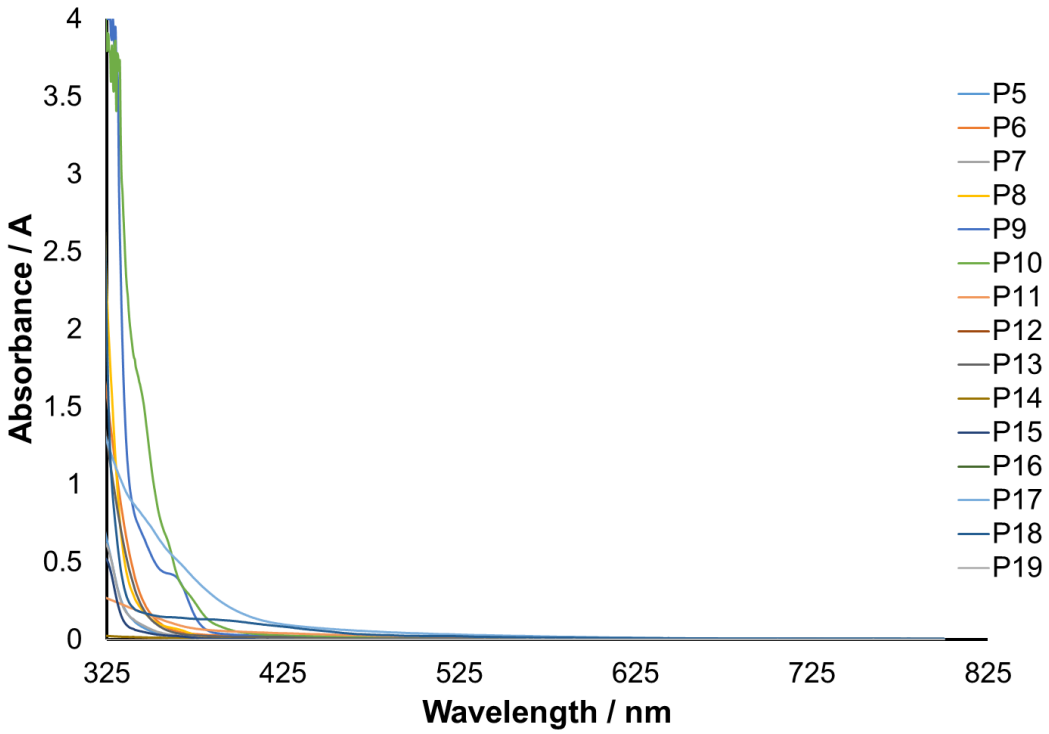

Figure 2.9: UV-vis spectra of the polyphosphonates.

The above spectra show that all polyphosphonates have good UV cut off points. All samples were in the range of 340-422 nm, giving them excellent optical clarity. The polymers synthesised display excellent refractive indices. Polymer **P5** gave the lowest refractive index because it only has one aromatic ring present in the backbone, and addition of a second ring in polymer **P7** increased the refractive index by 0.04. Reported polymers **P6** and **P7** show that conjugated rings have a higher refractive index than non-conjugated, as first shown by McGrath.[26] The transition from polymer **P5** to polymer **P6** shows no increase in refractive index, even though an additional aromatic ring has been added. This addition of the second aromatic ring is counteracted by the inclusion of two hard non-polarisable methyl groups, giving no net increase in refractive index. Polymers **P8-P12** all include fused aromatic rings. Comparing

polymers **P8** and **P9** showed that the 2,6- linkage in polymer **P9** compared to 2,7- in polymer **P8** gave a higher refractive index by 0.03. No difference in refractive index was seen between polymers **P9**, **P10** and **P11**, probably due to the similar angle of linkage. Polymer **P12** gave a slightly lower refractive index; it also has a linkage angle of 60°. Moving to 3 aromatic rings in polymer **P13** does not see an increase in refractive index compared to polymer **P6**, again due to the addition of two non-polarisable methyl groups. Keeping 3 aromatic groups but decreasing non-polarisable methyl groups in polymer **P14** does see an increase in refractive index. Polymer **P15** is the best performing sample with a refractive index of 1.66. The fluorenyl substituent prevents close molecular packing due to the geometry at the central carbon, which lowers the refractive index. Changing the side group from an aromatic phenyl group to a methyl group in polymer **P16** slightly reduces the refractive index, by 0.01. Polymers **P17**, **P18** and **P19** explored the use of heteroatoms. Polymers **P17** and **P18** both contain chlorine and increase the refractive index by 0.01 and 0.02 respectively. The *meta* linkage in polymer **P18** gives a slightly higher value, contradictory to the comparison with polymers **P8** and **P9**. Finally, thiol containing polymer **P19** improved the refractive index by 0.01, compared to analogous polymer **P7**. All polymers gave good Abbé numbers, with all samples over 22 and polymers **P7** and **P17** being above 30.

Abbé numbers were first calculated from refractive indices measured in solution, and then using the polymers in thin film form. The values can be seen in Table 2.6.

Table 2.6: Abbé numbers from solution and film measurements.

Polymer	v_D in solution[a]	v_D from thin films[a]
P5	57.0	29.9
P6	55.5	22.9
P7	54.9	31.0
P8	52.6	24.6
P9	52.2	24.7
P10	52.9	22.8
P11	52.7	23.2
P12	52.6	23.8
P13	54.5	31.6
P14	54.5	31.0
P15	53.4	22.4
P16	53.2	22.8
P17	54.7	28.2
P18	55.3	25.2
P19	52.8	n/a[b]

[a]calculated using Eq 2.1, [b]it was not possible to get reproducible readings for polymer **P19**.

Plots of refractive index as a function wavelength of light were constructed and can be seen in Figure 2.10.

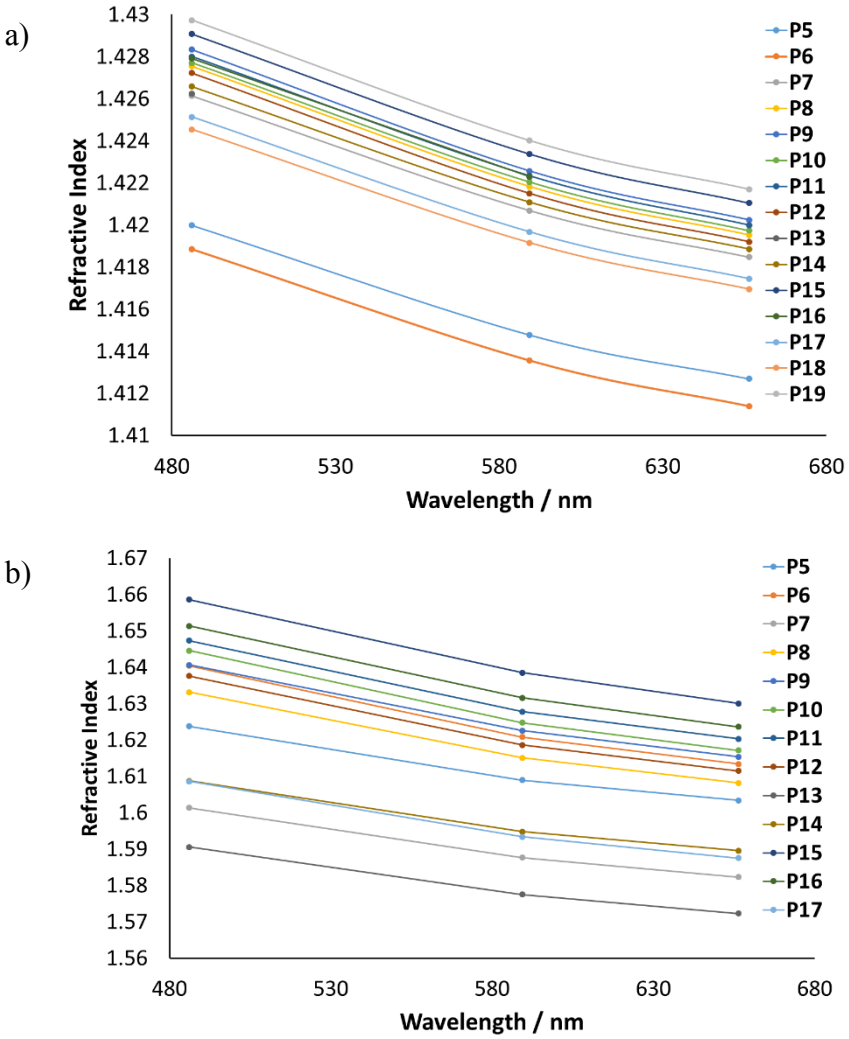

Figure 2.10: Plots of refractive index against wavelength of light for a) measurements in solution and b) in thin film form.

From Table 2.6 and Figure 2.10 it is clear the values differ drastically, and are much higher in solution than in thin film form. For those measurements taken in solutions the refractive index was measured at three different concentrations and extrapolated to obtain the refractive index at 100% polymer and 0% solvent. This is a standard approach to estimating the refractive index of an unknown polymer when it cannot be measured directly. A reason that solution is different to solid state readings is that when a polymer is in solution the absorbance of light in the UV region by the aromatic group

is diminished by the dilution factor of the solution. This would give a lower refractive index in that region of the spectrum, and so would inflate the Abbé number.

2.4 Conclusions

A series of poly(phosphate ester)s were synthesised, however, they discolour upon heating making them unsuitable as HRIPs. A family of polyphosphonates with varying aromatic backbones have been prepared and their thermal and optical properties explored. The T_g of these polymers can be tuned by changing the end capper used in the polymerisation. These polymers gave some of the highest reported refractive indices for polyphosphonates. The highest was polymer **P15** as it contained the most aromatic rings, and no methyl groups. The structure of the back bone also prevents close molecular packing, which can result in a lower refractive index. This study is also the first to report Abbé numbers for polyphosphonates, and they are all consistently high with some exceeding 30. It was also determined that the method used to measure refractive index, and hence Abbé number, can be crucial. In solution refractive index is lower than the actual value in one part of the spectrum, giving a much higher, and therefore incorrect Abbé number. Whilst this method is acceptable to estimate the refractive index for unknown samples it should not be used to calculate Abbé numbers. This study has expanded the scope of phosphorous containing HRIPs, and the findings can be used to design novel HRIPs. It has also shown that polyphosphonates have a low optical dispersity.

This work has been prepared for publication and has been accepted for publication in European Polymer Journal and is in press at time of writing. It has also been patented in Korea and the USA.[32]

2.5 References

(1) Gao, C.; Yang, B.; Shen, J. *J. Appl. Polym. Sci.* **2000**, *75*, 1474-1479.

(2) Matsuda, T.; Funae, Y.; Yoshida, M.; Yamamoto, T.; Takaya, T. *J. Appl. Polym. Sci.* **2000**, *76*, 50-54.

(3) Macdonald, E. K.; Shaver, M. P. *Polym. Int.* **2015**, *64*, 6-14.

(4) Krogman, K. C.; Druffel, T.; Sunkara, M. K. *Nanotechnology* **2005**, *16*, S338-343.

(5) K. Mentak, S. R. High refractive index polymers for ophthalmic applications. US Patent US 7,354,980 B1.

(6) Yen, H.-J.; Liou, G. S. *J. Mater. Chem.* **2010**, *20*, 4080-4084.

(7) Biron, M. *Optical Applications* **2010**, 49-53.

(8) Dislich, H. *Angew. Chem. Int. Ed. Engl.* **1979**, *18*, 49-59.

(9) Novak, B. *Adv. Mater.* **1993**, *5*, 422-433.

(10) Liu, L.; Zheng, Z.; Wang, X. *J. Appl. Polym. Sci.* **2010**, *117*, 1978-1983.

(11) Chang, C.-C.; Chen, W.-C. *J. Polym. Sci., Part A: Polym. Chem.* **2001**, *39*, 3419-3427.

(12) Su, H.-W.; Chen, W.-C. *J. Mater. Chem.* **2008**, *18*, 1139-1145.

(13) Tao, P.; Li, Y.; Rungta, A.; Viswanath, A.; Gao, J.; Benicewicz, B. C.; Siegel, R. W.; Schadler, L. S. *J. Mater. Chem.* **2011**, *21*, 18623-18629.

(14) Liu, J.-g.; Ueda, M. *J. Mater. Chem.* **2009**, *19*, 8907-8919.

(15) Gaudiana, R. A.; Minns, R. A.; Rogers, H. G. High refractive index polymers. US Patent US 5,132,430.

(16) Liu, J.-G.; Nakamura, Y.; Shibasaki, Y.; Ando, S.; Ueda, M. *J. Polym. Sci., Part A: Polym. Chem.* **2007**, *45*, 5606-5617.

(17) Liu, J. G.; Nakamura, Y.; Shibasaki, Y.; Ando, S.; Ueda, M. *Macromolecules* **2007**, *40*, 4614-4620.

(18) Liu, J. G.; Nakamura, Y.; Suzuki, Y.; Shibasaki, Y.; Ando, S.; Ueda, M. *Macromolecules* **2007**, *40*, 7902-7909.

(19) Li, Z.-m.; Zhang, G.; Li, D.-s.; Yang, J. *Chin. J. Polym. Sci.* **2014**, *32*, 292-304.

(20) Bhagat, S. D.; Chatterjee, J.; Chen, B.; Stiegman, A. E. *Macromolecules* **2012**, *45*, 1174-1181.

(21) Stiegman, A. High refractive index polymers. US Patent 2011/0054136 A1.

(22) Mosley, D. W.; Khanarian, G.; Conner, D. M.; Thorsen, D. L.; Zhang, T.; Wills, M. *J. Appl. Polym. Sci.* **2014**, *131*, 39824-39834.

(23) Paquet, C.; Cyr, P. W.; Kumacheva, E.; Manners, I. *Chem. Commun.* **2004**, 234-235.

(24) Hau; Lam, J.; Qin, A.; Tse, K.; Li, M.; Liu, J.; Jim, C.; Gao, P.; Tang, B. *Chem. Comm.* **2007**, 2584-2586.

(25) Hudson, R. F.: *Structure and Mechanism in organo-phosphorus chemistry*; Academic Press: London, 1965.

(26) Shobha, H. K.; Johnson, H.; Sankarapandian, M.; Kim, Y. S.; Rangarajan, P.; Baird, D. G.; McGrath, J. E. *J. Polym. Sci., Part A: Polym. Chem.* **2001**, *39*, 2904-2910.

(27) Shobha, H. K.; Sekharipuram, V.; McGrath, J. E.; Bhatnagar, A. High refractive index thermoplastic polyphosphonates. US Patent 6,288,210 B1.

(28) Olshavsky, M.; Allcock, H. R. *Macromolecules* **1997**, *30*, 4179-4183.

(29) Olshavsky, M. A.; Allcock, H. R. *Macromolecules* **1995**, *28*, 6188-6197.

(30) Quin, L. D.: *A Guide to Organophosphorus Chemistry*; Wiley: New York, 2000.

(31) Kuhl, O.: *Phosphorus-31 NMR Spectroscopy*; Springer: Berlin, 2008.

(32) Jung, H.; Shaver, M. P.; Macdonald, E. K. Polyphosphonate, and lens and camera module including the same. US Patent.

Chapter Three

Ring Opening Polymerisation of Cyclic Phosphonates

3.1 Introduction to Ring Opening Polymerisations of Phosphorus Monomers

The synthesis of phosphorus-containing polymers has been an active area of research for many decades. The range of chemical environments of the phosphorus atom makes the materials versatile, hence they are used in a variety of applications. One of the most common areas is the biomedical field, due to the biodegradability and biocompatibility of the materials. These materials are useful in dental applications,[1-3] where the phosphate chelates calcium ions on the tooth surface. Phosphorus containing polymers are also used in tissue engineering,[4,5] where a polymer matrix is seeded with cells with tissue regenerating from within this matrix. Often interactions between the polymer and the biomaterial are encouraged, and interactions between phosphorous polymers and proteins are extremely useful.[5] One of the main ways phosphorous rich polymers are used is in drug delivery. Polyphosphates are amongst some of the best performing

materials.[4] They display great biodegradability, which can be executed by enzymes in physiological conditions,[6] in a similar manner to ATP hydrolysis. Figure 3.1 shows some polyphosphates used in drug delivery.

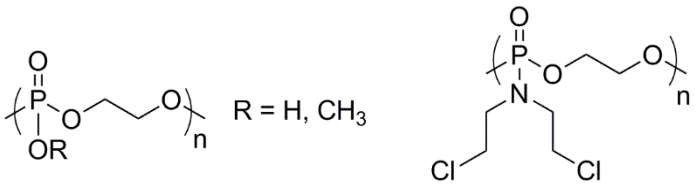

Figure 3.1: Polyphosphates used in drug delivery.

Aside from biomedical applications phosphorus polymers are useful as flame retardants,[7-9] as stated in Section 1.6. The materials that have been researched are phosphates, phosphonates, and phosphine oxides. Phosphorus is known as a char promoter; by promoting the formation of char this restricts the release of fuel so the amount of heat is reduced.[10,11] Also, as the level of char increases, this creates a protective layer which stops heat and oxygen reaching the material, acting like a barrier.[12] It is clear that phosphorus containing polymers are used in a wide variety of applications and the synthesis of new polymers, or modification to existing ones, may enhance their use.

Most phosphorus containing polymers for the mentioned applications can be prepared by polycondensation reactions, as seen in Chapter 2. However, with a polycondensation reaction there is little control over the reaction. By careful selection of monomers and catalysts, ROP can offer control over molecular weight, dispersity and tacticity of the polymers produced, which can alter their properties.

3.1.1 Metal Catalysed Polymerisations

Metal complexes were initially used as catalysts in the ROP of phosphorus containing polymers. Penczek and coworkers were the first to report polymerisation of a cyclic phosphorus monomer ,[13] where a six-membered phosphate underwent ROP with alkyl aluminium compounds. Later, Wang reported a kinetic and mechanistic study showing cyclic phosphates undergoing a coordination insertion mechanism. 6-Membered rings give lower molecular weights due to the decrease in ring strain compared to 5-membered rings.[14] Tin(II) 2-ethylhexanoate ($Sn(Oct)_2$) has also been used to polymerise cyclic phosphates, giving polymers that are biocompatible and biodegradable.[15] Phosphates have also been copolymerised with cyclic esters, some using lanthanides as catalysts.[16] Copolymers have also been synthesised in different topological structures, such as star and hyperbranched (Figure 3.2).[17]

3.1.2 Organocatalysed Polymerisations

Organocatalysts were first employed in the ROP of phosphates by Iwasaki and Yamaguchi.[18] They used 1,8-diazabicycloundec-7-ene (DBU) and triazabicyclodecene (TBD), with TBD acting as a dual activating catalyst and requiring shorter reaction times. Clèment combined DBU and a thiourea (TU) to achieve the same efficancy, with DBU activating the initiator and TU the monomer.[19] Whilst a lot of research effort has gone into phosphates and phosphoramidates, only three examples

of phosphonate ROP have been reported, each by Wurm and coworkers.[20-22] 2-Methyl-1,3,2-dioxaphosphalone-2-oxide was polymerised using DBU, giving polymers with dispersities all under 1.10. The resultant polymer showed no toxicity against HeLa cells and is biodegradable. More recently, a novel series of phosphonate monomers were reported and polymerised using DBU and TBD to give polymers with narrow dispersities, and showed no toxicity against HeLa cells and were water soluble.[21] A range of degradation times were observed, which could make them suitable for a variety of applications.

Control over polymerisation can be achieved by judicious catalyst choice, or choice of monomer. Polyphosphonates are known to undergo transphophonation either intra (green) or intermolecularly (purple) (Figure 3.2a). Polyphosphates contain an OR side group; this additional reactive site can also undergo transesterification (Figure 3.2b). Whilst polyphosphonates can be used for a lot of the same applications as polyphosphates, their structure can lower transesterification.

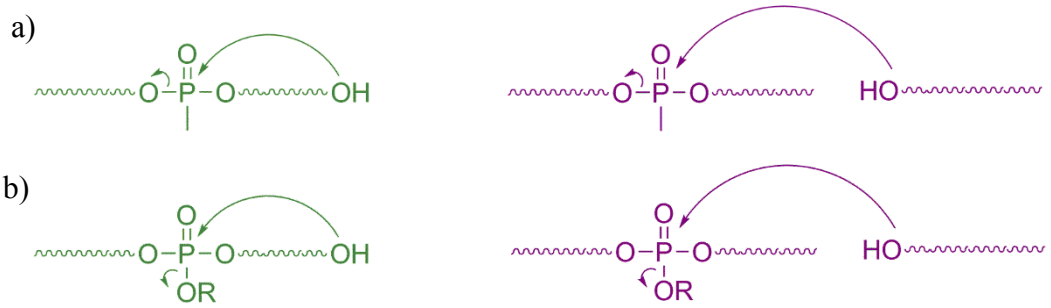

Figure 3.2: Intra and intermolecular transesterification of a) polyphosphonates and b) polyphosphates.

As shown in Chapter 2, nearly all HRIPs are synthesised *via* a polycondensation reaction, so have a wide range of molecular weights. We first wished to investigate

synthesising phosphorous containing HRIPs *via* a ROP mechanism, to produce polymers with controlled molecular weigths. The second aim is to expand the limited scope of phosphonate monomers and catalysts used in ROP. A wider monomer scope is needed to produce polymers with different physical properties, while having a range of available catalysts could possibly expand potential applications.

3.2 Synthesis of Monomers

3.2.1 Aromatic Monomers

Polycondensation synthetic strategies offer little control over molecular weight and dispersity. One way in which to promote control is to use ROP. The resulting polymers should have narrower dispersities. The two monomers shown in Figure 3.3 are potential target monomers for HRIPs synthesised through ROP, allowing incorporation of aromaticity in the backbone and side chain of the polymer, which may increase their respective refractive indices. The first route used to synthesise monomer **1** is shown in Scheme 3.1.

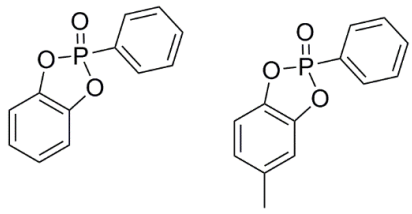

Monomer **1** Monomer **2**

Figure 3.3: Target monomers for HRIPs synthesised through ROP.

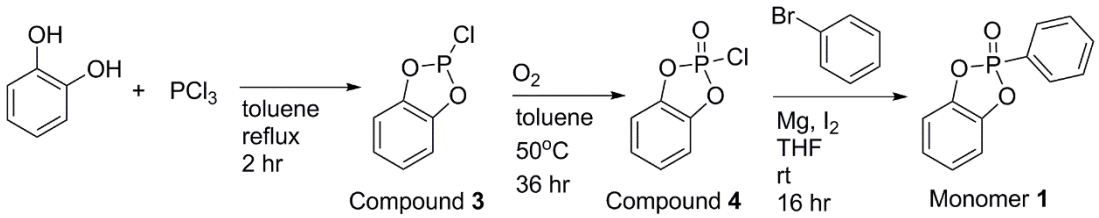

Scheme 3.1: First synthetic route for monomer **1**.

Step 1 of Scheme 3.1 initially gave low conversions. However, when a catalytic amount of water was added to the system and excess PCl_3 added in two aliquots, a 93% isolated yield was obtained. Figure 3.4 shows the ^{1}H and $^{31}P\{^{1}H\}$, NMR spectra of compound **3**, which are in agreement with the literature spectra of this compound.

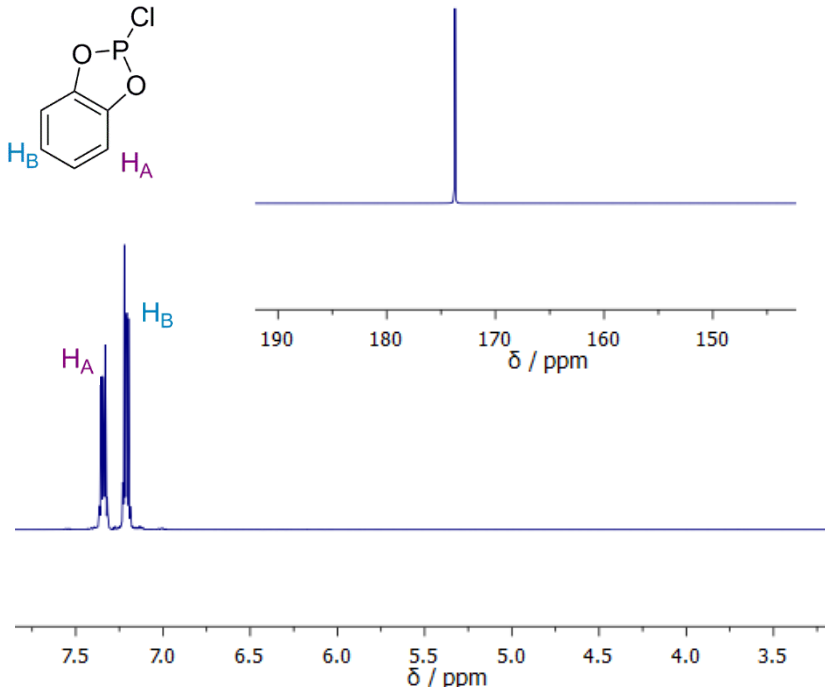

Figure 3.4: a) ^{1}H NMR spectrum ($CDCl_3$, 400 MHz) b) $^{31}P\{^{1}H\}$ NMR spectra ($CDCl_3$, 202 MHz) of compound **3.**

The second step of Scheme 3.1 to give compound **4** gave low conversions and caused problems in purification under a range of reaction conditions, as starting materials and the desired product have similar boiling points. Increasing the reaction time to 5 days

still only resulted in a 46% conversion of compound **4**, as shown by the $^{31}P\{^{1}H\}$ NMR spectrum in Figure 3.5. To minimise loss of material, a more productive route was designed starting from a P(V) species, as shown in Scheme 3.2.

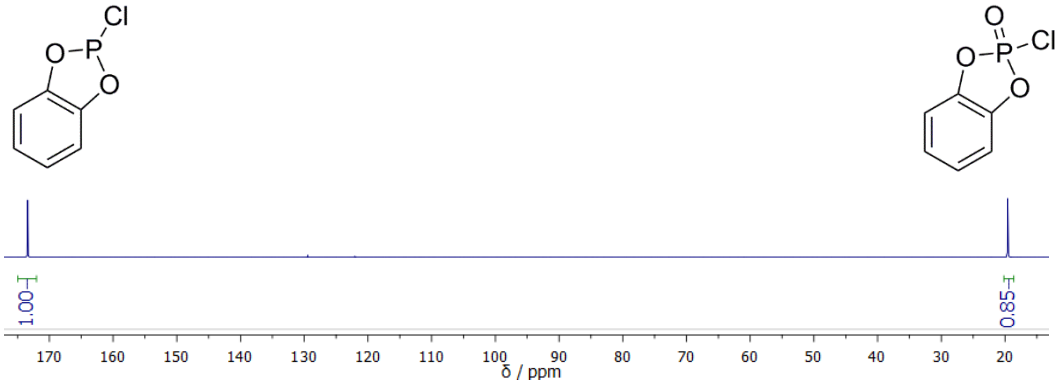

Figure 3.5: $^{31}P\{^{1}H\}$ spectrum of reaction to synthesis compound **4** ($CDCl_3$ at 102 MHz).

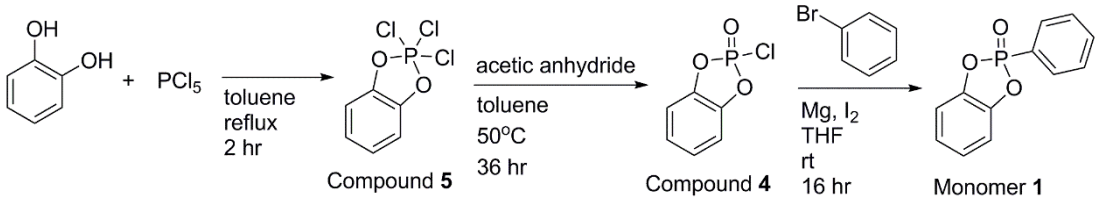

Scheme 3.2: Second synthetic route for monomer **1**.

Step one of Scheme 3.2 to synthesise compound **5** gave the desired product but with a major impurity identified as the di-substituted side product. Slowing the rate of addition of catechol, and decreasing the temperature of addition to -20°C increased conversion from 40 to 97%, as illustrated by the $^{31}P\{^{1}H\}$ NMR spectrum shown in Figure 3.6.

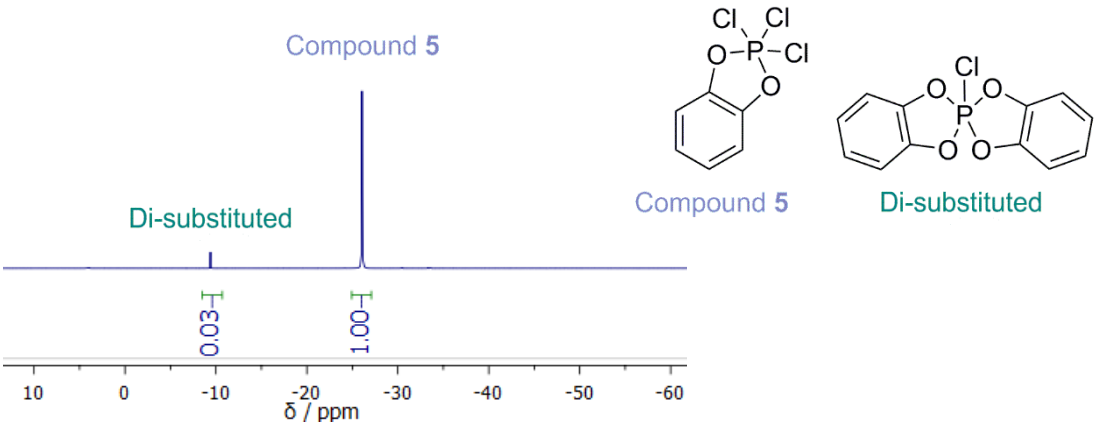

Figure 3.6: $^{31}P\{^{1}H\}$ NMR spectrum of reaction to synthesise compound **5** ($CDCl_3$, 102 MHz).

Step 2 of Scheme 3.2 to synthesise compound **4** resulted in a low conversion and side products with similar boiling points to that of the product. At this time, Wurm published a study[23] demonstrating a method to make cyclic phosphonates for ROP starting from the corresponding diol and phosphonic dichloride. Modifying this method resulted in successful synthesis of monomer **1** (Scheme 3.3).

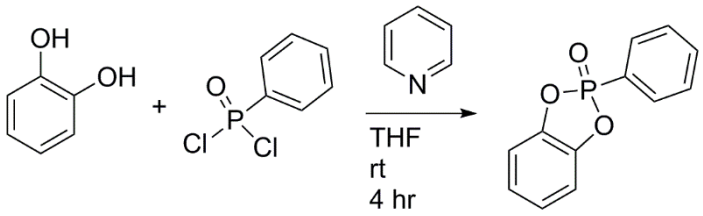

Scheme 3.3: Third synthetic route to monomer **1**.

Through this synthetic route, a high yield of pure monomer **1** was obtained in one step. In Figure 3.7 the ^{1}H and $^{31}P\{^{1}H\}$ NMR spectra of monomer **1** are shown. In the ^{1}H NMR spectrum, the proton environments of the phenyl group appear at a much higher chemical shift relative to the protons from the catechol substituent. A single peak in

the expected chemical shift region in the $^{31}P\{^{1}H\}$ NMR spectrum confirms formation of the monomer**.**

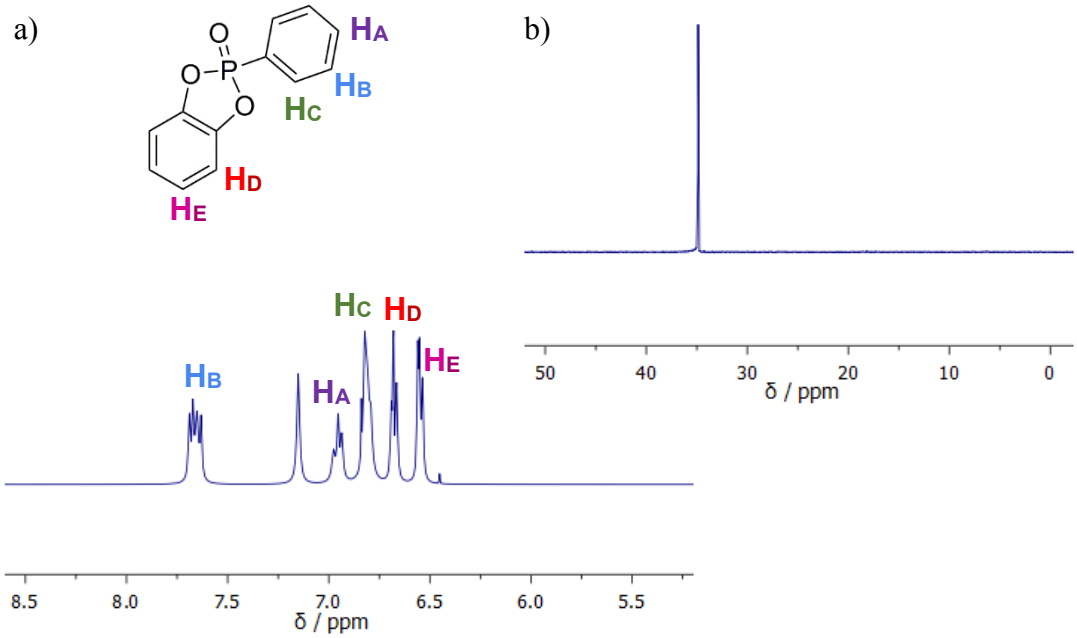

Figure 3.7: a) ^{1}H NMR spectrum (C_6D_6, 500 MHz) and b) $^{31}P\{^{1}H\}$ NMR spectra (C_6D_6, 202 MHz) of monomer **1**.

Monomer **2** was then synthesised using the same conditions (scheme 3.4). The ^{1}H and $^{31}P\{^{1}H\}$ NMR spectra of monomer **2** are shown in Figure 3.8. The ^{1}H NMR spectrum now contains two sets of doublets and a singlet from the presence of the methyl group on the catechol substituent. The $^{31}P\{^{1}H\}$ NMR spectrum also shows one sharp singlet at a similar chemical shift to monomer **1**. These monomers were then screened under ROP conditions, discussed in Section 3.3.1.

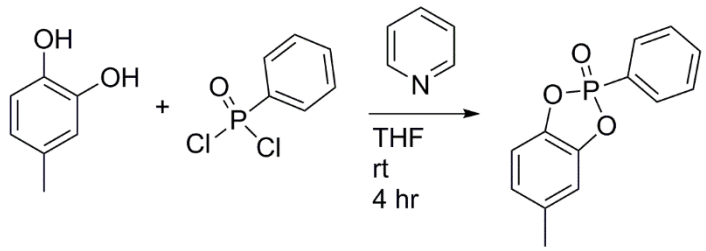

Scheme 3.4: Reaction conditions to synthesise monomer **2**.

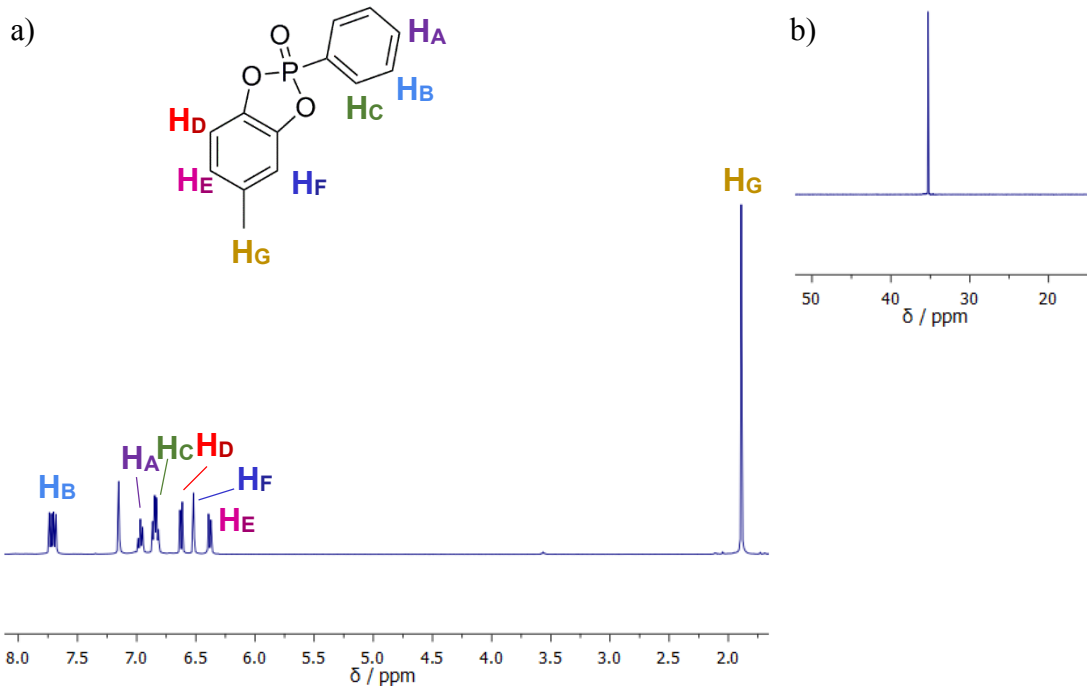

Figure 3.8: a) ^{1}H NMR spectrum (C_6D_6, 500 MHz) and b) $^{31}P\{^{1}H\}$ NMR spectra (C_6D_6, 202 MHz) of monomer **2**.

3.2.2 Novel Aliphatic Monomers

There have been no reports of polyphosphonate tactic microstructures. To solve this attention moved towards synthesising a phosphonate that could produce these types of microstructures. A bicyclic monomer was synthesised using the conditions outlined in Scheme 3.5. The ^{1}H and $^{31}P\{^{1}H\}$ NMR spectra for monomer **6** are shown in Figure 3.9.

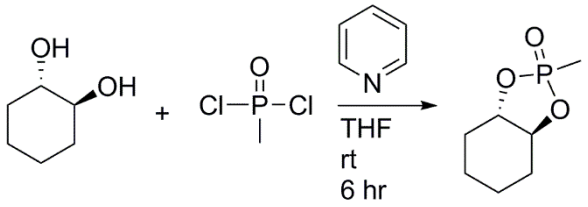

Scheme 3.5: Reaction scheme to synthesise bicyclic monomer **6**.

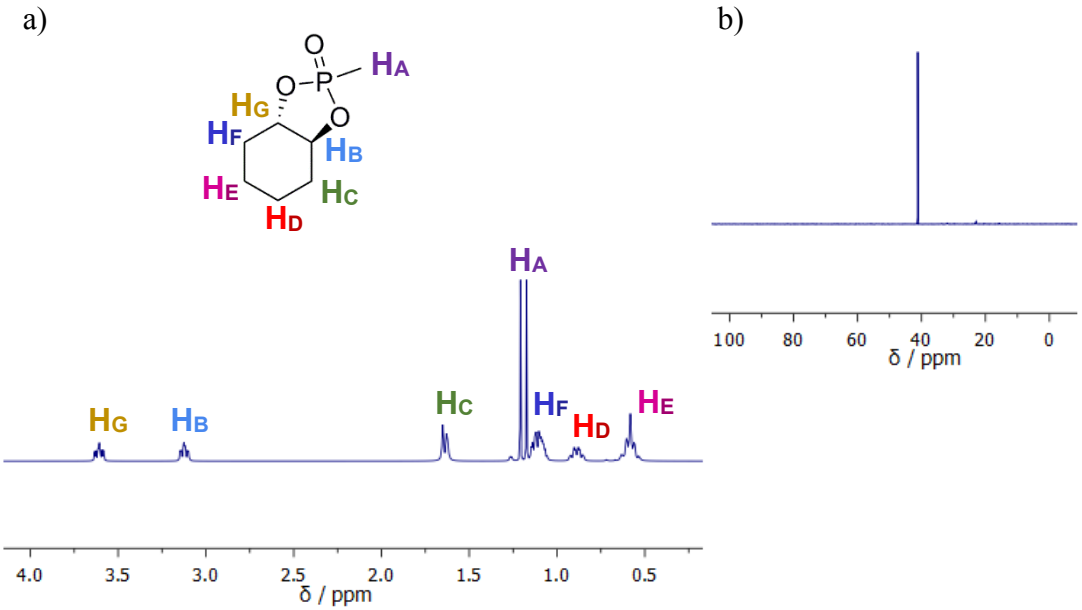

Figure 3.9: a) ^{1}H NMR spectrum (C_6D_6, 500 MHz) and b) $^{31}P\{^{1}H\}$ NMR spectrum (C_6D_6, 202 MHz) of monomer **6**.

The ^{1}H NMR spectrum of monomer **6** has a more complex splitting pattern compared to the aromatic monomers in Section 3.2.1, due to the likely non-planar nature of the cyclohexyl ring. The methyl side group is also split into a doublet due to coupling to phosphorus, with a coupling constant of 17.3 Hz as expected with $^{2}J_{HP}$. The $^{31}P\{^{1}H\}$ NMR shift of monomer **6** is higher than for the previous two monomers.

There are numerous functional cyclic phosphate monomers that can be modified post-polymerisation, such as monomers containing an alkene providing the opportunity to perform click chemistry on the resulting polymer.[24,25] However, there are no cyclic

phosphonates that have this property. Polyphosphonates synthesised *via* ROP all have similar properties, due to similar monomer structure. To address both of these problems, the synthesis of the monomers shown in Figure 3.10 was attempted. Similar reaction conditions were used as those to synthesise monomers **1**, **2** and **6**, were employed (Scheme 3.6).

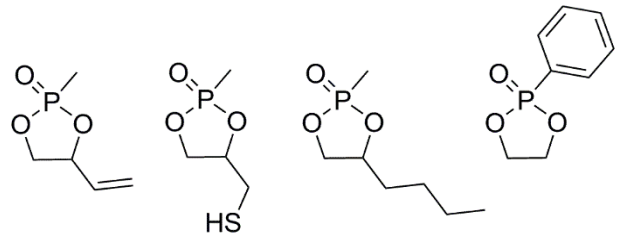

Figure 3.10: Functional phosphonate monomers.

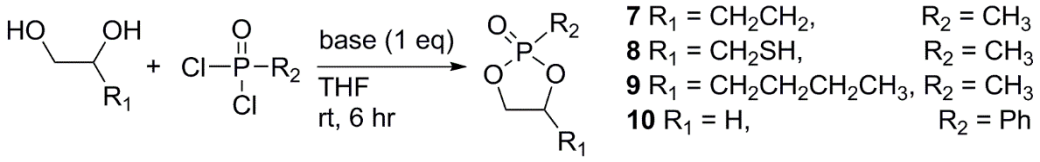

Scheme 3.6: Reaction scheme to synthesise functional phosphonate monomers.

^{1}H and ^{31}P NMR spectroscopy confirmed the presence of monomers **7**, **8**, **9**, and **10** in each of their respective reaction mixtures. However, they were all a mixture of product and starting materials. Originally, pyridine was used as the base which has a pK_a of 5.17. Later, stronger bases were employed such as 4-dimethylaminopyridine (DMAP), DBU and TBD. Nevertheless, none of the bases resulted in the conversion passing 60%. Increasing time and temperature also did not improve the conversion.

Purification of the cyclic monomers was challenging, with all reaction mixtures being colourless oils. First distillation of the crude product was used. However, it was not possible to separate the products from the reactants based on boiling point difference.

Precipitation in a range of solvents either resulted in the reaction mixture oil dissolving or being immiscible, possibly due to the monomers themselves being an oil. Column chromatography on silica decomposed the product, even with the addition of TEA to neutralise the silica. Due to the problems with purification, it was not possible to isolate these compounds and test them as monomers for ROP.

3.3 Polymerisations of Phosphonates

3.3.1 Bicyclic Monomers

Both aromatic monomers were tested under ROP conditions, Scheme 3.7 shows the ROP of monomer **1**. Two of the most commonly used organocatalysts were screened, TBD and DBU (pK_as of 26 and 24 respectively). Three commonly used metal catalysts in phosphate and ester ROP have also been screened in this study. Two are aluminium-based catalysts with salen and salan based ligand frameworks that were prepared by modified literature methods,[26,27] and the other is tin based. The three initiators that were used are benzyl alcohol (BnOH), 2-(benzyloxy)ethanol (BOE) and 3-phenyl-1-propanol (PPA). Table 3.1 shows all the reaction conditions tested with the two

organocatalysts and three metal based catalysts. DCM was used as solvent in the reactions performed at rt and toluene was used as solvent at temperatures above rt.

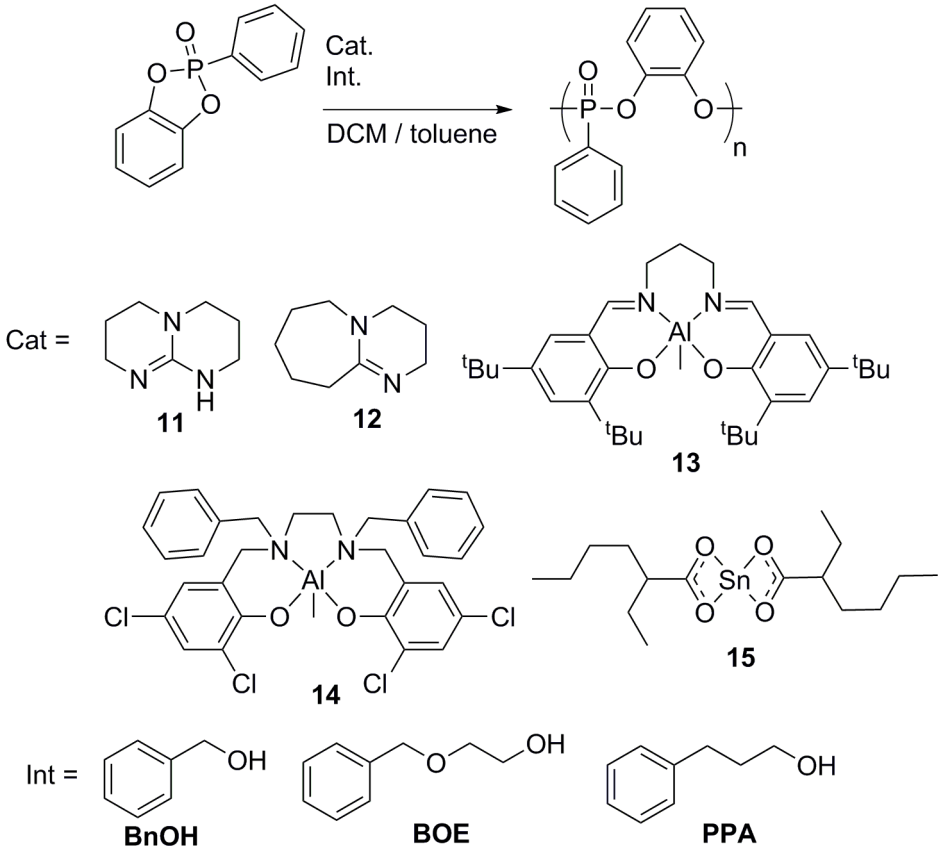

Scheme 3.7: ROP of monomer **1**.

Table 3.1: Reaction conditions for the ROP of monomer **1**.

Entry	Catalyst	Ratio [mon:int:cat]	Time / h	Temp / °C	Conversion / %[a]
1	**12**	100:1:1.5	4	rt	0
2	**11**	100:1:1.5	4	rt	0
3	**11**	100:1:1.5	4	50	0
4	**11**	100:1:1.5	4	100	0
5	**11**	100:1:1.5	24	rt	0
6	**11**	100:3.5:5	24	rt	0

7	**13**	100:1:1.5	4	rt	0
8	**13**	100:1:1.5	4	50	0
9	**13**	100:1:1.5	4	100	0
10	**13**	100:1:1.5	24	rt	0
11	**14**	100:1:1.5	4	rt	0
12	**14**	100:1:1.5	4	50	0
13	**14**	100:1:1.5	4	100	0
14	**14**	100:1:1.5	24	rt	0
15	**15**	100:1:1.5	4	rt	0
16	**15**	100:1:1.5	4	50	0

[a] determined by $^{31}P\{^{1}H\}$ NMR spectroscopy

Entry 1 uses reaction conditions that were reported by Wurm for 2-methyl-1,3,2-dioxaphosphalone-2-oxide,[20] however, no change was observed in the ^{1}H or ^{31}P NMR spectra. It was decided to use TBD (entry 2) as it is a stronger base (pK_a of 26) and has dual activating capability, however, still no conversion occurred. Increasing the temperature to 50 and 100°C (entries 3 and 4) still no change was observed. After 24 hours (entry 5) and increasing the catalyst loading to 20% again only monomer was observed. Entries 7-16 use organometallic catalysts, starting with Al(salen)Me at rt, 50 and 100°C with no reaction being observed. Increasing the reaction time to 24 hr also did not result in a reaction. Al(Salan)Me catalyst was used under the same conditions with a range of temperatures and times, though unfortunately no spectroscopic change was observed. Lastly, $Sn(Oct)_2$ was tested and no reaction occurred at either rt or 50°C.

Monomer **2** was screened using the same conditions outlined in Table 3.1 (Scheme 3.8).

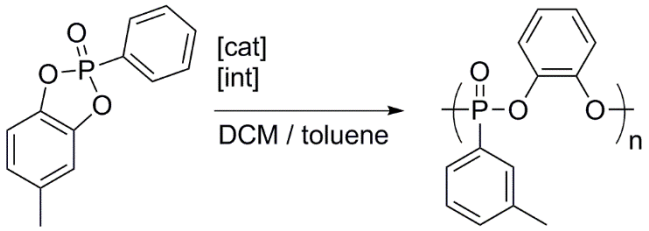

Scheme 3.8: ROP of monomer **2**.

As with monomer **1**, no change in the ^{1}H or $^{31}P\{^{1}H\}$ NMR spectra was observed under any of the conditions tested. None of the initiators promoted polymerisation. These negative results may be explained by the difference in bond strength of the phosphoryl bond between aromatic and aliphatic phosphonates. Table 3.2 shows the stretching frequencies of monomers **1** and **2** along with aliphatic phosphonates that have been successfully polymerised.[22,23] The phosphoryl bond is expected to break and reform when the phosphorus centre undergoes nucleophilic attack from either an initiator or chain end. If this bond is too strong, it may prevent polymerisation from occurring. In the aromatic monomers we see the stretching frequency is much higher than for any of the aliphatic monomers. The extra stability of this bond is likely due to delocalisation with the phosphonic aromatic ring.

Table 3.2: Stretching frequencies of phosphonate monomers.

Monomer	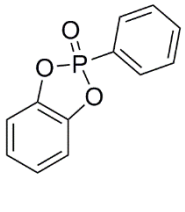	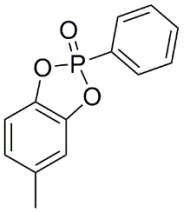	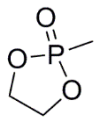	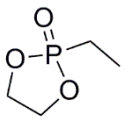	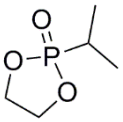
υ(P=O) / cm^{-1}	1298	1289	1255	1265	1244

The bicyclic phosphonate monomer **6** was also screened under the same reactions as monomers **1** and **2** (Scheme 3.9).

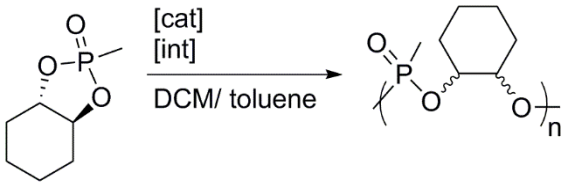

Scheme 3.9: ROP of bicyclic monomer **6**.

As with monomers **1** and **2**, no reaction was observed with monomer **6**. No reaction was detected for all temperatures, reaction times, catalysts, initiators and catalyst loadings tested. However, the P=O stretch of monomer **6** is at a similar frequency to monomers that are known to undergo ROP (Table 3.2), at 1256 cm^{-1}, suggesting that this monomer should be capable of polymerising under these conditions. Wurm and co-workers published findings where a phosphonate monomer containing a cyclohexyl side-group successfully undergoes ROP with good control over distribution and molecular weight.[22] It is possible that the cyclohexyl ring in monomer **6** adopts a structure that relieves strain in the connected five-membered dioxapholane ring. This may result in inadequate ring strain to favour ROP.

3.3.2 Organocatalyst Scope with Aliphatic Monomer 16

The first cyclic phosphonate (monomer **16**) to be opened has only been reported to undergo ROP with DBU.[20] To expand the catalyst scope, a range of nitrogen-containing bases were screened as organocatalysts in this polymerisation (Scheme 3.10).

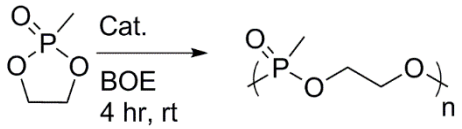

Scheme 3.10: Polymerisation of monomer **16** using a range of catalysts.

Conversion was determined by ^{31}P NMR spectroscopy, with the polymeric phosphorus is shielded compared to the monomeric phosphorous due to relief of ring strain and an associated increase in bond angle. BOE was used as an initiator (scheme 3.7) due to the ease of determining M_n using ^{1}H NMR spectroscopy. Table 3.3 shows the clear relationship between pK_a of the catalyst and conversion of the reaction.

Table 3.3: Polymerisation of monomer **16** catalysed by organocatalysts.

	Catalyst	pK_a[a]	Conversion / %[b]	$M_{n\ th}$[c]	M_n[d]	Đ[e]
11	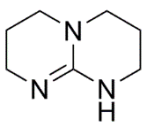	26	91	11,100	10,400	1.04
17	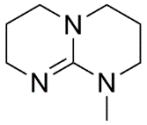	25	66	8,050	7,900	1.06
12	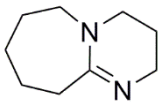	24	56	6,800	6,100	1.02

18	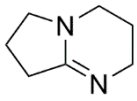	23	47	5,700	4,000	1.07
19	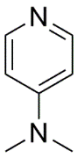	21	33	4,000	4,200	1.28
20	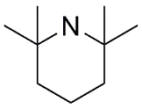	19	13	-	-	-
21	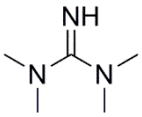	14	3	-	-	-
22	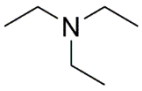	11	0	-	-	-

[a] in MeCN [b] calculated by ^{31}P NMR spectroscopy, [c] molecular weight of repeat unit × conversion, [d] calculated by ^{1}H NMR spectroscopy, [e] determined by GPC

A catalyst with a higher pK_a will have a greater ability to make the chain end nucleophilic. With a more nucleophilic chain end propagation steps are more likely to be successful, resulting in a higher conversion. Catalysts **21** and **22** provided little to no polymerisation due to their low pK_a values. Catalyst **20** only resulted in 13% conversion, indicating that a pK_a of 19 can only produce low molecular weight oligomers, at this low level of conversion accurate molecular weights were not able to be obtained. Catalyst **19** produced a polymer with a broad dispersity, suggesting that the slow initiation and less activated chain end results in a poor level of control over the polymerisation. All other catalysts (**11**, **17**, **12** and **18**) produced polymers with a high level of control with dispersities under 1.10, and ^{1}H NMR calculated molecular weights in good agreement with the theoretical values. Figure 3.11a shows the linear

relationship between pK_a and polymer conversion. TBD, with a pK_a of 26, does not fit this linear relationship. It has a much higher conversion than expected because it is "dual-activating", as it activates the chain end in the same way the basic catalysts do, but it also has an H-bonding donor that can activate the monomer by increasing its electrophilicity (Figure 3.11b).

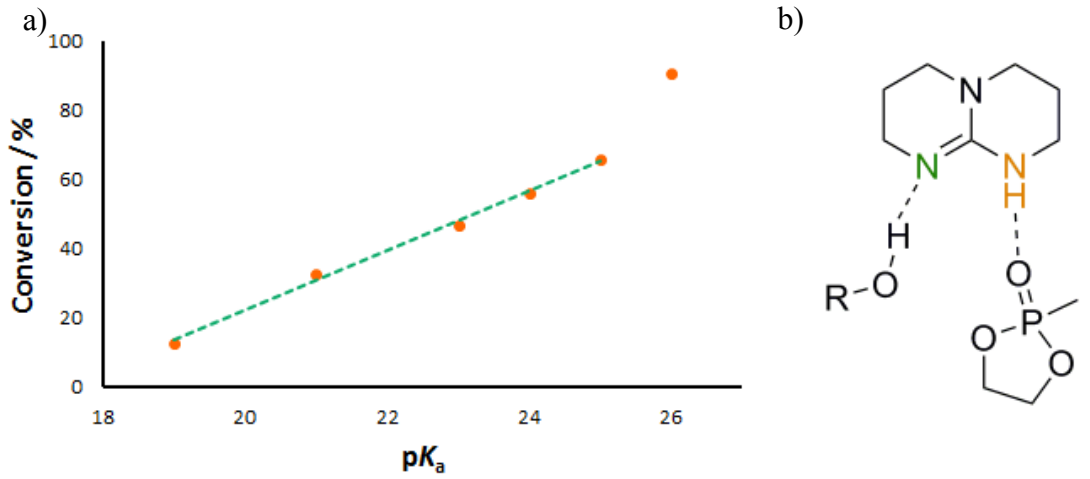

Figure 3.11: a) Conversion vs pK_a b) TBD's basic activation of the chain end (green) and acidic activation of the monomer (orange).

The two amino acids serine (catalyst **23**) and proline (catalyst **24**) were also tested for their catalytic ability, the results are summarised in Table 3.4. The basic substituents have a lower pK_a than 14 so it is unlikely they are basic enough to activate through a chain end mode. This suggests that the amino acids primarily activate through the acid moiety and hence proceeding *via* a cationic ROP.

Table 3.4: Amino acid catalyst screening with aliphatic monomer.

	Catalyst	pK_a acid/amine	Conversion / %[a]
23	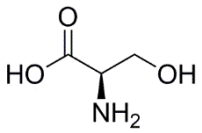	2/9	44
24	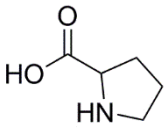	2/11	24

[a] calculated by ^{31}P NMR spectroscopy

3.3.3 Organometallic Catalyst Scope with Aliphatic Monomer 16

To further expand the catalytic scope with phosphonates, three of the commonly used organometallic catalysts outlined in Scheme 3.7 were screened. The results are displayed in Table 3.5.

Table 3.5: Organometallic catalyst screening with aliphatic monomer **16**.

Catalyst	Time / h	Conversion / %[a]	M_{nth} [b]	M_n [c]	Đ[d]
15	4	25	3,000	2,700	1.11
13	4	71	8,600	9,200	1.05
14	4	73	8,900	9,000	1.07

13	6	>99	12,000	11,200	1.06
14	6	>99	12,000	11,100	1.07

[a] calculated by ^{31}P NMR spectroscopy, [b] molecular weight of repeat unit × conversion, [c] calculated by ^{1}H NMR spectroscopy, [d] determined by GPC

From the data above $Sn(Oct)_2$ (catalyst **15**) is a poor catalyst for the ROP of this phosphonate. Aluminium salen and salan are effective under the same conditions, giving high conversions with a high level of control with dispersities of 1.05 and 1.07. Increasing the reaction time to 6 hr gave quantitative conversions and no loss of control was observed. This is the first instance of metal catalysed ROP of phosphonates.

3.3.4 Copolymerisations of Monomer 16 and Cyclic Esters

Copolymerisations were attempted with the aliphatic monomer **16** and lactide and ε-caprolactone. The reaction conditions are outlined in Scheme 3.11 and the results in Table 3.6. It was first attempted as a block copolymerisation, polymerising one monomer and this acting as a macroinitiator in the second polymerisation, as shown in Scheme 3.11a and 3.11b (Table 3.6 entries 1-9). A random copolymerisation was then attempted as shown in Scheme 3.11c (Table 3.6 entry 10).

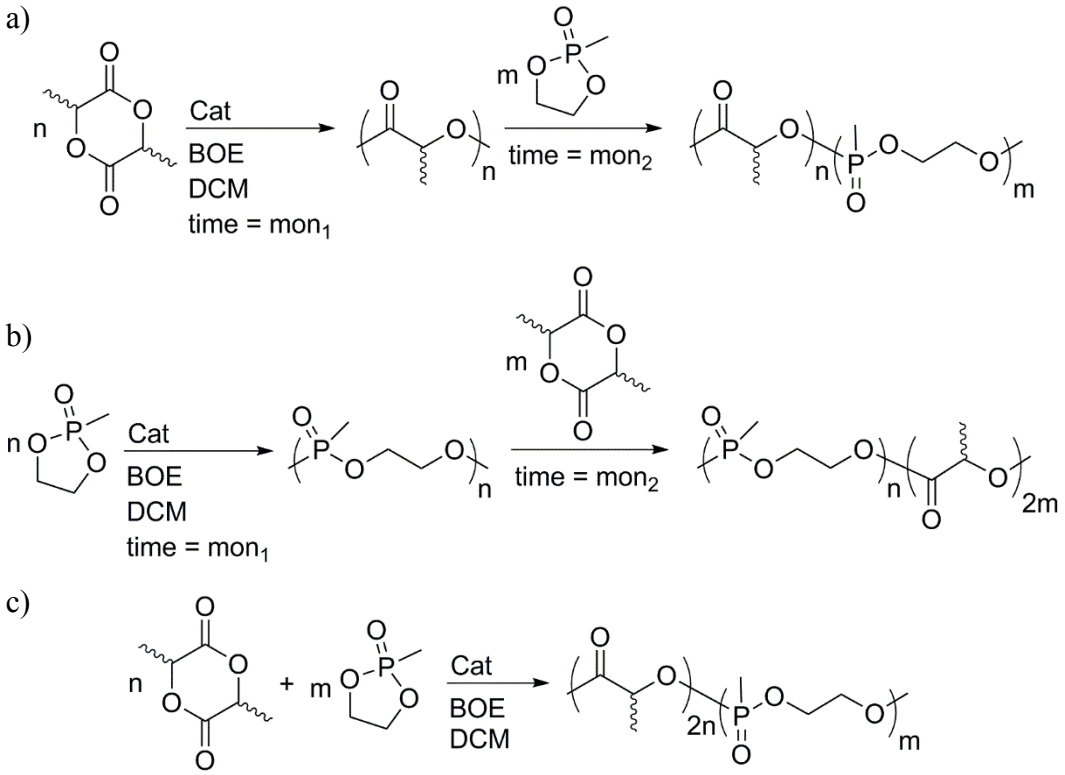

Scheme 3.11: a) Block copolymerisation of lactide and monomer **16**, b) block copolymerisation of monomer **16** and lactide, and c) random copolymerisation of lactide and monomer **16**.

Table 3.6: Copolymerisation data of monomer **8** and lactide.

Entry	1st monomer	2nd monomer	cat.	time (mon_1, mon_2)[a] / h	% PLA	% polyphosphonate
1	lactide	**16**	**13**	6, 6	>99	0
2	lactide	**16**	**13**	6, 12	>99	0
3	lactide	**16**	**14**	6, 6	>99	0
4	lactide	**16**	**14**	6, 12	>99	0
5	lactide	**16**	**11**	6, 6	>99	0
6	lactide	**16**	**11**	6, 12	>99	0

7	**16**	lactide	**13**	4, 6	0[b]	25
8	**16**	lactide	**13**	6, 6	0[b]	28
9	**16**	lactide	**11**	4, 6	0[b]	56
10	**16**	lactide	**11**	6	0	52

[a] mon_1 reaction time of first polymerisation, mon_2 reaction time after second monomer addition, [b] polymerisation of the polyphosphonates was observed before addition of lactide, however there was 0% conversion at the end of the reaction.

When lactide was polymerised first (entries 1-6), quantitative conversion to PLA was observed, then when the phosphonate was added, no conversion of the phosphorous containing monomer occurred. This was the case with Al(salen)Me, Al(salan)Me and TBD, with no conversion being observed after the extended reaction time for the phosphonate of 12 hr (entries 2, 4 and 6). Polymerising the phosphonate first was then tried (entries 7-9), after the phosphonate polymerisation conversion was observed as expected, however, after lactide was added very little polyphosphonate was observed and a low conversion of PLA was observed. It is likely that the conditions of the lactide polymerisation is causing degradation of the polyphosphonate. When both monomers were added at the same time (Scheme 3.11c and entry 10), there was no conversion of the phosphorous monomer and very little PLA was observed. It is possible the phosphonate could still bind to the catalyst blocking the site for lactide to reach higher conversions. Very similar results were produced using ε-caprolactone.

Copolymerisations were attempted using the aliphatic monomer **16** and aromatic monomer **1**. As monomer **16** is capable of undergoing ROP successfully it was hoped that it could encourage the aromatic monomer **1** to polymerise, it was a 1 step copolymerisation as shown in Scheme 3.12.

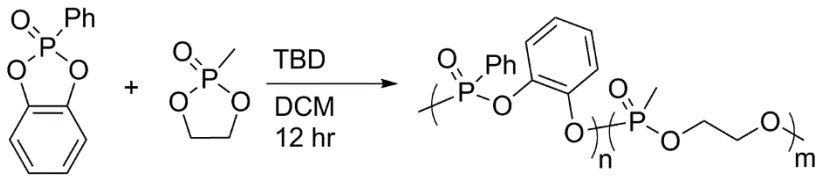

Scheme 3.12: Copolymerisation of monomer **1** and **16**.

No polymerisation was observed of the aromatic monomer **1**, even with reaction times up to 12 hr. There was a decrease in monomer **16** conversion, again indicating monomer **1** could be interacting with the catalyst and blocking monomer **16** from polymerising. This also agrees with the suggestion in Section 3.3.1 that the reason it may not polymerise is due to the higher bond strength of the phosphoryl, shown by its stretching frequency. It is likely monomer **1** interacts with TBD through a hydrogen bonding, but it cannot undergo polymerisation as the P=O does not break, preventing monomer **16** from hydrogen bonding in the same manner to undergo ROP itself.

3.4 Polymerisations of Polyphosphonates Containing a P-C Backbone

As both Shaver and Wurm (Max Planck Institute for Polymer Research) were working on phosphorus containing monomers for ROP, a collaboration was established. A novel monomer (**25**) kindly synthesised by Kristin Bauer in the Wurm group was screened to test its ability to undergo ROP, the general reaction is outlined in Scheme 3.14. The resulting polymer has a P-C bond present in the backbone. A P-C bond is

much more resistant to cleavage compared to P-O bonds. This should give the polymer different degradation properties compared to polyphosphates and polyphosphonates.

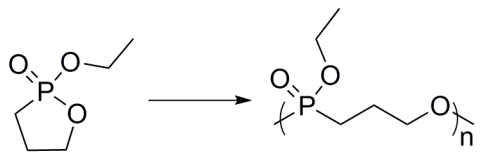

Scheme 3.14: ROP of polymer containing P-C in the backbone.

3.4.1 Optimising Synthetic Procedure

Polymerisations were attempted using the monomer as received and TBD as a catalyst, no change in the NMR of the starting material was observed. Figure 3.12 shows the ^{1}H NMR spectrum of the monomer as received is shown. There is an impurity at 0.92 ppm; after further purification by fractional distillation, this triplet impurity is no longer present (Figure 3.12 a) and b)). After further purification polymerisation was successful using TBD as the catalyst. Table 3.7 shows the reaction conditions screened using BOE as an initiator, TBD as the catalyst and $[mon]_0$:$[int]_0$:$[cat]_0$ of 100:1:1.

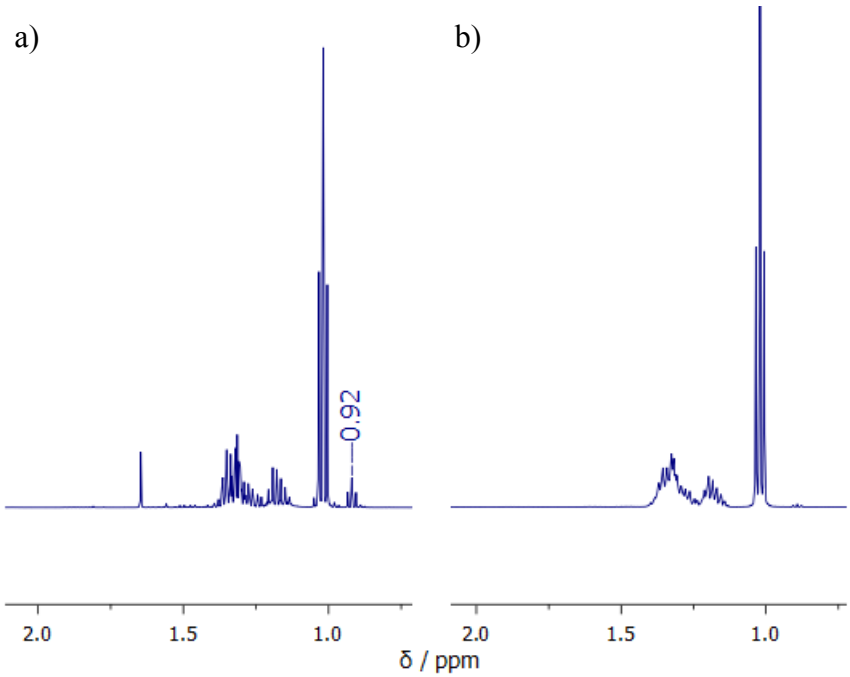

Figure 3.12: ^{1}H NMR spectrum of monomer **25** a) before and b) after further purification (C_6D_6, 500 MHz).

Table 3.7: Screening results of monomer **25** with catalyst **11**.

Entry	Solvent	time / h	temp / °C	Conversion / %[a]
1	DCM	6	0	7
2	DCM	6	rt	51
3	DCM	6	40	52
4	THF	6	rt	23
5	toluene	6	rt	62
6	neat	6	rt	76
7	toluene	1	rt	59

[a] calculated by ^{31}P NMR spectroscopy

When the reaction temperature was kept at 0°C very little conversion was observed. Raising the temperature to rt increased conversion, raising to 40°C did not significantly increase conversion. When THF was used as reaction solvent there was a decrease in conversion, however, when toluene was used there was an increase in conversion. Polymerisations carried out neat gave the highest conversion at 76% (entry 6). The polymerisation could reach similar conversion after 1 hr instead of 6 hr (entry 5 and 7).

3.4.2 Catalyst Scope

Work carried out in Edinburgh and Mainz then looked at expanding the catalyst scope of this reaction. Table 3.8 shows the catalysts tried in Scheme 3.15, with $[mon]_0$:$[int]_0$:$[cat]_0$ of 50:1:1, where the catalysts have been outlined previously and TU is catalyst **26**.

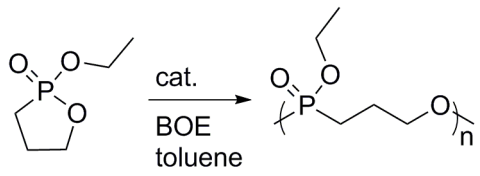

Scheme 3.15: Reaction scheme for catalyst screening.

Table 3.8: Data for catalyst screening.

Entry	Cat.	time / h	temp / °C	Polymerisation[a]
1	**11**	1	rt	Y
2	**12**	18	rt	N

3	**12/26**	18	rt	Y
4	**15**	18	95	Y
5	**14**	18	reflux	Y

[a] calculated by ^{31}P NMR spectroscopy

DBU (entry 2) did not work on its own, but when used with a TU (entry 3) polymerisation did occur. The TU has the ability to activate the monomer, so when used in conjunction with a base, dual-activation can occur. $Sn(Oct)_2$ (entry 4) and Al(salen) (entry 5) both polymerised monomer **26** but required much higher temperatures. It is also noteworthy that TBD was the fastest catalyst by a considerable amount.

3.5 Conclusions

Three novel monomers were synthesised and characterised, however productive ROP was inhibited. The two aromatic monomers **1** and **2** have a much stronger P=O bond, which is expected to break and reform during the polymerisation. The cyclohexyl monomer **6** could take on a structure that reduces ring strain, the main driving force for ROP. Work then focused on expanding catalyst scope for monomer **16**. First a range of organocatalysts were examined, where there is a linear relationship between pK_a of the catalyst and conversion. However, TBD did not fit this trend, as it gave a much higher conversion because it is dual-activating. Monomer **16** was also

successfully opened with Al(Salen) and Al(Salan), which is the first reported metal-catalysed ROP of phosphonate.

This work has been peer reviewed and accepted for publication.[28]

A novel phosphonate monomer was supplied from our collaborators at Max Planck Institute for Polymer Research, where the P-C bond would be present in the backbone. It was successfully polymerised with TBD and DBU/TU, as well metal catalysts, however, a higher temperature was needed.

This work is in preparation for publication.

3.6 References

(1) Mou, L.; Singh, G.; Nicholson, J. W. *Chem. Commun.* **2000**, 345-346.

(2) Fu, B.; Sun, X.; Qian, W.; Shen, Y.; Chen, R.; Hannig, M. *Biomaterials* **2005**, *26*, 5104-5110.

(3) Bayle, M. A.; Grégoire, G.; Sharrock, P. *J. Dent.* **2007**, *35*, 302-308.

(4) Monge, S.; Canniccioni, B.; Graillot, A.; Robin, J.-J. *Biomacromolecules* **2011**, *12*, 1973-1982.

(5) Sethuraman, S.; Nair, L. S.; El-Amin, S.; Nguyen, M.-T.; Singh, A.; Krogman, N.; Greish, Y. E.; Allcock, H. R.; Brown, P. W.; Laurencin, C. T. *Acta Biomaterialia* **2010**, *6*, 1931-1937.

(6) Renier, M. L.; Kohn, D. H. *J. Biomed. Mater. Res.* **1997**, *34*, 95-104.

(7) Wang, Q.; Undrell, J. P.; Gao, Y.; Cai, G.; Buffet, J.-C.; Wilkie, C. A.; O'Hare, D. *Macromolecules* **2013**, *46*, 6145-6150.

(8) Zhang, H.; Farris, R. J.; Westmoreland, P. R. *Macromolecules* **2003**, *36*, 3944-3954.

(9) Lu, S.-Y.; Hamerton, I. *Prog. Polym. Sci.* **2002**, *27*, 1661-1712.

(10) Jahromi, S.; Gabriëlse, W.; Braam, A. *Polymer* **2003**, *44*, 25-37.

(11) Braun, U.; Schartel, B. *J. Fire Sci.* **2005**, *23*, 5-30.

(12) Monge, S.; David, G.: *Phosphorous - Based Polymers: From Synthesis to Application*; The Royal Society of Chemistry: Cambridge, 2014.

(13) Pretula, J.; Kaluzynski, K.; Penczek, S. *Macromolecules* **1986**, *19*, 1797-1799.

(14) Xiao, C.-S.; Wang, Y.-C.; Du, J.-Z.; Chen, X.-S.; Wang, J. *Macromolecules* **2006**, *39*, 6825-6831.

(15) Wang, Y.-C.; Yuan, Y.-Y.; Wang, F.; Wang, J. *J. Polym. Sci., Part A: Polym. Chem.* **2011**, *49*, 487-494.

(16) Zhu, W.; Sun, S.; Xu, N.; Shen, Z. *J. Polym. Sci., Part A: Polym. Chem.* **2011**, *49*, 4987-4992.

(17) Liu, J.; Pang, Y.; Huang, W.; Zhai, X.; Zhu, X.; Zhou, Y.; Yan, D. *Macromolecules* **2010**, *43*, 8416-8423.

(18) Iwasaki, Y.; Yamaguchi, E. *Macromolecules* **2010**, *43*, 2664-2666.

(19) Clément, B.; Grignard, B.; Koole, L.; Jérôme, C.; Lecomte, P. *Macromolecules* **2012**, *45*, 4476-4486.

(20) Steinbach, T.; Ritz, S.; Wurm, F. R. *ACS Macro Letters* **2014**, *3*, 244-248.

(21) Wolf, T.; Steinbach, T.; Wurm, F. R. *Macromolecules* **2015**, *48*, 3853-3863.

(22) Wolf, T.; Na; Wurm, F. R. *Polym. Chem.* **2016**, *7*, 2934-2937.

(23) Steinbach, T.; Ritz, S.; Wurm, F. R. *Macro Letters* **2014**, *3*, 244-248.

(24) Yao, X.; Du, H.; Xu, N.; Sun, S.; Zhu, W.; Shen, Z. *J. Appl. Polym. Sci.* **2015**, *132*, 42647-42653.

(25) Zhang, S.; Li, A.; Zou, J.; Lin, L. Y.; Wooley, K. L. *ACS Macro Letters* **2012**, *1*, 328-333.

(26) Atwood, D. A.; Hill, M. S.; Jegier, J. A.; Rutherford, D. *Organometallics* **1997**, *16*, 2659-2664.

(27) Hormnirun, P.; Marshall, E. L.; Gibson, V. C.; White, A. J. P.; Williams, D. J. *J. Am. Chem. Soc.* **2004**, *126*, 2688-2689.

(28) Macdonald, E. K.; Shaver, M. P. *Green Materials* **2016**, *4*, 81-88.

Chapter Four

Phosphoric Acids as Organocatalysts for Ring Opening Polymerisations

4.1 Introduction to Phosphoric Acids as Catalysts

Synthetic plastics have become widely used throughout the modern world. However, the chemical and biological resistance of these materials is a growing concern for the environment, as well as areas such as surgery, pharmacology and agriculture. Biodegradable polyesters have emerged as a possible solution. Poly(lactic acid) (PLA) is one of the most commonly used synthetic biodegradable polymers and can be derived from renewable resources such as corn starch.[1] Poly(hydroxy butyrate) (PHB) is another commonly used biodegradable polymer, and biocompatible making it suitable for use in the biomedical field. PHB can be produced by bacteria, though, the polymer produced under fermentation conditions presents processing problems.[2] The majority of catalysts that have been explored for ROP contain metals, which are often toxic and expensive. Metal-free organocatalysts can produce materials which are highly desirable in biomedical and electronic applications, and thus are becoming increasingly popular.[3,4]

4.1.1 Phosphoric Acids as Catalysts

Many chemical transformations proceed *via* carbonyl activation. Acids simply do this by increasing the electrophilicity at the carbonyl carbon. A wide range of Lewis and Brønsted acids have been explored in this field. As the popularity of organocatalysis has grown over the last twenty years, the design of acid catalysts has become progressively elegant, producing high performing and selective organocatalysts. Figure 4.1 shows the number of publications per year containing the phrases organocatalyst or phosphoric acid as catalysts.

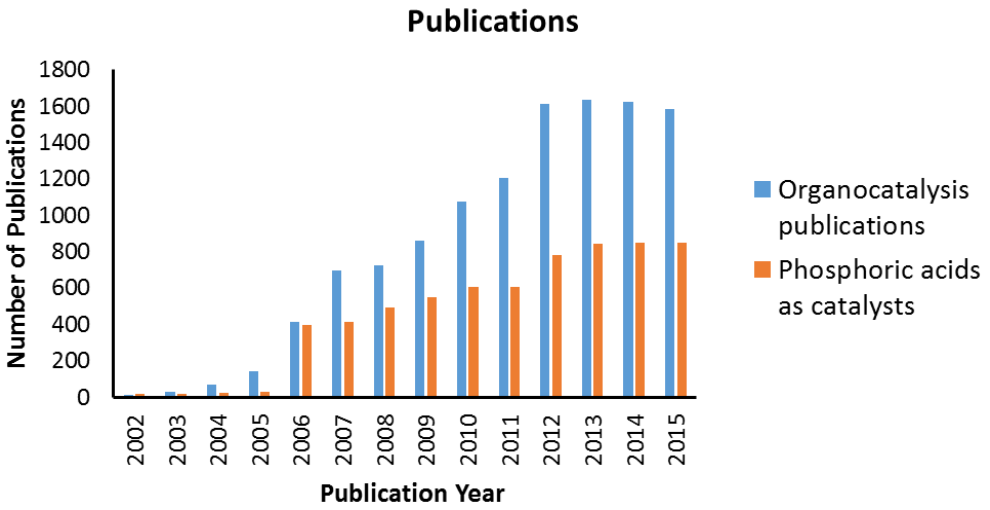

Figure 4.1: Graph showing publications per year containing key terms, data collected using scifinder.

Phosphoric acids have two features that make them excellent catalysts. As well as an acidic proton, these catalysts contain a phosphoryl oxygen, which can act as a hydrogen bond acceptor. The proximity of these two substituents allows for bifunctional catalysis, in a similar manner to how TBD acted in Chapter 3. The aryl

rings allow for varied substitution to fine tune the catalyst in terms of steric and electronic characteristics (Figure 4.2a). Akiyama and Terada independently developed phosphoric acid catalysts that contain an axially chiral binaphthol framework, and were successful in enantioselective Mannich type reactions.[5,6] A selection of the reported catalysts are shown in Figure 4.2b.

Many other organic reactions have been catalysed with phosphoric acids including the Baeyer-Villiger reaction, amination,[7,8] Nazarov cyclisation,[9] and Friedel-Crafts alkylation.[10]

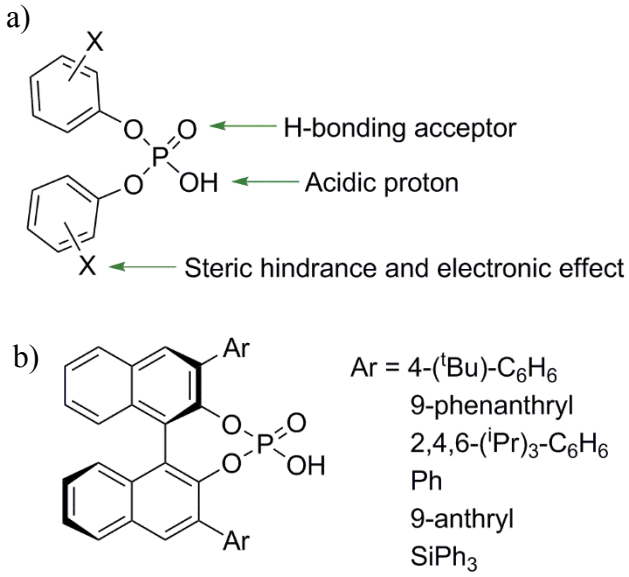

Figure 4.2: a) Structural features of phosphoric acid catalysts and b) chiral catalysts developed by Akiyama and Terada.

4.1.2 Phosphoric Acid Catalysts in Ring Opening Polymerisations

In the last few years, Brønsted acid-catalysed ROP has gathered interest.[11,12] Bourissou was one of the first groups to explore phosphoric acids.[13] They showed that phosphoric acids and phosphoramidic acids can polymerise ε-caprolactone in a controlled manner with dispersities as low as 1.06 and with molecular weights as high as 15,000 $gmol^{-1}$. Density functional theory (DFT) calculations suggest a transition state that contains the catalyst activating both the monomer and the initiator, by hydrogen bonding. In the same year Kakuchi also demonstrated that diphenyl phosphate was an excellent catalyst for the ROP of ε-caprolactone and δ-valerolactone.[14] With the use of NMR spectroscopy and MALDI-TOF-MS, they found the initiator residue at the chain end, indicating a monomer activated mechanism. Kinetic studies proved a living and controlled nature of the system up to 24 hours. In a later paper by Kakuchi, diphenyl phosphate was shown to polymerise carbonates effectively.[15] Chakraborty claimed to have synthesised a range of phosphates, with activity increasing with electron withdrawing power.[16] Kakuchi and Terada synthesised chiral binaphthol-derived phosphoric acids.[17] These catalysts showed a high level of enantiomeric-selectivity when polymerising *rac*-lactide, shown in Scheme 4.1. Their highly acidic catalyst led to the highest reported value for enantiomer-selective ROP of *rac*-lactide. Kakuchi later explored phosphates as catalysts for the ROP of β-butyrolactone (β-BL).[18] They found that a nitro-substituted phosphate was effective at loadings of 100:1, and still active after 40 hours. However, the unsubstituted diphenyl phosphate was much less effective, which they suggested was due to the lower acidity of the catalyst.

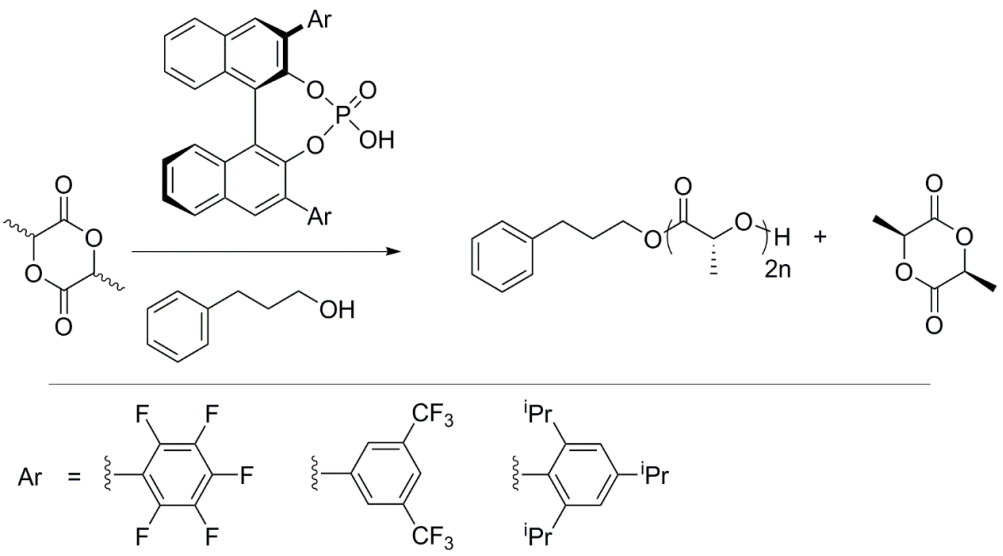

Scheme 4.1: Enantiomer-selective polymerisation of *rac*-lactide catalysed by chiral phosphoric acids.

It is clear that this family of catalysts are useful as ROP catalysts for a range of cyclic monomers, nevertheless, there is still little understood about how they work. There is a lack of success using β-BL compared to cyclic esters with less ring strain. This chapter explores these catalysts with respect to their mechanism and behaviour in the ROP of β-BL compared to ε-caprolactone and *rac*-lactide. Through investigation of reaction kinetics and *in situ* NMR studies a potential deactivation pathway was discovered with β-BL. By alteration of catalyst design, it is possible to prevent formation of the off-cycle deactivated species.

4.2 Synthesis of Substituted Phosphoric Acids

4.2.1 Synthetic Conditions

Chakraborty's 2013 paper outlines a synthesis of substituted phosphoric acids and their use as catalysts in the ROP of cyclic esters,[16] as shown in Scheme 4.2.

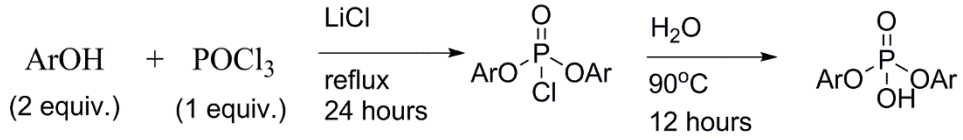

Scheme 4.2: Chakraborty's synthesis of substituted phosphoric acids.

As reported in the aforementioned paper, compounds synthesised using this route have ^{31}P NMR resonances in the range of -15 to -23 ppm. Using the conditions outlined, the synthesis of the unsubstituted product (catalyst **29**, Figure 4.3) was attempted.

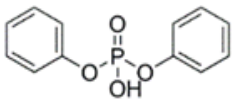

Figure 4.3: Structure of catalyst **29**.

The $^{31}P\{^{1}H\}$ NMR spectrum of the isolated product is provided in Figure 4.3a. This compound was inactive in ε-caprolactone, lactide and β-BL ROP. Commercially obtained diphenyl phosphate was then tested, with the $^{31}P\{^{1}H\}$ peak falling outside the range of any of the compounds reported by Chakraborty. We thus suspected that Charkroborty had not synthesised the desired catalysts. The $^{31}P\{^{1}H\}$ NMR resonance of commercially sourced triphenyl phosphate was at a comparable chemical shift to the product isolated with Charkroborty conditions. The $^{31}P\{^{1}H\}$ NMR spectra of

diphenyl and triphenyl phosphate are shown in Figure 4.3b. Thus it appears that the conditions outlined by Chakraborty favour the tri-substituted products. Changing the reaction stoichiometry to that shown in Scheme 4.3 resulted in the crude mixture shown in Figure 4.4

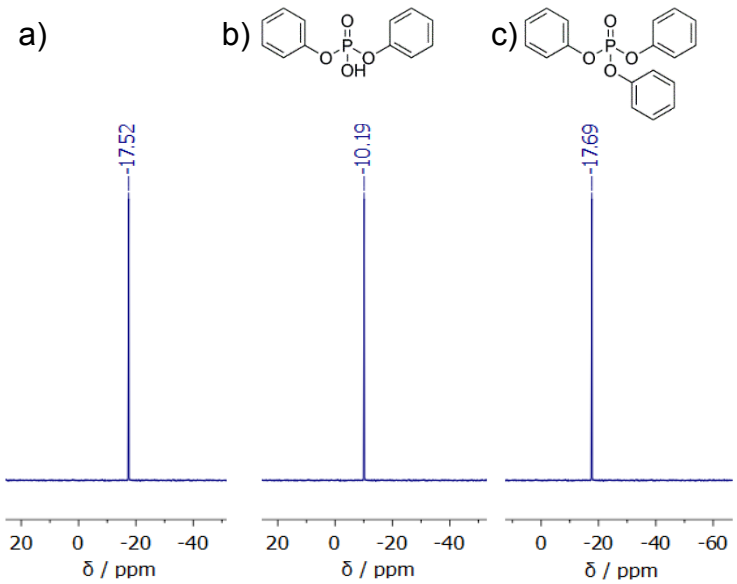

Figure 4.4: $^{31}P\{^{1}H\}$ NMR spectrum of a) catalyst **29** using Chakraborty's conditions and b) $^{31}P\{^{1}H\}$ diphenyl phosphate and c) triphenyl phosphate($CDCl_3$, 202 MHz).

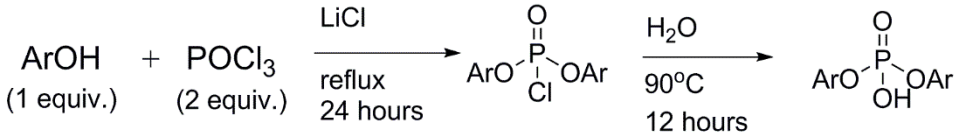

Scheme 4.3: New conditions for the synthesis of phosphoric acids.

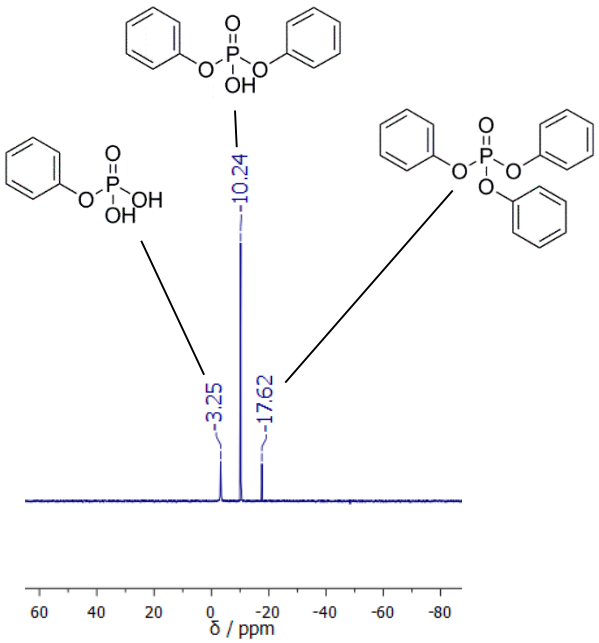

Figure 4.5: $^{31}P\{^{1}H\}$ NMR spectrum of crude mixture, in $CDCl_3$ at 202 MHz.

Using this new synthetic protocol, a range of substituted phosphoric acids were synthesised, bearing a variety of functional groups. Spectroscopic details are outlined in Table 4.1.

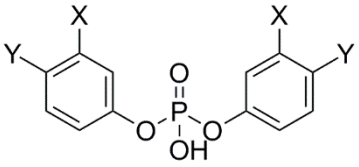

Table 4.1: Spectroscopic measurements of synthesised catalysts.

Catalyst	X	Y	$^{31}P\{^{1}H\}$ δ/ ppm[a]	ν(P=O) / cm^{-1} [b]	m/z [c]
27	H	OMe	-8.63	1215.9	309.05 $[M-H]^-$
28	H	^{t}Bu	-9.04	1210.5	361.16 $[M-H]^-$
29	H	H	-10.24	1219.9	251.05 $[MH]^+$
30	H	Cl	-10.30	1237.4	316.97 $[M-H]^-$ 318.97 $[MH]^+$

31	Cl	H	-11.16	1259.9	316.95 $[M-H]^-$
32	CF_3	H	-11.20	1234.5	387.02 $[MH]^+$
33	H	CF_3	-10.52	1235.8	385.00 $[M-H]^-$
34	CN	H	-11.66	1226.0	299.02 $[M-H]^-$
35	H	CN	-11.48	1248.6	299.02 $[M-H]^-$
					301.04 $[MH]^+$

[a] $^{31}P\{^1H\}$ spectra recorded in $CDCl_3$ at 202 MHz, [b] collected by IR spectroscopy, [c] collected by electrospray using positive and negative ion polarity.

Unexpectedly the $^{31}P\{^1H\}$ chemical shift decreases with increasing electron-withdrawing power of the aromatic substituent(s). However, semiempirical MO calculations attribute this to an increase in the positive charge on phosphorus, leading to more back-bonding from the phosphoryl oxygen, resulting in a more shielded phosphorus.[19] The mass spectrum peaks are in good agreement with expected values. The P=O stretching frequency generally increases as the electron-withdrawing power of the substituent(s) increases.

As mentioned earlier, ^{13}C-^{31}P coupling constants can provide useful characterisation information. Going from starting material to product, the ^{13}C resonances go from singlets to doublets. Table 4.2 contains the $^xJ_{CP}$ coupling constants for all of the catalysts. As seen in Section 2.3.1 $^2J_{CP} > {}^3J_{CP,}$ where normally with 4-coordinate phosphorous environments $^3J_{CP} > {}^2J_{CP.}$ Aside from the stereochemical influences discussed in Section 2.3.1, deviation from this trend is not uncommon in aromatic systems, normally where the difference between $^2J_{CP}$ and $^3J_{CP}$ is a few Hz. An example spectrum is shown in Figure 4.5. Figure 4.6 shows the ^1H-^{31}P HMBC NMR spectrum

of catalyst **35**. The only phosphorus signal strongly couples to the aromatic signals in the ^{1}H NMR spectrum.

Table 4.2: $^{x}J_{CP}$ values for phosphoric acid catalysts.

Catalyst	$^{2}J_{CP}$ / Hz[a]	$^{3}J_{CP}$ / Hz[a]
27	7.4	4.6
28	4.7	4.4
29	7.0	4.9
30	7.2	5.0
31	7.1	4.9
32	7.4	5.0
33	7.4	4.3
34	6.6	4.7
35	7.3	4.9

[a] ^{13}C NMR spectra taken in $CDCl_3$ at 126 MHz

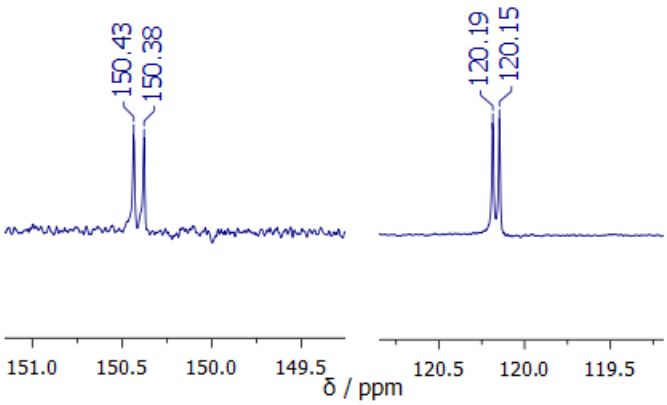

Figure 4.6: ^{13}C NMR resonances for catalyst **35**, in $CDCl_3$ at 126 HMz.

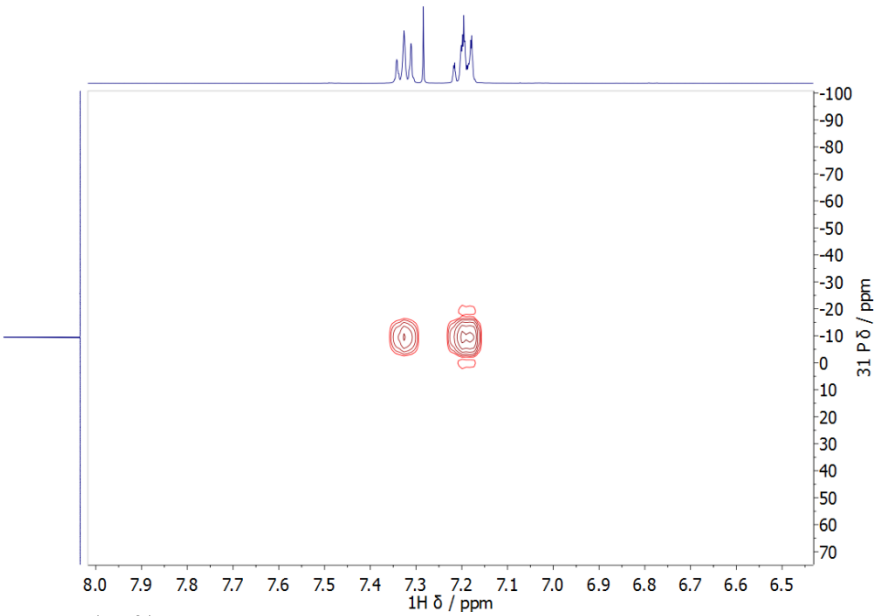

Figure 4.7: ^{1}H-^{31}P HMBC NMR spectrum of catalyst **35**, in $CDCl_3$ at 500 and 202 MHz.

4.2.1 pK_a Studies

The acidic proton of the phosphoric acid is expected to be crucial in their role as catalysts in ROP of esters. Thus, a series of titrations were carried out to determine the pK_a of the acids. In equation 4.1, the relationship between pH and pK_a is shown.

$$\mathrm{pH} = \mathrm{p}K_a + \log\frac{[\mathrm{A}^-]}{[\mathrm{HA}]} \qquad \text{(eqn 4.1)}$$

At the half-equivalents point pH = pK_a. The figure below shows this for catalyst **28** (pH curves for all catalysts can be found in Appendix 1) Table 4.3 shows the pK_a values determined for all catalysts. The table shows acidity of the hydroxyl proton

increasing with electron-withdrawing power, however, the cyano-containing catalysts have a lower acidity than expected. It is likely the nitrile group has become protonated hence, less acidic.

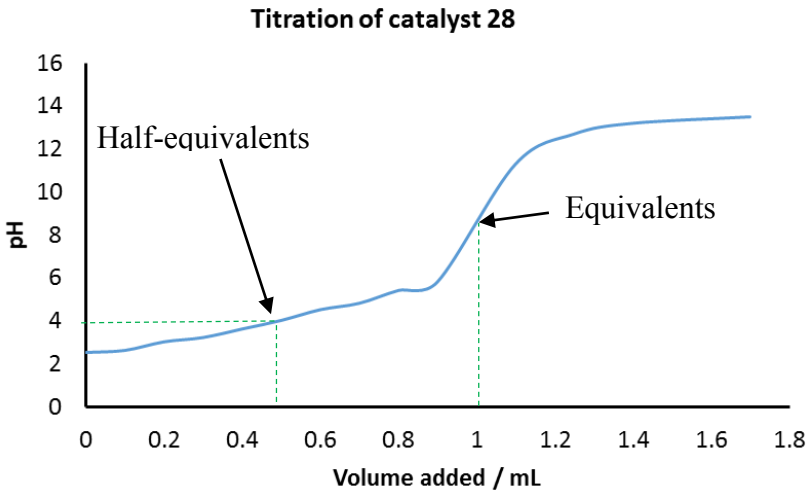

Figure 4.8: Titration curve for catalyst **28**.

Table 4.3: pK_a values of phosphoric acids.

Catalyst	X	Y	pK_a[a]
27	H	OMe	4.83
28	H	^{t}Bu	4.00
29	H	H	3.05
30	H	Cl	2.13
31	Cl	H	2.04
32	CF_3	H	1.95
33	H	CF_3	1.60
34	CN	H	2.95

35	H	CN	2.33
36	H	NO_2	0.75

[a]determined by titrating a 0.1 M of the acid in 10:1 v/v IPA/ methanol against tetrabutylammonium hydroxide solution (0.1M, 10:1 v/v IPA/ methanol).

4.3 Phosphates as ROP Catalysts

4.3.1 Catalytic Conditions

Catalyst **29** was used to determine the optimum reaction conditions for the ROP of β-BL (Scheme 4.4 and Table 4.4).

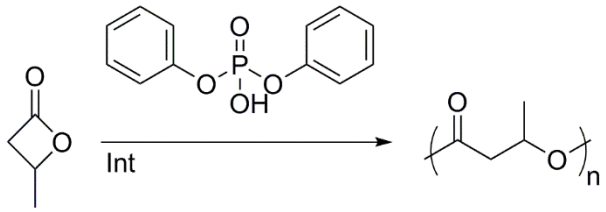

Scheme 4.4: ROP of β-BL using a phosphate catalyst.

Table 4.4: Screening conditions for ROP of βBL with catalyst **29**.

Entry	Initiator	Ratio ([Mon]:[Int]:[Cat])	Time / hr	Temp / °C	Conversion / %[a]
1	none	10:1:1	24	100	42
2	PPA	10:1:1	24	rt	0
3	PPA	10:1:1	24	80	34

4	PPA	10:1:1	24	100	56
5	PPA	10:1:1	24	120	55
6	PPA	10:1:1	60	100	48
7	PPA	100:1:1	24	100	9
8	PPA	50:1:1	24	100	23

[a]calculated by ^{1}H NMR spectroscopy

The polymerisation can occur without an initiator (entry 1), possibly by the catalyst also acting as the initiator using its hydroxyl group. The optimum temperature was found to be 100°C, with no significant increase in conversion above this temperature. When the reaction time was increased to 60 hr (entry 6), the conversion dropped slightly. The reaction stoichiometry was then changed to 100:1:1, and a drastic drop in conversion was observed. Even at loadings of 50:1:1, low conversions were obtained.

The optimum conditions (entry 5) were used for the ROP ε-caprolactone and *rac*-lactide (Schemes 4.5 and 4.6), producing conversion of 80 and 84 respectively.

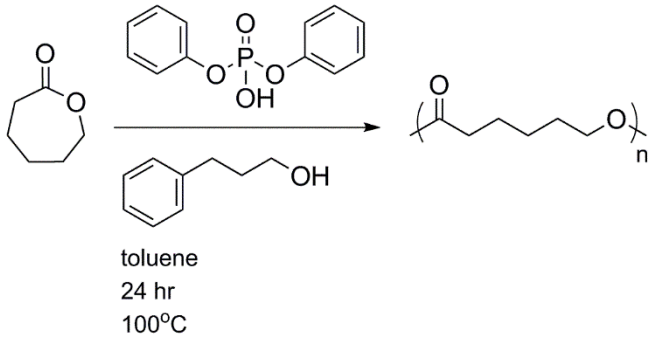

Scheme 4.5: ROP of ε-caprolactone catalysed by catalyst **29**.

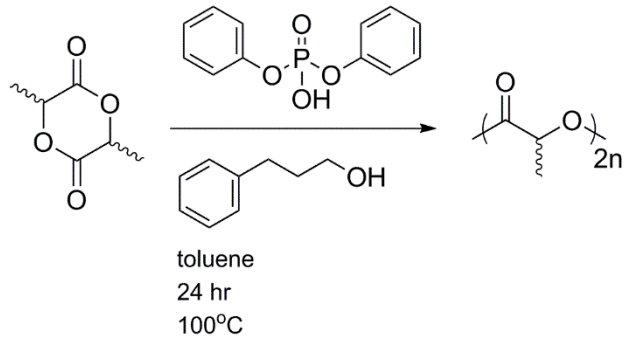

Scheme 4.6: ROP of *rac*-lactide catalysed by catalyst **29**.

Catalysts **27-36** were then used in the ROP of β-BL, to look at the effect of changing substituents. Scheme 4.7 shows the conditions used and Table 4.5 shows the conversions from the catalysts.

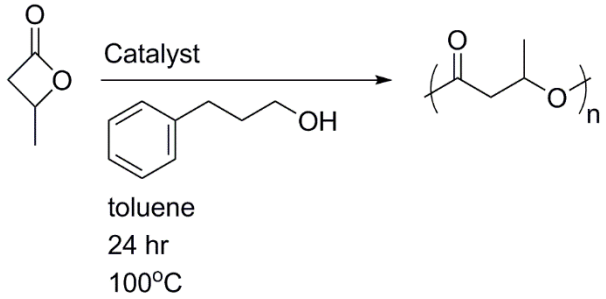

Scheme 4.7: Phosphate catalysed ROP of β-BL.

Table 4.5: Conversion of phosphoric acid catalysts.

Catalyst	X	Y	σ	Conversion / %[a]
27	H	OMe	-0.27	34
28	H	^{t}Bu	-0.20	31
29	H	H	0.00	56
30	H	Cl	0.23	63
31	Cl	H	0.37	64
32	CF_3	H	0.43	65

33	H	CF_3	0.54	68
34	CN	H	0.56	75
35	H	CN	0.60	86
36	H	NO_2	0.78	>99

[a] determined by ^{1}H NMR spectroscopy

Table 4.5 shows that monomer conversion increases with electron withdrawing ability, due to the increased acidity of the hydroxyl proton.

4.3.2 Dual-activation of Monomer / Chain End

To show that the catalysts activate both the carbon in the carbonyl and the OH in the initiator/ chain-end a series of ^{1}H and ^{13}C NMR experiments were run. First, the activation of the OH in the chain-end was explored by mixing ethyl 3-hydroxybutyrate with each catalyst. After addition of the phosphoric acid catalyst to ethyl 3-hydroxybutyrate, it is clear that the doublet at 3.82 ppm disappears and a singlet appears at a higher chemical shift, indicative of the above interaction with the phosphoryl oxygen of the catalyst (Figure 4.8). In Table 4.6, the OH ^{1}H NMR chemical shift (δ/ppm) and difference in chemical shift (Δδ/ppm) for each catalyst is shown. The difference in chemical shift increases with electron withdrawing power, making the initiator or chain end more nucleophilic.

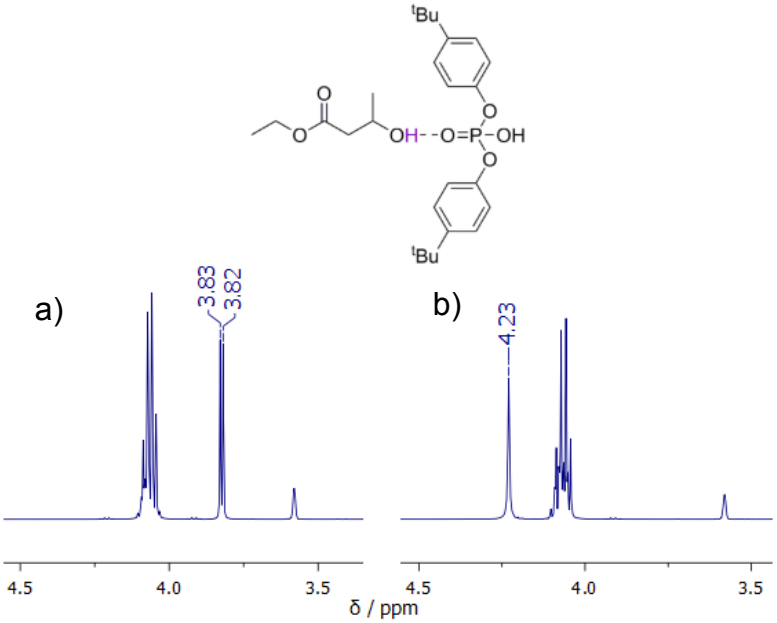

Figure 4.9: ^{1}H NMR spectra of ethyl 3-hydroxybutyrate a) before and b) after mixing with phosphoric acid catalyst **28**, THF-d_8 at 500 MHz.

Table 4.6: Chemical shift and difference in chemical shift of ethyl 3-hydrobutyrate with phosphoric acid catalysts.

Catalyst	X	Y	δ/ppm[a]	Δδ/ppm
27	H	^{t}Bu	4.21	0.39
28	H	OMe	4.23	0.42
29	H	H	4.30	0.48
30	H	Cl	4.51	0.69
31	Cl	H	4.63	0.81
32	CF_3	H	4.75	0.93
33	H	CF_3	4.79	0.97
34	CN	H	5.73	1.41
35	H	CN	6.85	3.03

36	H	NO_2	7.33	3.51

[a] ^{13}H NMR spectra taken in THF-d_8 at 500 MHz.

The activation of the carbonyl by the phosphoric acids was examined, a mixture of β-BL and each catalyst. Addition of the catalyst to β-BL sees an increases in the ^{13}C chemical shift of the carbonyl (Figure 4.9). In Table 4.7 shows the C=O ^{13}C NMR chemical shift (δ/ppm) and difference in chemical shift (Δδ/ppm) for each catalyst. A greater difference in the chemical shift is again observed as electron-withdrawing power increases.

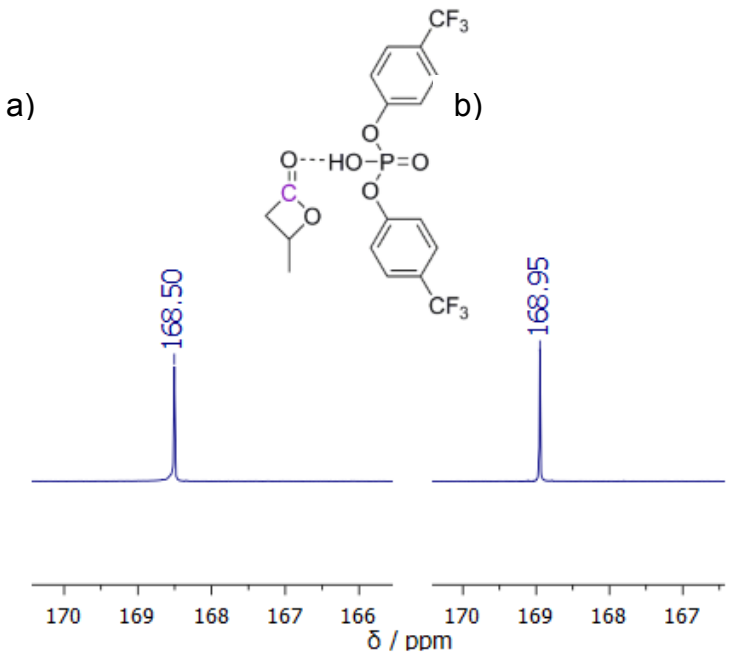

Figure 4.10: ^{13}C NMR spectra of βBL a) before and b) after mixing with phosphoric acid catalyst **33** (THF-d_8 at 126 MHz).

Table 4.7: Chemical shift and difference in chemical shift of β-BL with phosphoric acid catalysts.

Catalyst	X	Y	δ/ppm[a]	Δδ/ppm
27	H	^{t}Bu	168.59	0.09
28	H	OMe	168.52	0.02
29	H	H	168.68	0.18
30	H	Cl	168.78	0.28
31	Cl	H	168.80	0.30
32	CF_3	H	168.89	0.39
33	H	CF_3	168.95	0.45
34	CN	H	169.01	0.51
35	H	CN	169.07	0.57
36	H	NO_2	169.09	0.59

[a] ^{13}C NMR spectra taken in THF-d_8 at 126 MHz.

4.5 Hammett Substituent Constant Study

The activity of each catalyst in β-BL ROP was examined to look further into Kakuchi's findings that diphenyl phosphate is ineffective at polymerising β-BL at high monomer loadings,[18] and why ε-caprolactone and *rac*-lactide gave much higher conversions. Rate constants for each catalyst were determined for the initial 4 hours of the reaction

and are shown in Table 4.8, these rate constants were then used to construct a Hammett plot (Figure 4.10).

Table 4.8: Rate constants of phosphoric acid catalysts.

Catalyst	X	Y	σ	k / min^{-1}
27	H	OMe	-0.27	0.652 $x10^{-3}$
28	H	^{t}Bu	-0.20	0.574 $x10^{-3}$
29	H	H	0.00	0.374 $x10^{-3}$
30	H	Cl	0.23	1.96 $x10^{-3}$
31	Cl	H	0.37	3.16 $x10^{-3}$
32	CF_3	H	0.43	3.45 $x10^{-3}$
33	H	CF_3	0.54	2.22 $x10^{-3}$
34	CN	H	0.56	0.286 $x10^{-3}$
35	H	CN	0.60	0.286 $x10^{-3}$
36	H	NO_2	0.78	5.27 $x10^{-3}$

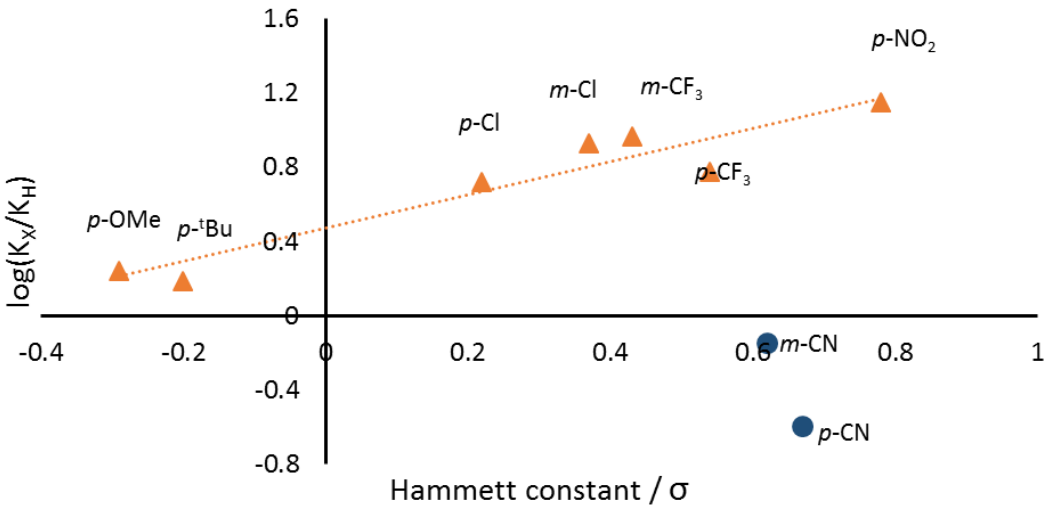

Figure 4.11: Hammett plot of phosphoric acid catalysts.

There is a correlation between reaction rate and the value of σ for the orange catalysts. The value of ρ for these catalysts is 0.90, which demonstrates that the reaction is significantly sensitive to different substituents attached to the catalysts. As ρ is positive this means more electrons are present in the transition state compared to the starting material in the rate determining step. This is common with acids when the rate determining step includes loss of the acidic proton. The magnitude of ρ gives information on the proximity of the acidic moiety and the benzene ring. If ρ is 1 or above the acidic moiety is delocalised within the benzene ring, which is not the case here. Normally, if the acidic moiety is 3 bonds away then ρ has a value of ~ 0.5,[20] here is it is much larger at 0.9, suggesting that the increase in electron density is not just from the acidic substituent, pointing towards dual functionality. It is possible that an interaction involving the catalyst and the chain end provides the extra electron density in the transition state. The blue catalysts in the Hammett plot (σ = 0.62 and 0.67) obviously do not fit the same trend as the orange catalysts, these catalysts are cyano

containing catalysts **34** and **35**. In Section 4.2.1 and Table 4.3 these catalysts were shown to have much lower pk_a values than expected. Due to the lower acidity, the activation energy is increased substantially, resulting in a much lower rate of reaction than expected.

4.4 Kinetic and Deactivation Studies

To look further at the behaviour of catalysts **34** and **35,** a kinetic study was conducted for 24 hr for each catalyst. Figure 4.11a shows the 24 hr kinetic study for catalyst **30** (the plots for catalysts **27**-**36** can be found in Appendix 1). The kinetic plot stops being linear after 250 minutes, and from this point the rate significantly drops and carries on falling, suggestive of the catalyst deactivating or a switch in mechanism. A polymerisation using catalyst **30** was doped with benzonitrile to see if having a cyano substituent present would lower the rate of reaction (Figure 4.11 b). It is clear to see Figure 4.11b follows a very similar curve to Figure 4.11a. There was also no significant drop in the initial rate of reaction. The fact that benzonitrile was added and no effect was observed suggests that the slower rate of reaction in catalysts **34** and **35** comes from an intramolecular effect rather than an intermolecular effect. Hillmyer also reported a non-first order kinetic relationship when using diphenyl phosphate as an ROP catalyst.[21] A similar kinetic plot was observed with a cyclic hemiacetal ester

monomer, and it was hypothesised that when the monomer concentration falls to a certain point, the catalyst switches mechanism, accounting for the change in the rate.[22]

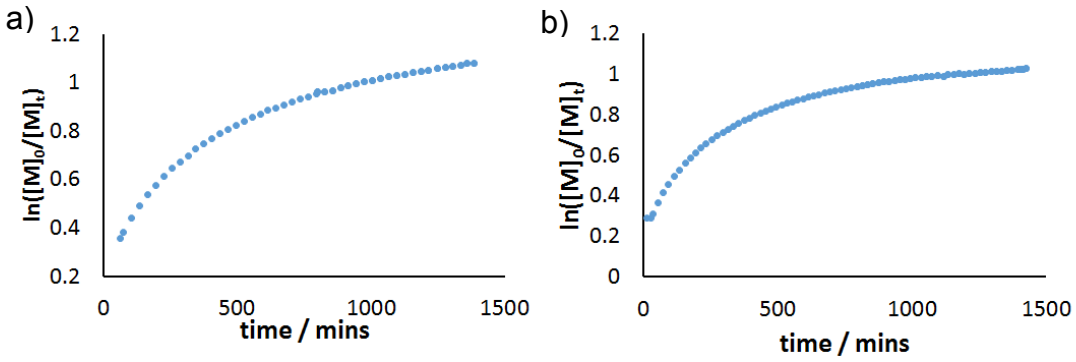

Figure 4.12: a) Kinetic plot of catalyst **30** and b) spiked with benzonitrile.

To test if the catalyst was switching mechanism or deactivating a reaction was set up and after a 1000 minutes a second aliquot of monomer was added maintaining the same initial monomer concentration. If the catalyst had undergone deactivation, there would be a drop in the rate of reaction after the second addition of monomer. If no deactivation had occurred, then the rate should be the same as the initial rate. Figure 4.12 shows the kinetic plot of this experiment using catalyst **30**. The initial rate of a reaction was 0.0011 $mins^{-1}$ and after the second addition of monomer the rate of reaction dropped to 0.0005 $mins^{-1}$. This experiment shows that a proportion of the catalyst has converted into a second species, which either has little or no activity. Although it is possible this compound could have a low level of activity, for simplicity it will henceforth be referred to as the deactive species.

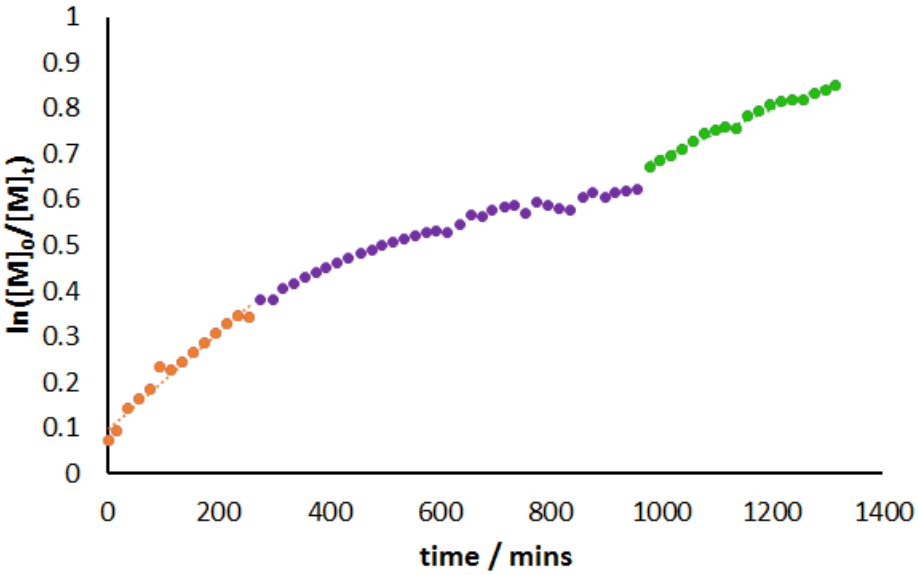

Figure 4.13: Kinetic plot of catalyst **30** with second monomer addition.

4.6 Deactivated Species

The polymerisation was also monitored by $^{31}P\{^{1}H\}$ NMR spectroscopy, the active catalyst (**A**) was observed, there is also a minor peak at -18.12 ppm which we propose is the deactive species (**B**) (Figure 4.13a). As the reaction progresses, decay of the active species and slow growth of **B** occurs. The rate of consumption of **A** (at -16.66 ppm) follows the same trend as the rate of reaction for the polymerisation shown in Figure 4.11a, with the kinetic plot of catalyst degradation shown in Figure 4.13b.

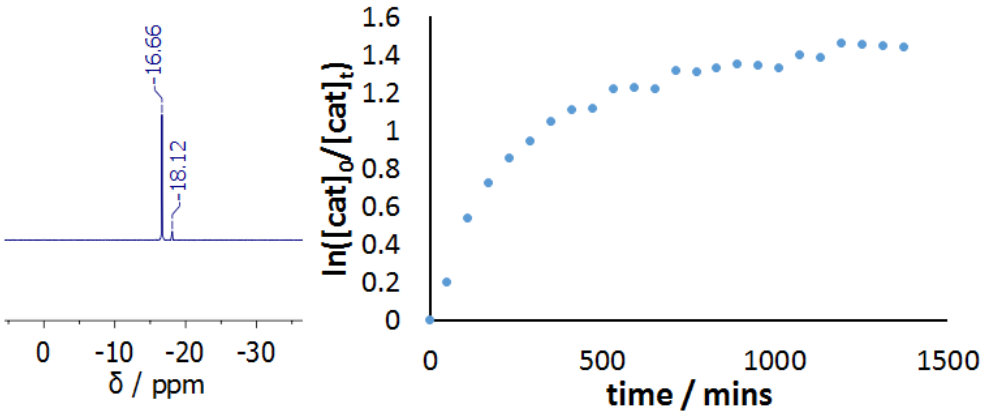

Figure 4.14: a) $^{31}P\{^{1}H\}$ NMR spectrum during a polymerisation using catalyst **30** (toluene-d_8 at 202 MHz) and b) kinetic plot of catalyst **30** degradation.

To gain information on the structure of the active and deactive species, ^{1}H-^{31}P HMBC NMR spectra were obtained during the polymerisations with β-BL, ε-caprolactone and *rac*-lactide (Figure 4.14). ^{1}H-^{31}P HMBC NMR spectra of ε-caprolactone and *rac*-lactide polymerisations only show one ^{31}P resonance indicating there is no second deactive species (Figure 4.14 b and c). This suggests a potential reason deactivation happens with β-BL is due to the smaller ring size. The active species is also only coupling to aromatic protons as expected. Moving onto β-BL, again the active catalyst is only coupling to aromatic protons. The deactive species, however, couples to aliphatic protons as well as aromatic protons. These aliphatic protons are at a comparable chemical shifts to β-BL protons, and integrate to match a β-BL fragment.

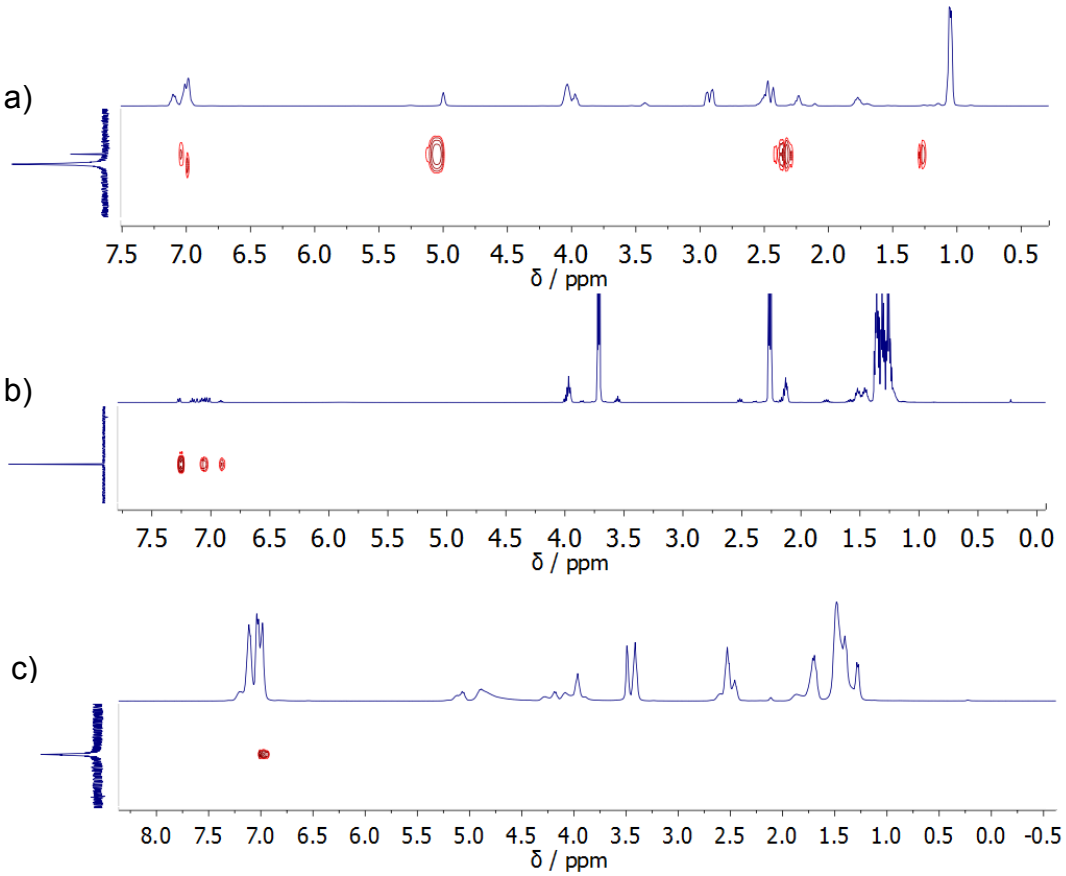

Figure 4.15: ^{1}H-^{31}P NMR during polymerisations with various monomers with catalyst **30** a) β-BL, b) ε-caprolactone and c) *rac*-lactide.

Catalyst **28** has a ^{t}Bu group that can be used to calculate how many aromatic substituents there are on the deactive species (**B**) compared to β-BL fragments. Figure 4.15 shows a section of the ^{1}H NMR spectrum of a polymerisation using catalyst **28**. From Figure 4.15 the integration ratio of the methane (H_A) on the β-BL fragment and ^{t}Bu protons (H_B) on the aromatic substituent is 1:9, meaning there is one β-BL fragment per aromatic substituent. A possible structure explaining these results is shown in Figure 4.15. If an analogous deactive species was formed with *rac*-lactide or ε-caprolactone, it would contain an 8 or 9 membered ring respectively but with β-BL

it forms a much more stable 6 membered ring structure, which is possibly why this only occurs with β-BL. The deactivation pathway is shown in Scheme 4.8. In this deactivation pathway, the first step is nucleophilic attack of the catalyst's hydroxyl oxygen on the carbonyl of β-BL, causing it to ring open, similar to how initiation occurs in Table 4.4 (entry 1). In the second step of the reaction, the β-BL fragment back bites to attack the phosphorous centre, again *via* nucleophilic attack with the loss of one of the aromatic substituents. To prevent the loss of one of the aromatic groups a catalyst (catalyst **37**) was synthesised that had extra stability *via* the chelate effect (Figure 4.16a.)

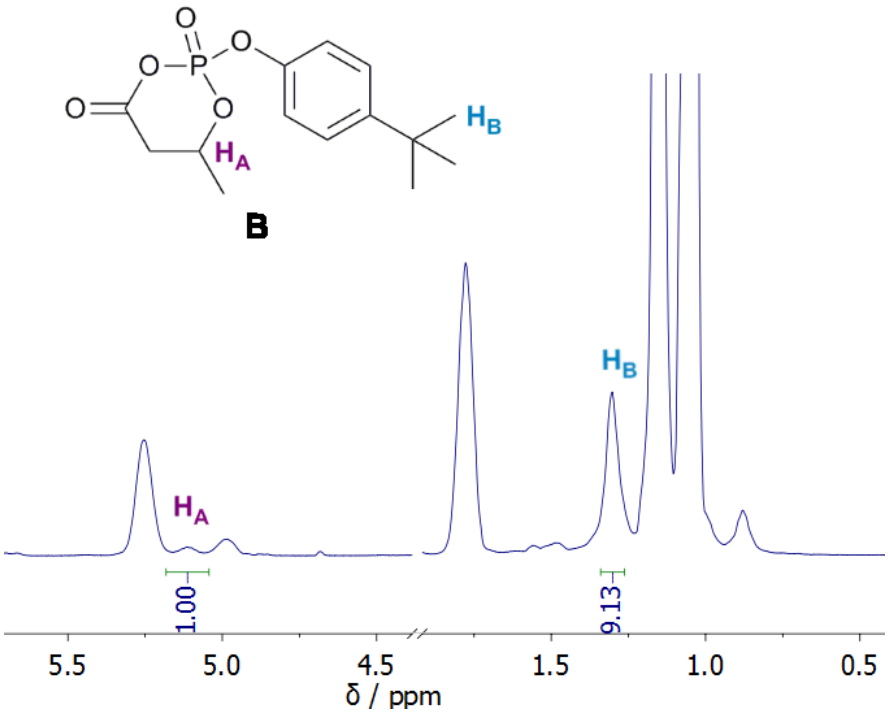

Figure 4.16: ^{1}H NMR spectrum of β-BL polymerisation with catalyst **28**, in toluene-d_8 at 400 MHz.

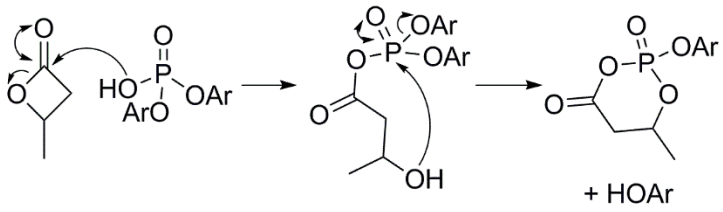

Scheme 4.8: Proposed deactivation pathway of catalysts in β-BL polymerisation.

When catalyst **37** used in a polymerisation, there was no conversion of β-BL. It is possible the 7-membered ring poses a geometry on the phosphorous atom that hinders polymerisation. Another way to block this deactivation pathway, is to replace the P-OAr with more chemically resistance P-Ar bonds, catalyst **38** (Figure 4.16b). A polymerisation was carried out using phosphinic acid as the catalyst and after 3 days no deactivation was observed whilst polymerisation still occurred (Figure 4.16c).

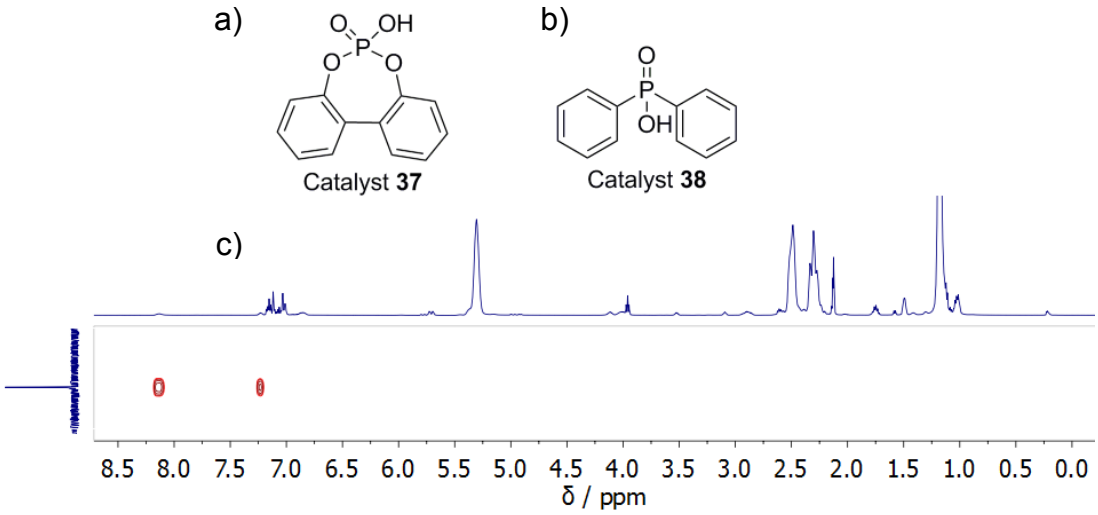

Figure 4.17: a) Biphenyl based catalyst **37**, b) phosphinic acid catalyst **38** c) $^{31}P\{^{1}H\}$ of reaction mixture after 3 days using catalyst **38**.

Attention was then turned to isolation of the deactive species. Unreacted monomer can be removed under vacuum, which leaves deactive and active versions of the catalyst and the oligomers produced by the reaction. It was possible to remove the oligomers

by precipitation. However, all solvents tested had the same solubility properties with the active and deactive species. It was hoped that separation may be possible by deprotonation of the hydroxyl proton on the active species, nevertheless every attempt degraded the deactive species. As the active species should have the hydroxyl group still attached column chromatography may separate the two species. All fractions collected from the column did not contain any phosphorous species, suggesting both the active and deactive species reacted during purification and did not elute. The column was attempted again with TEA added, however, the same outcome was observed. Isolation of the deactive species was then tried through a synthetic route, shown below in Scheme 4.9.

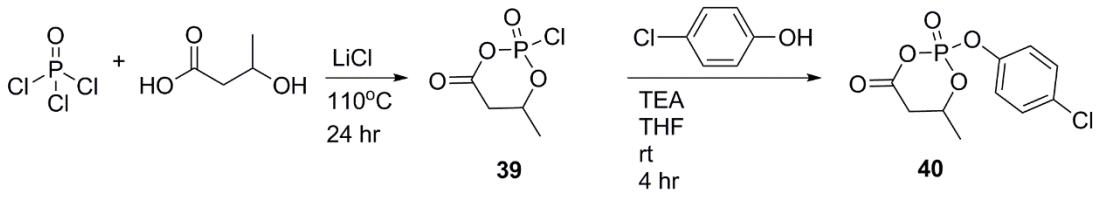

Scheme 4.9: Synthetic route for deactive species.

Step one of this reaction mirrors the reaction conditions to synthesise the phosphoric acid catalysts. The major product is the desired product, through there are two other species which it was not possible to separate from the product. The reaction conditions were then changed to those outlined in Scheme 4.10, similar to conditions used to synthesise monomers in Chapter 3.

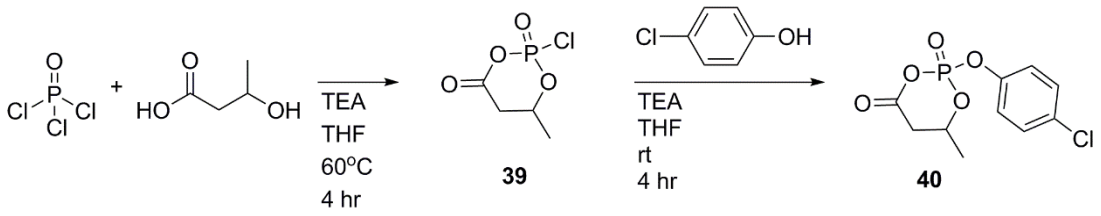

Scheme 4.10: Second synthetic route for deactive species.

This second route gave compound **39** with trace amounts of impurities, the $^{31}P\{^{1}H\}$ NMR spectrum is shown in Figure 4.17. It was then used without further purification. In the second step, a range of products was obtained, with the deactive species not being the major product. It was then decided to change the synthetic route to attach the aromatic substituent first (Scheme 4.11).

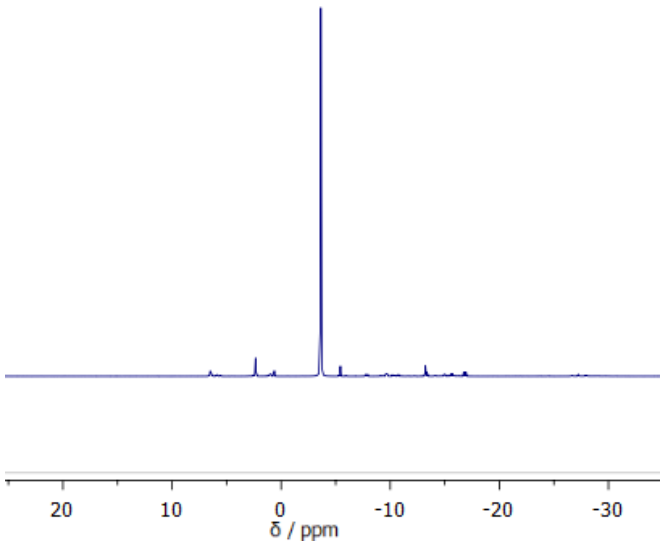

Figure 4.18: $^{31}P\{^{1}H\}$ NMR spectrum of compound **39** after step 1 of second synthetic route, in $CDCl_3$ at 202 MHz.

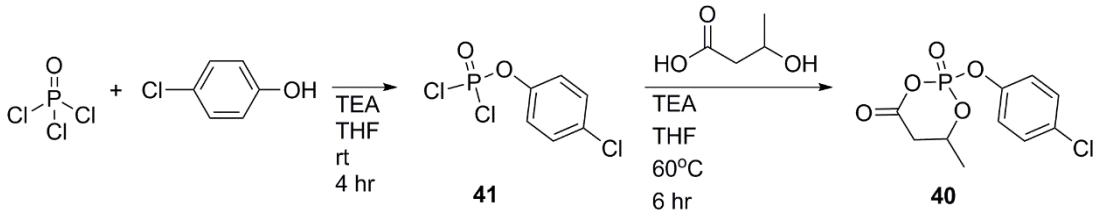

Scheme 4.11: Third synthetic route to deactive species.

In the first step, a mixture of mono and di-substituted products were observed, which were difficult to separate. After increasing the equivalents of $POCl_3$ to phenol to 3:1, it was possible to purify the mixture, giving the mono-substituted product (in 97% yield), the spectroscopic data for this compound is provided in Figure 4.18. In the second step of the reaction, again a range of products were observed and it was not possible to purify the reaction mixture. Unfortunately, due to time constraints, no further investigation into synthesising the deactive species was carried out.

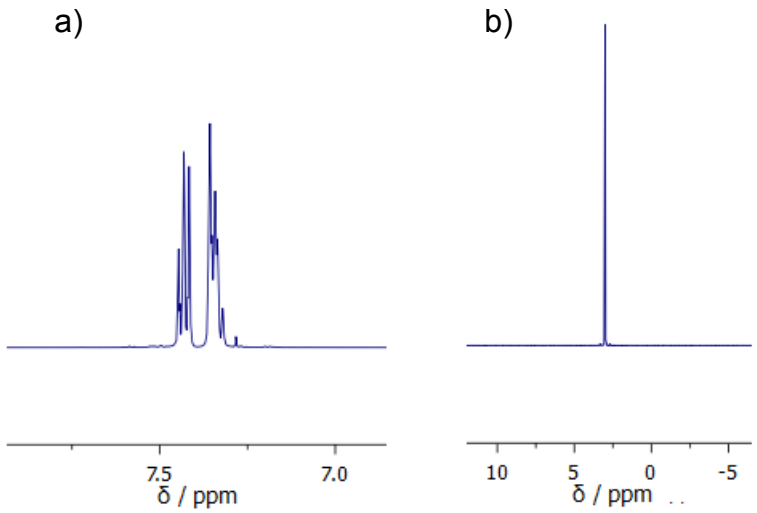

Figure 4.19: a) ^{1}H NMR and b) ^{31}P NMR spectra of compound **41**, in $CDCl_3$ at a) 500 and b) 202 MHz.

4.7 Conclusions

A series of phosphoric acid derivatives were synthesised. It was found that literature conditions produced the tri-aryl product.[16] Altering the stoichiometry and purification method gave the desired di-aryl product, and 9 catalysts were synthesised with

different substituents. Through ^{1}H and ^{13}C NMR spectroscopic studies, the catalysts were shown to be dual activating. After optimising the ROP conditions with β-BL, a Hammett plot was constructed. The plot gave a positive ρ value of 0.9, which is common with Brønsted acids. However, the value is larger than expected, indicating the transition state has gained electron density by an additional mode to donating a proton. Cyano-containing catalysts **34** and **35** did not fit this positive correlation of reaction rate and σ. It is likely this is due to the lower acidity of these catalysts. A deactivation pathway was observed which is probably why difficulties were experienced with these catalysts in the literature.[18] The deactive species contains a 6 membered ring which is possibly why this deactivation does not occur with ε-caprolactone or *rac*-lactide. To produce this deactive species, an aromatic substituent has to dissociate from the phosphorous centre. Replacing these cleavable P-OAr bonds with P-Ar bonds by using a phosphinic acid gave no deactive species after 3 days.

This work has been submitted to the *Catalysis Science & Technology* journal for peer review.

4.8 References

(1) Luckachan, G. E.; Pillai, C. K. S. *J. Polym. Environ.* **2011**, *19*, 637-676.

(2) Ebrahimi, T.; Hatzikiriakos, S. G.; Mehrkhodavandi, P. *Macromolecules* **2015**, *48*, 6672-6681.

(3) Fiore, G. L.; Jing, F.; Young, J. V. G.; Cramer, C. J.; Hillmyer, M. A. *Polym. Chem.* **2010**, *1*, 870-877.

(4) Martello, M. T.; Burns, A.; Hillmyer, M. *ACS Macro Letters* **2012**, *1*, 131-135.

(5) D. Uraguchi, M. T. *J. Am. Chem. Soc.* **2004**, *126*, 5356-5357.

(6) Akiyama, T.; Itoh, J.; Yokota, K.; Fuchibe, K. *Angew. Chem. Int. Ed.* **2004**, *43*, 1566-1568.

(7) Yang, X.; Toste, F. D. *J. Am. Chem. Soc.* **2015**, *137*, 3205-3208.

(8) Rueping, M.; Ieawsuwan, W. *Adv. Synth. Catal.* **2009**, *351*, 78-84.

(9) Yang, B.-M.; Cai, P.-J.; Tu, Y.-Q.; Yu, Z.-X.; Chen, Z.-M.; Wang, S.-H.; Wang, S.-H.; Zhang, F.-M. *J. Am. Chem. Soc.* **2015**, *137*, 8344-8347.

(10) Rueping, M.; Nachtsheim, B. J.; Moreth, S. A.; Bolte, M. *Angew. Chem. Int. Ed. Engl.* **2008**, *47*, 593-596.

(11) Zhu, W.; Du, H.; Huang, Y.; Sun, S.; Xu, N.; Ni, H.; Cai, X.; Li, X.; Shen, Z. *J. Polym. Sci., Part A: Polym. Chem.* **2013**, *51*, 3667-3673.

(12) Xu, J.; Song, J.; Pispas, S.; Zhang, G. *J. Polym. Sci., Part A: Polym. Chem.* **2014**, *52*, 1185-1192.

(13) Delcroix, D.; Couffin, A.; Susperregui, N.; Navarro, C.; Maron, L.; Martin-Vaca, B.; Bourissou, D. *Polym. Chem.* **2011**, *2*, 2249-2256.

(14) Makiguchi, K.; Satoh, T.; Kakuchi, T. *Macromolecules* **2011**, *44*, 1999-2005.

(15) Makiguchi, K.; Ogasawara, Y.; Kikuchi, S.; Satoh, T.; Kakuchi, T. *Macromolecules* **2013**, *46*, 1772-1782.

(16) Malik, P.; Chakraborty, D. *Inorg. Chim. Acta* **2013**, *400*, 32-41.

(17) Makiguchi, K.; Yamanaka, T.; Kakuchi, T.; Terada, M.; Satoh, T. *Chem. Commun.* **2014**, *50*, 2883-2885.

(18) Makiguchi, K.; Saito, T.; Satoh, T.; Kakuchi, T. *J. Polym. Sci., Part A: Polym. Chem.* **2014**, *52*, 2032-2039.

(19) Cajaiba Da Silva, J. F.; Pedrosa, M. S.; Nakayama, H. T.; Neto, C. C. *Phosphorus, Sulfur Silicon Relat. Elem.* **1997**, *131*, 97-105.

(20) Clayden, J.; Greeves, N.; Warren, S.; Wothers, P.: *Organic Chemistry*: Oxford, 2009; Vol. Oxford University Press.

(21) Schneiderman, D. K.; Hillmyer, M. A. *Macromolecules* **2016**, *49*, 2419-2428.

(22) Neitzel, N.; Haversang, T.; Hillmyer, M. A. *Ind. Eng. Chem. Res.* **2016**, In Press.

Chapter Five

Conclusions and Further Work

5.1 Conclusions

This thesis captures a broad scope of roles that phosphorus can play in polymer chemistry. From condensation polymerisations to make HRIPs to organocatalysts for ROP of cyclic esters.

It is known that phosphorus rich HRIPs give low optical dispersion and good optical clarity, but, only a handful of systems have been published. Poly(phosphate ester)s proved to be unsuitable for this application, due to problems with thermal stability. A range of polyphosphonates were successful synthesised with high levels of thermal stability. Their thermal properties could be tuned by using different end cappers in the polymerisation. The study also showed that whilst it is important to incorporate highly polarisable substituents, it is just as crucial to avoid non-polarisable groups. For example, the effect of increasing the number of aromatic rings was negated by the incorporation of extra methyl groups, yielding no net increase in the refractive index of the polymer. All polymers also showed good optical dispersion with high Abbé

numbers, the first reported for polyphosphonates. Figure 5.1 shows the polymer with the highest refractive index.

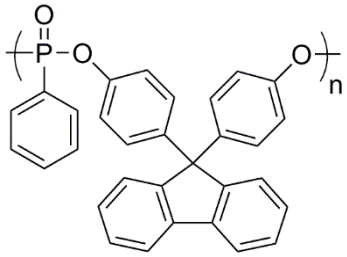

η = 1.66

υ = 22.4

Figure 5.1: Polymer **P15** possessing the highest reported refractive index for polyphosphonates.

Polyphosphonates made by ROP instead of convention polycondensation reactions are still underexplored. No aromatic or bicyclic phosphonate monomers had been reported. Three novel monomers were successfully synthesised, however, none successfully underwent ROP using the conditions tested. Aromatic monomers **1** and **2** have a stronger phosphoryl bond than phosphonates capable of undergoing ROP, which could prevent the polymerisation from proceeding. Bicyclic monomer **6** could adopt a structure that relieves ring strain, again preventing polymerisation. All reports of ROP of phosphonates use the two most common organocatalysts, DBU and TBD. Here a full range of organocatalysts were screened with monomer **16**, and there is a clear linear relationship between pK_a and conversion of the polymerisation. TBD did not fit with this linear relationship, with conversion much higher than expected based on its pK_a. This is because TBD is dual activating. To date there have been no other reports of phosphonates undergoing ROP with metal catalysts. Figure 5.2 shows monomers **1**, **2**, and **6**, with the metal catalysts that successfully polymerise monomer **16**.

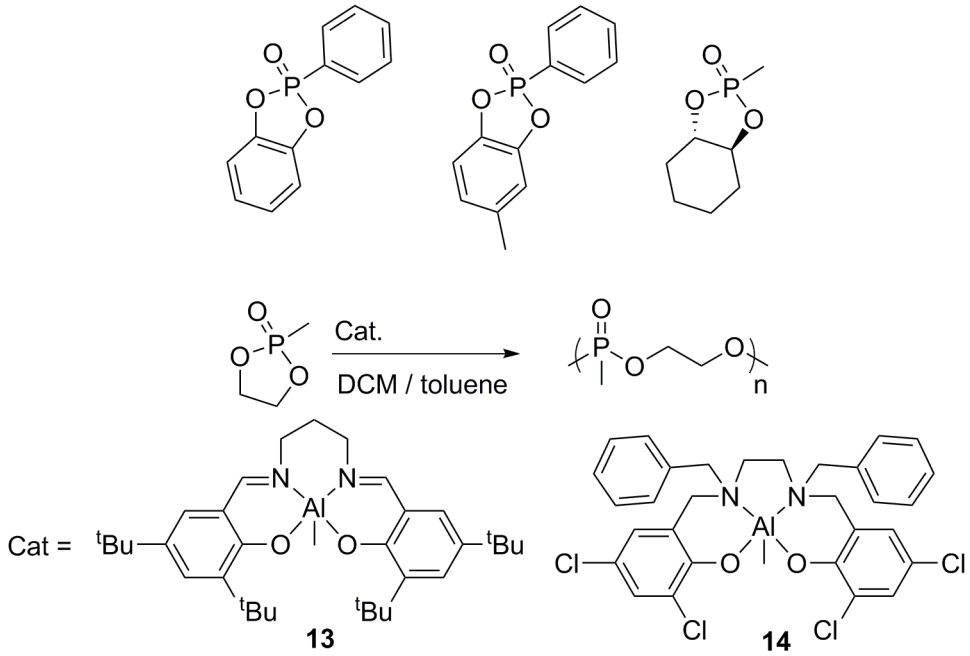

Figure 5.2: Phosphonate monomers unable to undergo ROP, and first reported metal catalysed phosphonate ROP.

Chapter Four includes the synthesis of a family of substituted phosphoric acids, and through spectroscopic methods it was shown that the catalysts were dual-activating. A Hammett plot was constructed which gave a positive ρ value of 0.9, indicating the loss of the acidic proton during the rate determining step. However, the value of ρ is much higher for the proximity of the acidic hydroxyl, and it is probable that the transition state picks up electron density from an interaction with the chain end. Cyano-containing catalysts **34** and **35** do not fit this trend, due to their lower acidity. An off-cycle deactive species was observed when these catalysts were used with β-BL. This species contained a 6-membered ring, which is likely why this is less favoured with larger rings such as ε-caprolactone and *rac*-lactide. Replacement of the reactive P-OAr bonds with P-Ar, bonds in the form of phosphinic acid, blocks this deactivation

pathway. Figure 5.3 shows the phosphoric catalysed ROP of β-BL and the deactive pathway.

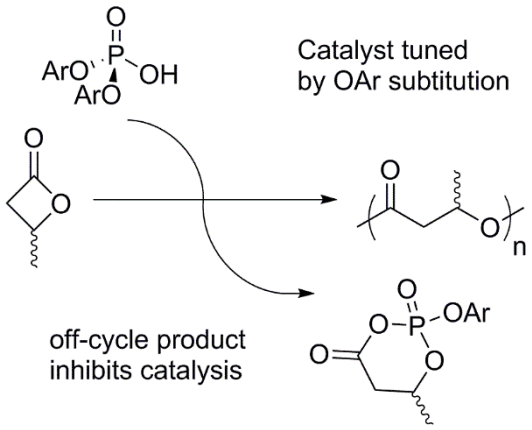

Figure 5.3: ROP of β-BL with deactivation of phosphoric acids.

5.2 Further Work

All the polymers synthesised in Chapter Two contain oxygen atoms, which are known to decrease refractive index. Two ways to decrease the number of oxygen atoms present are shown in Figure 5.4. The first method is to use amines instead of alcohols to synthesise the polymers, and the second is to replace P=O with P=S bonds.

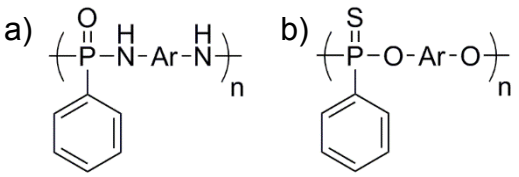

Figure 5.4: Possible phosphorus containing HRIPs with less oxygen atoms present a) polymer **P26** and b) polymer **P27**.

All starting materials required for polymers in Figure 5.4 are commercially available. This study only looked at one case of changing the side group from a phenyl group, and that was to a non-polarisable methyl group. Further work could include synthesising polymers with a higher level of aromaticity in the side group, with two examples shown in Figure 5.5.

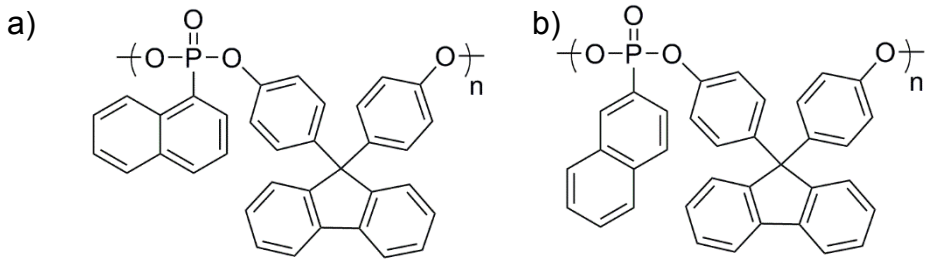

Figure 5.5: Phosphorus containing HRIPs with a higher level of aromaticity in the side group a) polymer **P28** and b) polymer **P29**.

The starting material for the polymers in Figure 5.5 are not commercially available but can be synthesised from the corresponding phosphonic acid, oxalyl chloride and a DMF catalyst, as shown in Scheme 5.1.

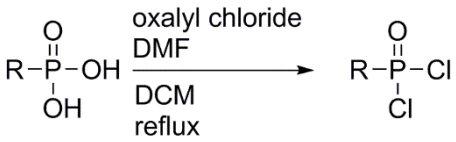

Scheme 5.1: Synthesis of starting materials for polymers **P28** and **P29**.

It is not known why these polymers possess high Abbé numbers, a specific study into the relationship between structure and Abbé number may aid design of future HRIPs. The structure of the polymers in Chapter Two are extremely similar to commercial fire retardants, it is hypothesised that these polymers could also be good flame retardants with further testing.

To further the work of Chapter Three other metal catalysts could be used with this family of monomer. Such as zinc and magnesium β-diiminates, which are extremely useful in cyclic ester ROP. Broadening the ligand scope to include phosphorous could see the use of phosphasalen ligands, which have been used mainly with yttrium for the ROP of many cyclic esters. These structures are shown in Figure 5.6.

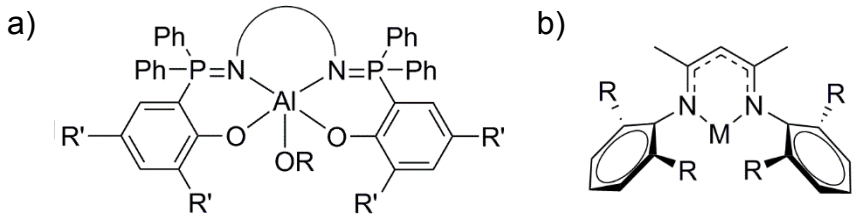

Figure 5.6: Structure of a) phosphasalen M = Sc, Y b) β-diiminate M = Zn, Mg

Chapter Four showed phosphinic acids are effective ROP catalysts, an obvious route to carry on this work is to explore a range of phosphinic acids. However, a novel body of work would be to look into new phosphorous containing ROP catalysts. These could include phosphonium salts, where the phosphorous carries a formal positive charge. These would be similar to compounds used to make ylides for the Wittig reaction. These catalysts could have the ability to catalyse the cationic ROP of cyclic esters.

Chapter Six

Experimental Procedures

6.1 General Considerations

All reactions were carried out under an inert atmosphere using standard Schlenk or glovebox techniques, unless stated otherwise. ^{1}H NMR spectra were recorded using BrukerAsance (400 or 500 MHz) spectrometers, $^{13}C\{^{1}H\}$ NMR spectra were recorded using Bruker Asance (at 126 MHz) both are referenced to tetramethylsilane. $^{31}P\{^{1}H\}$ NMR spectra were recorded using a BrukerAsance (202 or 102 MHz) spectrometer referenced to 80% H_3PO_4. All spectra were recorded at room temperature. UV-vis spectra were obtained as DMSO solutions at rt in 1 cm glass cuvettes using a Shimadzu UV-1800 UV spectrophotometer. IR spectra were recorded with solid samples on a Perkin Elmer spectrum 65 FT-IR spectrometer. GPC was conducted with THF samples at a flow rate of 1 mL/min on a Malvern Instruments Viscotek 270 GPC Max triple detection system with 2 x mixed bed styrene DVB columns (300 x 7.5 mm) using THF as the eluent at rt and an injection volume of 100 µL. Refractive indices of polyphosphonates were obtained from solutions prepared in THF at concentrations of 75 mg/mL and 150 mg/mL. Polymer films were prepared by using 80 µL of polymer

solutions (150 mg/mL) in THF. Polyphosphate solutions were measured in 300 μL volumes and polymer thin films and solutions were measured at 20°C using a digital multiple wavelength refractometer DSR-L (Schmidt Haensch, Germany) using the full range of available wavelengths (404.7, 435.8, 486.1, 546.1, 587.6, 589.3, 632.8, 656.3, 706.5 nm). The refractive index for THF was then measured and the refractive index of the polymer extrapolated. DSC analyses were carried out on a TA Instruments DSC Q2000 through heat / cool cycles at rate of 10°C/min. TGA measurements were carried out on a SDTQ600 up to a temperature of 800°C with temperature gradient at 10°C/min. Mass spectroscopy was carried out at the University of Edinburgh using a Bruker Daltonics micro TOP instrument. The pK_a's of the phosphoric acids were determined by titrating a 0.1 M of the acid in 10:1 v/v IPA/ methanol against tetrabutylammonium hydroxide solution (0.1M, 10:1 v/v IPA/ methanol).

6.2 Starting Materials

DCM, toluene, THF and chloroform were obtained from an Innovative Technologies solvent purification system and lyophilised three times before use. BOE was distilled from sodium prior to use. Phenol was purchased from Sigma Aldrich and recrystallized from chloroform. TEA, ε-caperlactone, DCM, DBU, 1,5-diazabicyclo[4.3.0]non-5-ene (DBN), 2,2,6,6-tetramethylpiperidine (TMP), 1,1,3,-tetramethylguanidine (TMG), 7-methyl-1,5,7-triazabicyclo[4.4.0]dec-5-ene (MeTBD), pyridine, PPA, β-BL and d_8-toluene were purchased from Sigma-Aldrich and dried over calcium hydride and distilled before use. ε-Caprolactone and 3-hydroxybutyric acid were received from

Fisher Scientific and dried over calcium hydride and distilled prior to use. Phenylphosphonic dichloride, phenyl dichlorophosphate, bisphenol-A, 4,4'-dihydroxybiphenol, 4,4'-(1,4-phenylenediisopropylidene)phenol, 4,4'-(9-fluorenylidene)phenol, 4,4'-(1-phenylethylidene)biphenol, 1,5-dihydroxynaphthalene, 4,4-thiophenol, benzyl alcohol, 2-naphthol, 4-cumylphenol, 2,4-bis(α,α-dimethylbenzyl)phenol, TBD, 3-butene-1,2-diol, methylphosphonic dichloride, catechol, phenylphosphonic dichloride, trans-1,2-cyclohexanediol, phosphorus pentachloride, 4-methylcathehol, phosphorus oxychloride, lithium chloride, 4-cyanophenol, 3-chlorophenol, 4-tert-butylphenol 3-(trifluoromethyl) phenol, 2,2-biphenol were supplied by Sigma Aldrich and used as received. Methylphosphonic dichloride, chlorohydroquinone, 4-chlororesorcinol, 1,7-dihydroxynaphthalene, 1-thioglycerol, ethylene glycol and 3-cyanophenol were obtained from Alfa Aesar, and used as received. Hydroquinone, ethyl dichlorophosphate and 2,7-dihydroxynaphthalene were supplied from Acros Organics, and used as received. N-methyl imidazole, DMAP, phosphorus trichloride, sodium hydroxide pellets, 4-methyloxyphenol and 4-(trifluoromethyl) phenol were purchased from Merck Schuchardt, and used as received. 4-Chlorophenol was order from Fluka and used as received. *Rac*-lactide was obtained from Purac and sublimed 3 times prior use.

6.3 Synthesis of Polycondensation Polymers

Synthesis of poly(phosphate ester)s

Representative synthesis of poly(phosphate ester)s: TEA (0.033 mol) and N-methyl imidazole (0.393 mmol) were added to a stirred solution of diol (0.0313 mol) in DCM (20 mL). A solution of dichlorophosphate (0.0313 mol) was added dropwise at 0°C. The mixture was then stirred at room temperature for 4 hr. Phenol (0.0313 mol) was then added and left to stir for 1 hr. The solution was then washed twice with water, once with 5% HCl aqueous solutions and finally washed three more times with water. The polymer was then precipitated into methanol. The product was then purified by heating at 120°C under vacuum.

Polymer P1

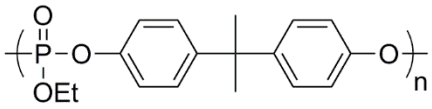

^{1}H NMR (DMSO-d_6, ppm): δ7.18-7.08 (m, 8H, Ar C-H), 4.23 (s, 2H, CH_2,CH_3), 1.55 (s, 6H, C-CH_3) 1.21 (s, 3H, CH_2,CH_3). ^{13}C{^{1}H} NMR (DMSO-d_6, ppm): δ148.41 (d, $^{2}J_{CP}$ = 7.1 Hz, Ar O-C-$(CH)_2$), 147.56 (Ar C-C-C-$(CH_3)_2$), 128.46 (Ar C-C-C-$(CH_3)_2$), 119.83 (d, $^{3}J_{CP}$ = 4.3 Hz, O-C-$(CH)_2$), 65.81 (d, $^{2}J_{CP}$ = 6.1 Hz, O-CH_2-CH_3), 42.31 (C-$(CH_3)_2$), 30.81 (C-$(CH_3)_2$), 16.22 (d, $^{3}J_{CP}$ = 6.0 Hz, O-CH_2-CH_3). ^{31}P{^{1}H} NMR (DMSO-d_6, ppm): δ-11.61. FTIR (cm^{-1}): 1285 (P=O).

Polymer P2

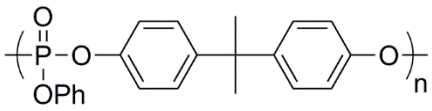

^{1}H NMR (DMSO-d_6, ppm): δ7.45-7.34 (m, 5H), 7.29-7.09 (m, 8H), 1.57 (s, 6H). ^{13}C{^{1}H} NMR (DMSO-d_6, ppm): δ150.31 (d, $^{2}J_{CP}$ = 7.4 Hz), 148.20 (d, $^{2}J_{CP}$ = 7.5 Hz), 130.63, 128.65, 127.77, 126.31, 120.34 (d, $^{4}J_{CP}$ = 3.0 Hz), 119.69 (d, $^{3}J_{CP}$ = 4.8 Hz), 42.39, 30.77. ^{31}P{^{1}H} NMR (DMSO-d_6, ppm): δ-17.02. FTIR (cm^{-1}): 1295 (P=O).

Polymer P3

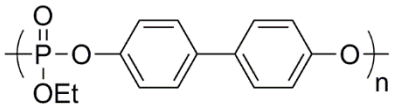

^{1}H NMR (DMSO-d_6, ppm): δ7.37 (d, J = 8.6, 4H), 6.80 (d, J = 8.6, 4H), 3.05 (q, J = 7.3, 2H), 1.19 (t, J = 7.3, 3H). ^{13}C{^{1}H} NMR (DMSO-d_6, ppm): δ150.11 (d, $^{2}J_{CP}$ = 7.3 Hz), 136.86, 128.77, 120.85 (d, $^{3}J_{CP}$ = 4.5 Hz), 66.21 (d, $^{2}J_{CP}$ = 6.3 Hz), 16.31 (d, $^{3}J_{CP}$ = 6.0 Hz). ^{31}P{^{1}H} NMR (DMSO-d_6, ppm): δ-11.58. FTIR (cm^{-1}): 1277 (P=O).

Polymer P4

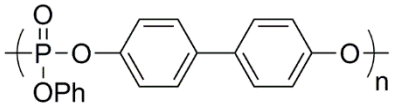

^{1}H NMR (DMSO-d_6, ppm): δ7.74 (d, J = 6.6 Hz, 4H), 7.46 (d, J = 7.5 Hz, 2H), 7.39 (d, J = 7.22 Hz, 4H), 7.32 (d, J = 8.2 Hz, 2H), 7.28 (d, J= 8.6 Hz, 1H). ^{13}C{^{1}H} NMR (DMSO-d_6, ppm): δ150.28 (d, $^{2}J_{CP}$ = 7.4 Hz), 149.95 (d, $^{2}J_{CP}$ = 7.1 Hz), 137.17, 130.17,

129.00, 126.49, 120.91, 120.87 (d, $^{2}J_{CP}$ = 4.7 Hz), 120.37 (d, $^{2}J_{CP}$ = 4.8 Hz). $^{31}P\{^{1}H\}$ NMR (DMSO-d_6, ppm): δ-17.28. FTIR (cm^{-1}): 1256 (P=O).

Synthesis of Polyphosphonates

Representative synthesis of polyphosphonate: TEA (0.033 mol) and N-methyl imidazole (0.393 mmol) were added to a stirred solution of diol (0.013 mol) in DCM (20 mL). A solution of phosphonic dichloride (0.0313 mol) was added dropwise at 0 °C. The mixture was then stirred at rt for 4 h and phenol (0.0313 mol) was then added, and the reaction was left to stir for a further 1 h. The reaction vessel was then opened to air, and washed with water twice, followed by two washings with 10% HCl aqueous solution and finally washed with water three more times. The resulting polymer was precipitated into methanol. A DCM solution of the polymer was then filtered through a Celite® plug. After removal of the solvent the samples were purified by heating at 100°C under vacuum for 16 hr.

Polymer P5

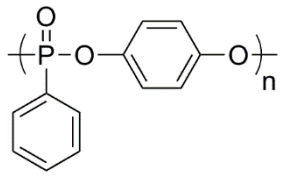

^{1}H NMR ($CDCl_3$, ppm): δ7.97-7.83 (m, 2H, Ar P-C-$(CH)_2$-$(C\underline{H})_2$-CH), 7.60 (t, J = 7.6 Hz, 1H, P-C-$(CH)_2$-$(CH)_2$-C$\underline{H}$), 7.48 (q, J = 7.3 Hz, 2H, P-C-$(C\underline{H})_2$-$(CH)_2$-CH), 7.08 (s, 4H, Ar O-C-$(C\underline{H})_2$-$(C\underline{H})_2$). $^{13}C\{^{1}H\}$ NMR ($CDCl_3$, ppm) δ147.18 (d, $^{2}J_{CP}$ = 7.5 Hz,

P-O-C), 133.46 (d, $^{4}J_{CP}$ = 2.6 Hz, P-C-(CH)$_2$-(CH)$_2$-CH), 132.22 (d, $^{2}J_{CP}$ = 10.7 Hz, P-C-(CH)$_2$-(CH)$_2$-CH), 128.75 (d, $^{3}J_{CP}$ = 15.9 Hz, P-C-(CH)$_2$-(CH)$_2$-CH), 126.17 (d, $^{1}J_{CP}$ = 192.2 Hz, P-C-(CH)$_2$-(CH)$_2$-CH), 121.72 (d, $^{3}J_{CP}$ = 4.4 Hz, O-C-(CH)$_2$). $^{31}P\{^{1}H\}$ NMR ($CDCl_3$, ppm): δ12.22. FTIR (cm^{-1}): 1264 (P=O).

Polymer P6

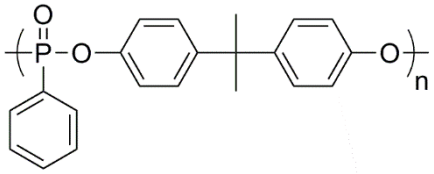

^{1}H NMR ($CDCl_3$, ppm): δ7.95 (dd, J = 13.8, 7.5 Hz, 2H), 7.60 (t, J = 7.0 Hz, 2H), 7.50 (t, J = 6.3 Hz, 1H), 7.08 (m, 8H), 1.59 (s, 6H). $^{13}C\{^{1}H\}$ NMR ($CDCl_3$, ppm) δ148.26 (d, $^{2}J_{CP}$ = 7.7 Hz), 147.13, 133.15 (d, $^{4}J_{CP}$ = 3.3 Hz), 132.23 (d, $^{2}J_{CP}$ = 10.4 Hz), 128.61 (d, $^{3}J_{CP}$ = 15.8 Hz), 127.08 (d, $^{1}J_{CP}$ = 192.8 Hz), 128.04, 119.98 (d, $^{3}J_{CP}$ = 4.5 Hz), 42.26, 30.87. $^{31}P\{^{1}H\}$ NMR ($CDCl_3$, ppm): δ11.87. FTIR (cm^{-1}): 1262 (P=O).

Polymer P7

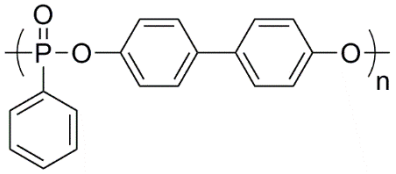

^{1}H NMR ($CDCl_3$, ppm): δ8.02 (dd, J = 14.14, 7.4 Hz, 2H), 7.63 (t, J = 6.9 Hz, 1H), 7.53 (td, J = 7.3, 3.7 Hz, 2H), 7.44 (d, J = 8.7 Hz, 2H), 7.26 (d, J = 8.1 Hz, 2H). $^{13}C\{^{1}H\}$ NMR ($CDCl_3$, ppm) δ149.80 (d, $^{2}J_{CP}$ = 7.5 Hz), 137.27, 133.42 (d, $^{4}J_{CP}$ = 3.1 Hz),

132.29 (d, $^{2}J_{CP}$ = 10.5 Hz), 128.77 (d, $^{3}J_{CP}$ = 15.9 Hz), 128.49 (d, $^{3}J_{CP}$ = 14.2 Hz), 128.04 (d, $^{1}J_{CP}$ 158.9 Hz), 120.95 (d, $^{4}J_{CP}$ = 4.5 Hz). $^{31}P\{^{1}H\}$ NMR ($CDCl_3$, ppm): δ12.15. FTIR (cm^{-1}): 1267 (P=O).

Polymer P8

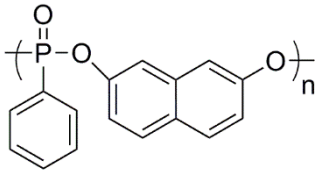

^{1}H NMR ($CDCl_3$, ppm): δ8.00 (dd, J=13.9, 7.5 Hz, 2H), 7.77 (m, 1H), 7.72 (d, J = 9.0 Hz, 2H), 7.57 (s, 2H), 7.49 (dt, J = 12.2, 5.8 Hz, 2H), 7.31 (d, J = 8.8, 2H). $^{13}C\{^{1}H\}$ NMR ($CDCl_3$, ppm) δ148.75 (d, $^{2}J_{CP}$ = 7.5 Hz), 134.53, 133.46 (d, $^{4}J_{CP}$ = 3.2 Hz), 132.31 (d, $^{2}J_{CP}$ = 10.4 Hz), 129.77, 129.43, 128.79 (d, $^{3}J_{CP}$ = 15.9 Hz), 126.39 (d, $^{1}J_{CP}$ = 191.9 Hz), 120.17 (d, $^{3}J_{CP}$ = 4.5 Hz), 116.88 (d, $^{3}J_{CP}$ = 4.9 Hz). $^{31}P\{^{1}H\}$ NMR ($CDCl_3$, ppm): δ12.18. FTIR (cm^{-1}): 1262 (P=O).

Polymer P9

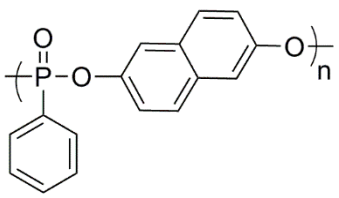

^{1}H NMR ($CDCl_3$, ppm): δ8.01 (dd, J = 14.1, 7.5 Hz, 2H), 7.71-7.64 (m, 2H), 7.64-7.57 (m, 1H), 7.51 (t, J= 6.2 Hz, 2H), 7.34 (d, J = 9.2 Hz, 2H). ^{13}C{^{1}H} NMR ($CDCl_3$, ppm) δ147.76 (d, $^{2}J_{CP}$ = 7.8 Hz), 133.44 (d, $^{4}J_{CP}$ = 3.0 Hz), 132.31 (d, $^{2}J_{CP}$ = 10.3 Hz), 131.37, 129.50, 128.77 (d, $^{3}J_{CP}$ = 15.9 Hz), 126.49 (d, $^{1}J_{CP}$ = 191.9 Hz), 121.39 (d, $^{3}J_{CP}$ = 4.5 Hz), 117.19 (d, $^{3}J_{CP}$ =4.5 Hz). ^{31}P{^{1}H} NMR ($CDCl_3$, ppm): δ12.32. FTIR (cm^{-1}): 1262 (P=O).

Polymer P10

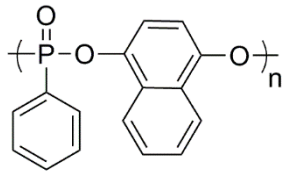

^{1}H NMR ($CDCl_3$, ppm): δ8.03 (dd, J = 13.8, 7.4 Hz, 2H), 7.96 (br s, 2H), 7.56 (m, 1H), 7.45 (Br s, 2H), 7.40 (Br s, 2H), 7.30 (Br s, 2H). ^{13}C{^{1}H} NMR ($CDCl_3$, ppm) δ143.38 (d, $^{2}J_{CP}$ = 7.9 Hz), 133.60, 132.19 (d, $^{2}J_{CP}$ = 10.5 Hz), 128.90 (d, $^{3}J_{CP}$ = 15.6 Hz), 128.55 (d, $^{1}J_{CP}$ = 243.8 Hz), 127.50, 127.19, 121.79, 115.04. ^{31}P{^{1}H} NMR ($CDCl_3$, ppm): δ12.53. FTIR (cm^{-1}): 1258 (P=O).

Polymer P11

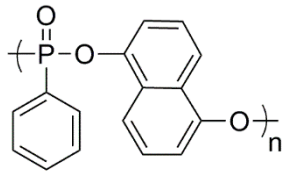

^{1}H NMR ($CDCl_3$, ppm): δ8.06 (d, J = 13.6 Hz, 2H), 7.83 (t, J = 11.2 Hz, 2H), 7.59 (t, J = 7.5 Hz, 1H), 7.49 (d, J= 9.9 Hz, 4H), 7.28 (m, 2H). ^{13}C{^{1}H} NMR ($CDCl_3$, ppm) δ146.33 (d, $^{2}J_{CP}$ = 8.3 Hz), 133.62, 132.16 (d, $^{3}J_{CP}$ = 10.6 Hz), 128.92 (d, $^{3}J_{CP}$ 16.1 Hz), 127.96, 126.50 (d, $^{1}J_{CP}$ = 190.6 Hz), 126.08, 118.77 (d, $^{2}J_{CP}$ = 6.6 Hz), 116.43. ^{31}P{^{1}H} NMR ($CDCl_3$, ppm): δ12.40. FTIR (cm^{-1}): 1268 (P=O). FTIR (cm^{-1}): 12.71 (P=O).

Polymer P12

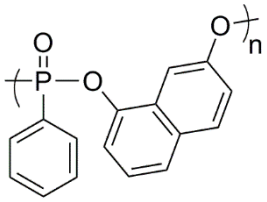

^{1}H NMR ($CDCl_3$, ppm): δ7.96-7.84 (m, 2H), 7.67-7.56(m, 2H), 7.55-7.48 (m, 1H), 7.45-7.33 (m, 4H), 7.23-7.14 (m, 2H). ^{13}C{^{1}H} NMR ($CDCl_3$, ppm) δ148.58, 145.92, 133.40, 132.87 (d, $^{1}J_{CP}$ = 151.0 Hz), 129.86, 128.65 (d, $^{3}J_{CP}$ =11.4 Hz), 127.02, 125.20 (d, $^{2}J_{CP}$ = 5.3 Hz), 124.77, 121.32, 116.44, 116.38, 115.31, 11.46 (d, $^{2}J_{CP}$ = 5.92 Hz). ^{31}P{^{1}H} NMR ($CDCl_3$, ppm): δ12.50. FTIR (cm^{-1}): 1271 (P=O).

Polymer P13

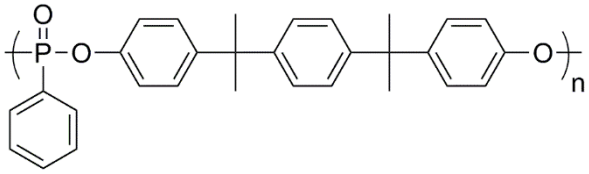

^{1}H NMR ($CDCl_3$, ppm): δ7.94 (dd, J = 14.0, 8.3 Hz, 2H), 7.56 (t, J = 7.4 Hz, 1H), 7.46 (q, J = 7.7 Hz, 2H), 7.12 (d, J = 8.6 Hz, 4H), 7.04 (d, J = 8.7 Hz, 8H), 1.55 (s, 12H). ^{13}C{^{1}H} NMR ($CDCl_3$, ppm) δ148.16 (d, $^{2}J_{CP}$ = 7.7 Hz), 147.49, 147.46, 133.05 (d, $^{4}J_{CP}$ = 3.0 Hz), 132.22 (d, $^{2}J_{CP}$ = 10.4 Hz), 128.57 (d, $^{3}J_{CP}$ = 15.6 Hz), 128.07, 126.27, 119.89 (d, $^{3}J_{CP}$ =4.4 Hz), 42.17, 30.80. ^{31}P{^{1}H} NMR ($CDCl_3$, ppm): δ11.77. FTIR (cm^{-1}): 1252 (P=O).

Polymer P14

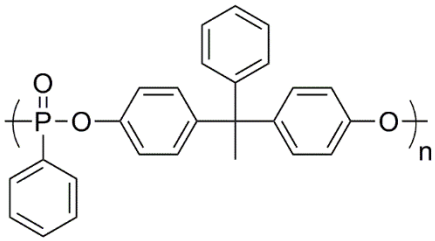

^{1}H NMR ($CDCl_3$, ppm): δ7.96 (dd, J = 14.0, 7.2 Hz, 2H), 7.60 (t, J = 7.4 Hz, 1H), 7.49 (td, J = 7.5, 4.6 Hz, 2H), 7.22 (q, J = 7.2 Hz, 2H), 7.18 (d, J = 6.8 Hz, 1H), 7.06 (d, J = 6.8 Hz, 2H), 7.00 (d, J = 7.4 Hz, 2H), 6.97 (d, J = 8.0 Hz, 2H), 2.06 (s, 3H). ^{13}C{^{1}H} NMR ($CDCl_3$, ppm) δ148.48 (d, $^{2}J_{CP}$ = 7.6 Hz), 145.63, 133.23 (d, $^{4}J_{CP}$ =3.0 Hz), 132.23 (d, $^{2}J_{CP}$ = 10.3 Hz), 129.96, 128.80 (d, $^{1}J_{CP}$ = 197.95 Hz), 128.62 (d, $^{3}J_{CP}$ = 15.8 Hz), 128.49, 127.96, 126.17, 120.20, 119.85 (d, $^{3}J_{CP}$ = 4.5 Hz), 51.69, 50.82. ^{31}P{^{1}H} NMR ($CDCl_3$, ppm): δ11.95. FTIR (cm^{-1}): 1252 (P=O).

Polymer P15

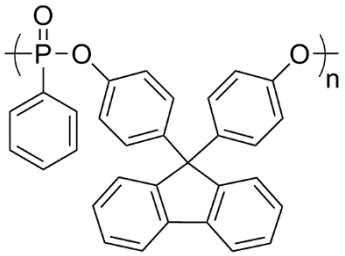

^{1}H NMR ($CDCl_3$, ppm): δ7.99-7.88 (m, 2H), 7.75-7.69 (m, 2H), 7.57 (d, J = 8.6 Hz, 1H), 7.50-7.44 (m, 2H), 7.36-7.30 (m, 2H), 7.26-7.21 (m, 2H), 7.20-7.13 (m, 2H), 7.08-6.91 (m, 8H). $^{13}C\{^{1}H\}$ NMR ($CDCl_3$, ppm) δ142.44 (d, $^{2}J_{CP}$ = 13.8 Hz), 139.93, 133.22, 132.16 (d, $^{2}J_{CP}$ = 10.72 Hz), 129.46, 129.37 (d, $^{4}J_{CP}$ = 6.5 Hz), 128.64 (d, $^{3}J_{CP}$ = 15.2 Hz), 128.31 (d, $^{1}J_{CP}$ 213.5 Hz), 127.74 (d, $^{3}J_{CP}$ = 17.12 Hz), 126.03, 120.25 (d, $^{4}J_{CP}$ = 5.64 Hz), 115.23, 64.33. $^{31}P\{^{1}H\}$ NMR ($CDCl_3$, ppm): δ11.79. FTIR (cm^{-1}): 1253 (P=O).

Polymer P16

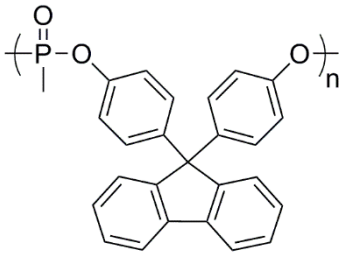

^{1}H NMR ($CDCl_3$, ppm): δ7.74 (d, J= 7.5 Hz, 2H), 7.33 (q, J = 6.8 Hz, 3H), 7.28-7.13 (m, 5H), 7.09 (d, J = 8.2 Hz, 3H), 6.96 (d, J = 8.4 Hz, 3H), 1.80-1.70 (m, 3H). $^{13}C\{^{1}H\}$ NMR ($CDCl_3$, ppm) δ150.93, 142.32, 140.00, 139.77, 129.48 (d, $^{4}J_{CP}$ = 6.1 Hz), 129.16, 127.81 (d, $^{3}J_{CP}$ = 15.3 Hz), 126.09, 120.21, 120.12, 64.36, 53.39. $^{31}P\{^{1}H\}$ NMR ($CDCl_3$, ppm): δ24.13. FTIR (cm^{-1}): 1253 (P=O).

Polymer P17

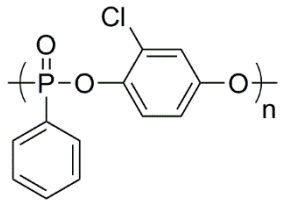

Polymer **P17** was synthesised using DMAP as a catalyst and left to stir for 16 hours. ^{1}H NMR ($CDCl_3$, ppm): δ 8.12-7.86 (m, 2H), 7.64 (Br S, 1H), 7.52 (Br S, 2H), 7.40-7.23 (m, 2H), 7.01 (s, 1H). $^{13}C\{^{1}H\}$ NMR ($CDCl_3$, ppm) δ154.98 (s), 146.88 ($^{2}J_{CP}$ = 9.2 Hz), 143.69 (d, $^{2}J_{CP}$ = 11.3 Hz), 134.00, 132.34 (d, $^{2}J_{CP}$ = 11.5 Hz), 128.88 (d, $^{3}J_{CP}$ = 16.2 Hz), 127.52 (d, $^{1}J_{CP}$ = 218.2 Hz), 122.98 (d, $^{3}J_{CP}$ = 20.2 Hz), 122.46 (d, $^{3}J_{CP}$ = 21.8 Hz), 120.05 (d, $^{3}J_{CP}$ = 18.6 Hz). $^{31}P\{^{1}H\}$ NMR ($CDCl_3$, ppm): δ12.92. FTIR (cm^{-1}): 1251 (P=O).

Polymer P18

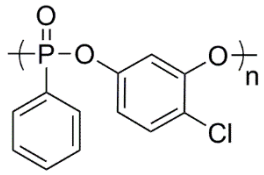

Polymer **P18** was synthesised using DMAP as a catalyst and left to stir for 16 hours. ^{1}H NMR ($CDCl_3$, ppm): δ8.06-7.89 (m, 2H), 7.74-7.63 (m, 1H), 7.62-7.45 (m, 2H), 7.27-7.08 (m, 3H). $^{13}C\{^{1}H\}$ NMR ($CDCl_3$, ppm) δ149.11(d, $^{2}J_{CP}$ = 7.5 Hz), 148.89 (d, $^{2}J_{CP}$ = 8.2 Hz), 134.15, 132.13 (d, $^{2}J_{CP}$ = 11.0 Hz), 130.83 (d, $^{3}J_{CP}$ = 5.1 Hz), 130.59 (d, $^{3}J_{CP}$ = 7.4 Hz), 129.20 (d, $^{1}J_{CP}$ = 202.5 Hz), 128.88 ($^{3}J_{CP}$ = 16.1 Hz), 128.60 (d, $^{4}J_{CP}$ = 2.1 Hz), 155.28. $^{31}P\{^{1}H\}$ NMR ($CDCl_3$, ppm): δ12.77. FTIR (cm^{-1}): 1251 (P=O).

Polymer P19

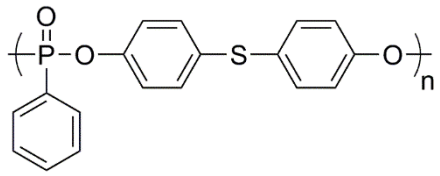

^{1}H NMR ($CDCl_3$, ppm): δ7.94 (dd, J = 14.0, 7.11 Hz, 2H), 7.62 (t, J = 7.5 Hz, 1H), 7.52 (qd, J = 8.3, 7.43 Hz, 2H), 7.22 (d, J = 8.4 Hz, 2H), 7.12 (d, J = 8.4 Hz, 2H). ^{13}C {^{1}H} NMR ($CDCl_3$, ppm) δ149.49 (d, $^{2}J_{PC}$ = 7.4 Hz), 133.61, 132.81 (d, $^{1}J_{CP}$ = 174.91 Hz), 132.52, 132.25 (d, $^{2}J_{CP}$ = 10.3 Hz), 128.83 (d, $^{3}J_{CP}$ = 16.0 Hz), 121.47 (d, $^{3}J_{CP}$ = 4.5 Hz), 116.71. ^{31}P {^{1}H} NMR ($CDCl_3$, ppm): δ12.17. FTIR (cm^{-1}): 1252 (P=O).

6.4 Synthesis of Monomers and Catalysts

Compound 3

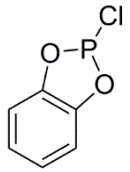

Synthesis of compound 3: PCl_3 (12.15 mL, 0.14 mol) was added dropwise to a solution of catechol (10.00 g, 0.091 mol) in toluene (20 mL) with water (0.13 mL, 7.20 mmol), the mixture left to stir for an hr at rt. A second portion of PCl_3 (5.00 mL, 0.057 mol) was added and the reaction stirred at 100°C for a further 2.5 hr. Solvent was removed under vacuum. Yield: 13.14 g (83%). ^{1}H NMR ($CDCl_3$): δ7.36-7.29 (m, 2H), 7.23-7.16 (m, 2H). ^{31}P{^{1}H} NMR ($CDCl_3$, ppm): δ173.64.

Compound 4

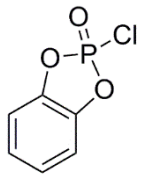

Synthesis of compound 4: O_2 was bubbled through a solution of compound **3** (4,00 g, 2.30 mmol) in toluene (30 mL) at a constant rate for 36 hr. The solvent was then removed under vacuum. Yield: 0.18 g (43%).^{1}H NMR ($CDCl_3$): δ7.32-7.27 (m, 2H), 7.21-7.15 (m, 2H). $^{31}P\{^{1}H\}$ NMR ($CDCl_3$, ppm): δ19.89.

Compound 5

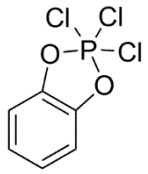

Synthesis of compound 5: PCl_5 (14.35 g, 0.069 mol) was added to a solution of catechol (6.00 g, 0.054 mol) in toluene (15 mL) and refluxed for 2 hr under a dynamic flow of nitrogen which was passed through the reaction head space and into a 1M NaOH aqueous solution to remove HCl. Yield: 9.61 g (73%). ^{1}H NMR ($CDCl_3$, ppm): δ7.26-7.15 (m, 2H), 7.13-7.05 (m, 2H). $^{31}P\{^{1}H\}$ NMR ($CDCl_3$, ppm): δ-26.09.

Monomer 1

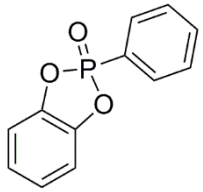

Synthesis of monomer 1: A solution of catechol (2.79 g, 0.025 mol) and pyridine (4.00 mL, 0.050 mol) in THF (15 mL) was added at −20°C to a stirred solution of phenylphosphonic dichloride (4.87 g, 0.025 mol) in THF (20 mL). The mixture was then allowed to warm to rt and stirred for 6 hr. It was then filtered, the solvent was removed and the white solid dried under vacuum to give 1,3,2-benzodioxaphosphole,1-phenyl-2-oxide. Yield: 4.29 g (74%). ^{1}H NMR (C_6D_6, ppm): δ7.74-7.58 (m, 2H, P-C-$(CH)_2$-$(C\underline{H})_2$-CH), 7.01-6.92 (m, 1H, P-C-$(CH)_2$-$(CH)_2$-C$\underline{H}$), 6.82 (q, J = 7.6, 2H, P-C-$(C\underline{H})_2$-$(CH)_2$-CH), 6.72-6.63 (m, 2H, O-C-$(C\underline{H})_2$-$(CH)_2$), 6.55 (dt, J = 5.9, 3.7 Hz, 1H, O-C-$(CH)_2$-$(C\underline{H})_2$). ^{13}C{^{1}H} NMR (C_6D_6, ppm): δ145.64 (O-$(\underline{C}H)_2$-$(CH)_2$), 134.06 (d, $^{4}J_{CP}$ = 3.3 Hz, P-C-$(CH)_2$-$(CH)_2$-$\underline{C}$H), 132.55 (d, $^{3}J_{CP}$ = 11.5 Hz, P-C-$(CH)_2$-$(\underline{C}H)_2$-CH), 125.44 (d, $^{1}J_{CP}$ = 187.5 Hz, P-$\underline{C}$-$(CH)_2$-$(CH)_2$-CH), 123.77 (O-$(CH)_2$-$(\underline{C}H)_2$), 112.78 (d, $^{2}J_{CP}$ = 10.4 Hz, P-C-$(\underline{C}H)_2$-$(CH)_2$-CH). ^{31}P{^{1}H} NMR (C6D6, ppm): δ34.87. FTIR (cm^{-1}): 1298 (P=O). MS ($[MCH_3]^+$) m/z) calculated: 232.03, found: 232.03.

Monomer 2

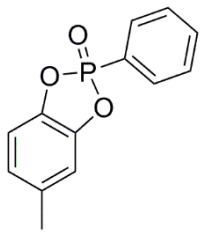

Synthesis of monomer 2: A solution of 4-methylcatechol (3.10 g, 0.025 mol) and pyridine (4.00 mL, 0.050 mol) in THF (15 mL) was added at −20°C to a stirred solution of phenylphosphonic dichloride (4.87 g, 0·025 mol) in THF (20 mL). The mixture was

then allowed to warm to rt and stirred for 6 hr. It was then filtered and the solvent removed. The white solid was dried under vacuum to give 1,3,2-benzodioxaphosphole-6-methyl, 2-phenyl-2-oxide. Yield: 5.35 g (87%). ^{1}H NMR (C_6D_6, ppm): δ7.77-7.65 (m, 2H), 7.02-6.93 (m, 1H), 6.89-6.80 (m, 2H), 6.62 (d, J = 8.1 Hz, 1H), 6.52 (s, 1H), 6.38 (d, J = 8.1 Hz, 1H), 1.89 (s, 3H). ^{13}C{^{1}H} NMR (C_6D_6, ppm): δ145.54, 143.53, 134.02 (d, $^{4}J_{CP}$ = 3.4 Hz), 133.82, 132.51 (d, $^{3}J_{CP}$ = 11.4 Hz), 128.96 (d, $^{3}J_{CP}$ =16.1 Hz), 125.70 (d, $^{1}J_{CP}$ = 124.0 Hz), 123.95, 113.52 (d, $^{2}J_{CP}$ = 10.4 Hz), 112.21 (d, $^{2}J_{CP}$ = 10.4 Hz), 20.98. ^{31}P{^{1}H} NMR (C_6D_6, ppm): δ35.27. FTIR (cm^{-1}): 1289 (P=O). MS ($[MCH_3]^{+}$) m/z) calculated: 247.05, found: 247.05.

Monomer 6

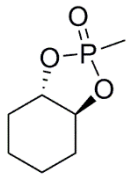

Synthesis of monomer 6: A solution of trans-1,2-cyclohexanediol (2.90 g, 0.025 mol) and pyridine (4.00 mL, 0.050 mol) in THF (15 mL) was added at −20°C to a stirred solution of methylphosphonic dichloride (3.30 g, 0.025 mol) in THF (20mL). The mixture was then allowed to warm to rt and stirred for 6 hr. It was then filtered and solvent was removed and the white solid was dried under vacuum to give 1,3,2-benzodioxaphosphole, hexahydro-2-methyl-2-oxide. Yield: 3.17 g (72%). ^{1}H NMR (C_6D_6, ppm): δ3.65-3.59 (m, 1H), 3.18-3.07 (m, 1H), 1.64 (d, J = 14.0 Hz, 1H), 1.19 (d, J = 17.3 Hz, 3H), 1.15-1.06 (m, 3H,), 0.89 (qd, J = 11.8, 3.7 Hz, 1H), 0.66-0.52 (m, 2H). ^{13}C{^{1}H} NMR (C_6D_6, ppm): δ83.83, 81.61, 29.62 (d, $^{2}J_{CP}$ = 10.5Hz), 29.40 (d,

$^{2}J_{CP}$ = 9.2 Hz), 23.36, 23.33, 11.86 (d, $^{1}J_{CP}$ = 134.3 Hz). $^{31}P\{^{1}H\}$ NMR (C_6D_6, ppm): δ41.21. FTIR (cm^{-1}): 1256 (P=O). MS ($[MH]^{+}$) m/z) calculated: 176.06, found: 176.07.

Monomer 16

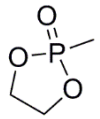

Synthesis of monomer 16: A solution of ethylene glycol (1.55 g, 0.025 mol) and pyridine (4.00 mL, 0.050 mol) in THF (15 mL) was added at −20°C to a stirred solution of methylphosphonic dichloride (3.30 g, 0.025 mol) in THF (20mL). The mixture was then allowed to warm to rt and stirred for 6 hr. It was then filtered and solvent was removed and the oil was purified using fractional distillation to give 2-methyl-1,3,2-dioxaphospholane 2-oxide. Yield 1.43 g (47%). ^{1}H NMR (C_6D_6, ppm): δ3.52-3.41 (m, 2H), 3.15-3.04 (m, 2H), 1.07 (d, J = 17.3 Hz, 3H, CH_3). $^{31}P\{^{1}H\}$ NMR (C_6D_6, ppm): δ45.33.

Monomers 7, 8, 9 and 10

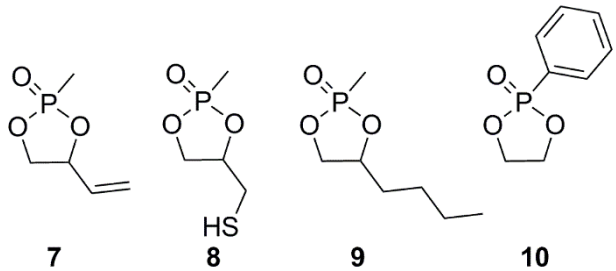

Representative attempted synthesis of functional phosphonate monomers (7, 8, 9 and 10): A solution of diol (3-butene-1,2-diol, 1-thioglycerol, 1,2-hexanediol,

ethylene glygcol) and base (pyridine, DMAP, DBU, TBD) were made up in THF. A solution of phosphonic dichloride (phenylphosphonic dichloride, methylphosphonic dichloride) was added to the diol solution at 0°C. The mixture was allowed to warm to rt for 6 h. The resulting mixture was filtered through Celite® and THF was removed under vacuum.

Representative ROP of cyclic phosphonates: reagent ratios for polymerisations were $[Monomer]_0:[Initiator]_0:[Catalyst]_0 = 100:1:1{\cdot}5$ unless otherwise stated. A solution of monomer and initiator were made up in 1.5 mL of DCM. The mixture was freeze-thaw degassed three times. The catalyst in 0.3 mL of DCM was added to the monomer initiator solution at 0°C. The reaction was then terminated by addition of excess formic acid in DCM and the polymer precipitated into cold hexane. The precipitate was then filtered and dried under vacuum.

Phosphoric Acid Catalyst Synthesis

Representative synthesis of phosphoric acid catalysts: phenol (0.019 mol), phosphorus oxychloride (2.89 g, 0.019 mol) and lithium chloride (0.01 g, 0.240 mmol) were heated to 110°C in a sealed schlenk flask for 24 hr. The mixture was allowed to cool to rt and a crude NMR spectrum taken. The mixture was then used without purification. Water (4 mL, 0.22 mol) was added and the reaction mixture was heated to 90°C for 16 hr. The organic layer was extracted with DCM. The product was then extracted using an aqueous 1M sodium carbonate solution (20 mL). The basic solution

was neutralised with an aqueous 1M hydrochloric acid solution and the product extracted using DCM and dried in under vacuum.

Catalyst 27

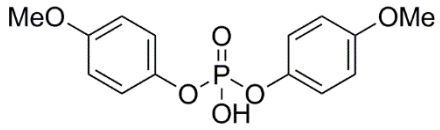

Yield: 3.42 g (58%). ^{1}H NMR ($CDCl_3$, ppm): δ7.10 (dd, J = 9.1, 1.2 Hz, 4H, O-C-(C<u>H</u>)$_2$-(CH)$_2$), 6.83 (d, J = 9.0 Hz, 4H, O-C-(CH)$_2$-(C<u>H</u>)$_2$), 3.79 (s, 3H, O-C<u>H</u>$_3$). ^{13}C{^{1}H} NMR ($CDCl_3$, ppm) δ156.95 (O-C-(CH)$_2$-(CH)$_2$-<u>C</u>), 143.97 (d, $^{2}J_{CP}$ = 7.4 Hz, O-<u>C</u>-(CH)$_2$-(CH)$_2$), 121.06 (d, $^{3}J_{CP}$ = 4.6 Hz, O-C-(<u>C</u>H)$_2$-(CH)$_2$), 114.63 (O-C-(CH)$_2$-(<u>C</u>H)$_2$), 55.57 (O-<u>C</u>H$_3$) ^{31}P{^{1}H} NMR ($CDCl_3$, ppm): δ-8.63. FTIR (cm^{-1}): 1216 (P=O). MS ([M-H]$^{-}$) m/z) calculated: 309.06, found: 309.05.

Catalyst 28

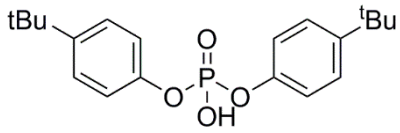

Yield: 4.23 g (61%). ^{1}H NMR ($CDCl_3$, ppm): δ7.33 (d, J = 8.6 Hz, 4H), 7.12 (dd, J = 8.8, 1.0 Hz, 4H), 1.31 (s, 18H). ^{13}C{^{1}H} NMR ($CDCl_3$, ppm) δ148.16 (d, $^{2}J_{CP}$ = 4.1 Hz), 126.53, 119.50 (d, $^{3}J_{CP}$ = 4.4 Hz), 110.92, 34.38, 31.37. ^{31}P{^{1}H} NMR ($CDCl_3$, ppm): δ-9.04. FTIR (cm^{-1}): 1210 (P=O). MS ([M-H]$^{-}$) m/z) calculated: 361.17, found: 361.16.

Catalyst 29

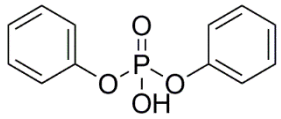

Yield: 2.08 g (43%). ^{1}H NMR ($CDCl_3$, ppm): δ7.30 (t, J = 8.3, 4H), 7.20-7.14 (m, 6H). $^{13}C\{^{1}H\}$ NMR ($CDCl_3$, ppm) δ150.39 (d, $^{2}J_{CP}$ = 7.0 Hz), 129.72, 125.40, 120.16 (d, $^{3}J_{CP}$ = 5.0 Hz). $^{31}P\{^{1}H\}$ NMR ($CDCl_3$, ppm): δ-10.24. FTIR (cm^{-1}): 1220 (P=O). MS ($[MH]^{+}$) m/z) calculated: 251.05, found: 251.05.

Catalyst 30

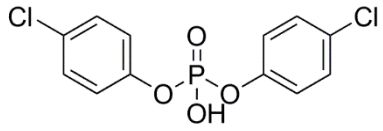

Yield: 3.37 g (56%). ^{1}H NMR ($CDCl_3$, ppm): δ7.30 (d, J = 8.8 Hz, 4H), 7.10 (d, J = 8.2 Hz, 4H). $^{13}C\{^{1}H\}$ NMR ($CDCl_3$, ppm) δ148.63 (d, $^{2}J_{CP}$ = 7.2 Hz), 131.20, 129.88, 121.46 (d, $^{3}J_{CP}$ = 5.0 Hz). $^{31}P\{^{1}H\}$ NMR ($CDCl_3$, ppm): δ-10.03. FTIR (cm^{-1}): 1237 (P=O). MS ($[MH]^{+}$) m/z) calculated: 318.97, found: 318.97, ($[M-H]^{-}$) m/z) calculated: 316.95, found: 316.96.

Catalyst 31

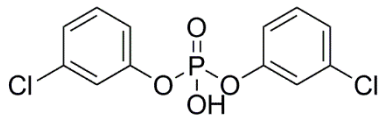

Yield: 2.98 g (49%). ^{1}H NMR ($CDCl_3$, ppm): δ7.23 (d, J = 8.4 Hz, 2H), 7.19 (q, J = 2.8 Hz, 2H), 7.18-7.16 (m, 2H), 7.08 (q, J = 2.3 Hz, 2H). $^{13}C\{^{1}H\}$ NMR ($CDCl_3$, ppm) δ150.52 (d, $^{2}J_{CP}$ = 7.1 Hz), 135.10, 130.53, 126.02, 120.83 (d, $^{3}J_{CP}$ = 5.4 Hz), 118.39

(d, $^{3}J_{CP}$ = 4.9 Hz). ^{31}P {^{1}H} NMR ($CDCl_3$, ppm): δ-1260. FTIR (cm^{-1}): 1260 (P=O). MS ([M-H]$^{-}$) m/z) calculated: 316.95, found: 316.95.

Catalyst 32

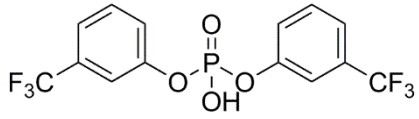

Yield: 3.81 g (52%). ^{1}H NMR ($CDCl_3$, ppm): δ7.50-7.43 (m, 4H), 7.42 (s, 2H), 7.40-7.35 (m, 2H). ^{13}C{^{1}H} NMR ($CDCl_3$, ppm) δ150.12 (d, $^{4}J_{CP}$ = 7.4 Hz), 132.57 (q, $^{1}J_{CF=}$ 32.8, 32.2 Hz), 130.52, 124.30, 123.47 (d, $^{3}J_{CP}$ = 4.9 Hz), 122.48, 117.37 (d, $^{3}J_{CP}$ = 5.0 Hz). ^{31}P{^{1}H} NMR ($CDCl_3$, ppm): δ11.20. FTIR (cm^{-1}): 1234 (P=O). MS ([MH]$^{+}$) m/z) calculated: 387.02, found: 387.02.

Catalyst 33

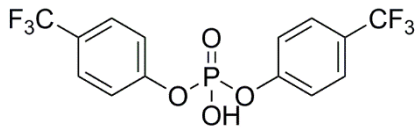

Yield: 3.52 g (48%). ^{1}H NMR ($CDCl_3$, ppm): δ7.64 (d, J = 8.4 Hz, 4H), 7.33 (d, J = 8.5 Hz, 4H). ^{13}C{^{1}H} NMR ($CDCl_3$, ppm) δ152.24 (d, $^{2}J_{CP}$ = 7.35 Hz), 132.75 (d, $^{3}J_{CP}$ = 4.3 Hz), 127.35 (q, $^{1}J_{CP}$ = 3.8 Hz), 122.29 (d, J = 3.9 Hz), 120.48, 115.54. ^{31}P{^{1}H} NMR ($CDCl_3$, ppm): δ-10.52. FTIR (cm^{-1}): 1236 (P=O). MS ([M-H]$^{-}$) m/z) calculated: 385.01, found: 385.00.

Catalyst 34

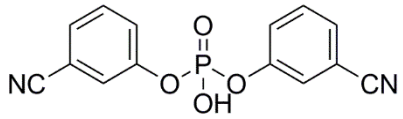

Yield: 3.98 g (70%). ^{1}H NMR ($CDCl_3$, ppm): δ7.36 (t, J = 8.0 Hz, 2H), 7.24 (dt, J = 7.7, 1.2 Hz, 2H), 7.16 (t, J = 2.0 Hz, 2H), 7.13 (dd, J = 8.3, 2.6, 2H). ^{13}C{^{1}H} NMR ($CDCl_3$, ppm) δ150.33 (d, $^{2}J_{CP}$ = 6.6 Hz), 131.11, 129.33, 125.15 (d, $^{3}J_{CP}$ = 4.7 Hz), 123.72 (d, $^{3}J_{CP}$ = 4.6 Hz), 118.58, 113.69. ^{31}P{^{1}H} NMR ($CDCl_3$, ppm): δ-11.66. FTIR (cm^{-1}): 1226 (P=O). MS ([M-H]$^{-}$) m/z) calculated: 299.02, found: 299.02.

Catalyst 35

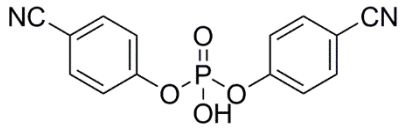

3.98 g (70%). ^{1}H NMR ($CDCl_3$, ppm): 7.33 (t, J = 7.3, 4H), 7.19 (m, 4H). ^{13}C{^{1}H} NMR ($CDCl_3$, ppm) 150.41 (d, $^{2}J_{CP}$ = 7.3 Hz), 129.71, 125.36, 120.17 (d, $^{3}J_{CP}$ = 4.9 Hz), 117.81. ^{31}P {^{1}H} NMR ($CDCl_3$, ppm): δ-9.48. FTIR (cm^{-1}): 1249 (P=O). HRMS ([MH]$^{+}$) m/z) calculated: 301.04, found 301.04. HRMS ([M-H]$^{-}$) m/z) calculated: 299.02, found: 299.02.

Catalyst 37

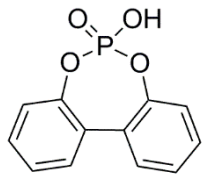

3.98 g (70%). ^{1}H NMR ($CDCl_3$, ppm): 7.36 (dd, J = 8.1, 7.4 Hz, 2H), 7.31 (dd, J = 7.7, 1.8 Hz, 2H), 7.08 (td, J = 7.5, 1.2 Hz, 2H), 7.04 (dd, J = 8.1, 1.2 Hz, 2H). ^{13}C{^{1}H} NMR ($CDCl_3$, ppm): 152.84, 130.67 (d, $^{1}J_{CP}$ = 173.2 Hz), 123.69, 121.67, 116.69. ^{31}P{^{1}H} NMR ($CDCl_3$, ppm): 3.78. FTIR (cm^{-1}): 1224 (P=O). MS ([MNa]$^{+}$) m/z) calculated: 270.01, found 270.01.

Representative β-BL polymerisation using phosphoric acid catalysts: All polymerisations were set up in a glovebox. For a β-BL polymerisation, a solution of β-BL (0.019 g, 0.023 mmol), PPA (0.63 mg, 0.0046 mmol) and catalyst **27-38** (0.0023 mmol) were made up in toluene (2 mL). The mixture was stirred at 100°C for 24 hr. A crude NMR was taken and the polymerisations quenched by precipitation into cold hexane.

Representative β-BL kinetic study using phosphoric acid catalysts: All kinetic runs were set up in the glovebox. A solution of β-BL (0.010 g, 1.2 mmol), PPA (0.030 g, 0.23 mmol) and catalyst **15-25** (0.12 mmol) were made up in d_8-toluene (0.70 mL). The sample was kept at 100°C in the magnet for 24 hr. A ^{1}H NMR spectrum was taken every 20 mins and a ^{31}P{^{1}H} NMR spectrum recorded every 60 min.

Compound 39

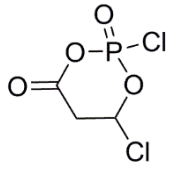

Attempted synthesis of compound 39 using method A: Not under inert conditions, 3-hydroxybutyric acid (0.27 g, 2.61 mmol), phosphorus oxychloride (0.40 g, 2.913 mmol) and lithium chloride (0.01 g, 0.236 mmol) were heated to 110°C in a sealed schlenk flask for 24 hr. The mixture was allowed to cool to rt and a crude NMR taken.

Synthesis of compound 39 using method B: A solution of 3-hydroxybutyric acid (0.68 g, 6.52 mmol) and TEA (0.98 mL, 7.00 mmol) in THF (15 mL) were added to a solution of $POCl_3$ (1.00 g, 6.52 mmol) in THF (15 mL), dropwise at 0°C. Once the addition was complete the reaction mixture was allowed to warm to rt and stirred for 4 hr. The mixture was then filtered through Celite® and the solvent removed under vacuum. ^1H NMR ($CDCl_3$, ppm): δ5.21 (s, 1H), 3.04 (qd, J = 7.3, 4.8 Hz, 2H), 1.25 (t, J = 7.4 Hz, 3H). $^{31}P\{^1H\}$ NMR ($CDCl_3$, ppm): δ-3.64.

Compound 40

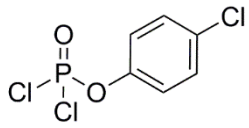

Synthesis of 40: A solution of 4-chloropehnol (0.28 g, 2.17 mmol) and TEA (0.22 mL, 3.00 mmol) was made up in THF (15 mL) and added to a solution of $POCl_3$ (1.00 g, 6.52 mmol) in THF (15 mL), dropwise at 0°C. Once the addition was complete the reaction mixture was allowed to warm to rt and stirred for 4 hr. The mixture was then filtered through Celite® and the solvent removed under vacuum. ^1H NMR ($CDCl_3$,

ppm): δ7.42 (dd, J = 9.06, 1.14 Hz, 2H), 7.27 (dq, J = 8.99, 2.44 Hz, 2H). $^{31}P\{^{1}H\}$ NMR ($CDCl_3$, ppm): δ3.70.